Elektroprivreda

Electric Power Industry Journal

ISSN 3009-2892 (Online)

UDC 620.9
621.31

2026

Godina 4, Broj 2
Volume 4, Issue 2

SPECIAL EDITION

cigre
СРБИЈА

VOLUME. 4, ISSUE. 2 / 2026
GODINA 4, BROJ 2 / 2026
Electric Power Industry Journal
ELEKTROPRIVREDA

ISSN 3009-2892 (Online)
UDC 620.9
621.31

Elektroprivreda
Electric Power Industry Journal

Scientific and professional journal of the joint-stock company "Elektroprivreda Srbije"
in co-publishing with the Nikola Tesla Institute of Electrical Engineering JSC Belgrade

Volume 4, Issue 2

Content

ISSN 3009-2892 = Elektroprivreda (Online)

EXECUTIVE PUBLISHER
JOINT STOCK COMPANY ELEKTROPRIVREDA SRBIJE BELGRADE
11000 Belgrade, 13 Balkanska Street
Website: www.eps.rs
Editor-in-Chief phone: +381-11-365-23-63
E-mail: epijournal.editor@eps.rs
The Journal web platform: https://epijournal.eps.rs

CO-PUBLISHER
NIKOLA TESLA INSTITUTE OF ELECTRICAL ENGINEERING JSC BELGRADE
11000 Belgrade, 8a Koste Glavinića Street
Website: www.ieent.org
Phone: +381-11-39-52-000
Fax: +381-11-36-90-487

FOR EXECUTIVE PUBLISHER
Dušan Živković, Dipl. El. Ing.
General Manager, EPS JSC

FOR CO-PUBLISHER
Dr. Jelena Lukić, Dipl. Ing. Techn.
Director, ETI Nikola Tesla

Electric Power Industry Journal - „Elektroprivreda“
is published twice a year, exclusively in electronic form,
at https://epijournal.eps.rs as *Open Access* journal type

COBISS.SR-ID - 121874441

FOREWORD BY THE EDITORIAL BOARD AND THE GUEST EDITOR

Dear Readers and Contributors,

We are pleased to present the latest issue of Elektroprivreda – *Electric Power Industry Journal*. As a continuation of the journal's partnership with the CIGRE Serbia National Committee, this is another special edition featuring extended and enhanced versions of six selected conference papers that received awards at the organisation's 37th National Conference, held in Zlatibor from 26 to 30 May 2025. Distinguished experts from academia and industry, specialising in the fields covered by these papers, served on the Guest Editorial Board, which, in collaboration with the journal's permanent Editorial Board, reviewed and peer-reviewed the manuscripts and prepared this issue for publication.

The first paper presents the technical solution, characteristics and functionalities of the new excitation systems for the motor-generators at the Bajina Bašta Pumped-Storage Hydropower Plant (PSHPP). The replacement of the legacy excitation systems was carried out as part of the recently completed refurbishment of the plant's generating units, a key undertaking for maintaining the stability of Serbia's power system and facilitating the integration of renewable energy sources. The newly installed state-of-the-art excitation controllers provide full control of the units under all operating conditions, with high reliability ensured by a redundant (1+1) architecture of the thyristor bridges and control units. The units are capable of operating in all four quadrants of the operating diagram and support both synchronous start-up and electrical braking. The paper concludes with illustrative dynamic response recordings obtained during the acceptance testing of the units, which were used to evaluate and verify the system's dynamic performance indicators.

The second paper begins with an overview of the key technological principles, advantages and limitations of modern green hydrogen production methods, with particular emphasis on electrolysis. It also highlights the technological trends driving the increasing adoption of hydrogen in energy systems. The authors then present a practical conceptual proposal for the construction of a hydrogen production and storage facility to provide a substitute fuel for the potential future gas turbines of Units A1 and A2 at the Nikola Tesla Thermal Power Plant. The proposed location benefits from an already established supporting infrastructure. The paper analyses the conditions required for the development of an integrated energy complex for hydrogen production, storage and utilisation, examines the associated challenges, and proposes suitable locations for water supply facilities, electrolysers, and hydrogen storage systems. As such, it offers a coherent assessment of one of the potential pathways towards the decarbonisation of Serbia's power sector.

Building on the theme of the development and application of hydrogen technologies, the next paper also addresses issues related to electrolyser operation. Specifically, it presents the development and practical implementation of specialised power converter topologies for supplying alkaline electrolysers used in the production of "green" hydrogen. Its particular value lies in the fact that it goes beyond theoretical analyses and simulation models, describing instead a fully realised 40 kW industrial installation that has been successfully commissioned within a thermal power generation system for generator cooling purposes. The innovative nature of this solution, developed by domestic experts, is reflected in a unique twelve-pulse topology that eliminates the need for an interphase reactor between the two thyristor bridges. Instead, a three-winding transformer with secondary voltages of unequal amplitudes is employed. The paper is richly illustrated with diagrams and experimental results that confirm the theoretical principles presented.

The following paper is likewise devoted to the field of power electronics. It examines the modelling of dynamic losses in gallium nitride (GaN) power switches, a modern wide-bandgap semiconductor technology used to achieve high efficiency and high-power density. Unlike existing approaches reported in the literature, the proposed analytical model simultaneously accounts for the nonlinear dependence of the parasitic capacitances (Ciss, Coss and Crss) on the drain-source voltage, as well as the nonlinear variation of the GaN switch transconductance (gm). An algorithm is defined and implemented to discretise the nonlinear characteristic curves provided in manufacturers' datasheets into more than 100 points, thereby avoiding the analytical approximations that introduce errors at high switching frequencies. The key innovation is the detailed mathematical separation of the total current into channel conduction current and parasitic capacitance current. This distinction enables the precise identification of losses during hard-switching, soft-switching and quasi-soft-switching commutation processes in a half-bridge configuration. The paper also has significant practical value, as the proposed theoretical model was validated using a 1 kW synchronous buck converter prototype designed and built by the authors themselves, who conducted measurements across its entire operating voltage range.

The penultimate paper describes a controlled switching technique as a means of limiting the adverse effects of switching transients. This is a highly topical issue in modern transmission systems. The controlled switching function and its potential benefits within a transmission network were tested under laboratory conditions. The experimental setup consisted of a microprocessor-based protection and control device acting as the controller, together with a real-time Hardware-in-the-Loop (HIL) simulator on which a model of a 400 kV shunt reactor and a circuit breaker was implemented. The effects of switching transients associated with the energisation of different types of loads are presented, and a comparison is made with the conventional switching of a shunt reactor circuit breaker. The laboratory validation of the results adds significant practical value to the conclusions presented in the paper.

The final paper examines the implementation of the European regulatory framework and operational practices within the work of transmission system operators (TSOs) in the Western Balkans region. It outlines the coordination of processes carried out at the level of European transmission system operators and the principal changes being introduced into the operational activities of Serbia's TSO, Elektromreža Srbije (EMS JSC). The two most important processes, coordinated security analysis and transmission capacity calculation, are being aligned with the requirements of ENTSO-E. The paper also presents the regulatory process through which EMS JSC is joining the European capacity calculation regions, namely the CORE and SEE regions, and highlights the challenges associated with this integration. The fundamental concepts of the coordinated processes are explained, some of which will be implemented directly by the TSO, while others will be carried out through regional coordination centres. In this context, compliance with the requirement to make available 70% of the capacity of critical network elements, particularly interconnecting transmission lines, is essential. This requirement also applies to the management of internal transmission line loading affecting cross-border interconnections within the broader congestion management process in the South-East European interconnection and the Serbian transmission network. The particular value of this paper lies in its clear presentation of the current European landscape in comparison with Serbia's position and degree of implementation, as well as in its identification of the processes and activities that must be undertaken in the coming period. The implementation of the mechanisms analysed is one of the key prerequisites for Serbia's integration into the single European electricity market, including participation in day-ahead and intraday market coupling, as well as accession to the European balancing platforms.

In view of the timeliness of the topics addressed and the innovative nature of the solutions presented in these papers, we are confident that the content of this issue will capture your interest and prove valuable to your work. Most of the articles focus on power electronics, a field to which the late Professor Vladimir Katić, former Chairman of the journal's permanent Editorial Board, made an outstanding contribution. In addition to a tribute reviewing his remarkable career and lasting impact on both the profession and the scientific community, this issue concludes with an Excerpt from his extensive bibliography. We hope that the titles collected in this selection will serve as a useful resource for experts working in the fields to which Professor Katić devoted his research, thereby further enhancing the accessibility and value of his scientific and professional legacy.

We would also like to take this opportunity to renew our invitation to readers to participate actively in the life of the Journal. We warmly encourage you to submit manuscripts of scholarly and professional articles, as well as discussions, commentaries, polemics, or personal viewpoints relating to previously published papers and to the specific technical and scientific issues they address. We will be pleased to consider all materials received and to explore opportunities for their publication in future issues of the Journal.

On behalf of the Guest Editorial Board
of this Special Issue of the Journal,

Nebojša Petrović, Dipl. El. Ing.
President of CIGRE Serbia
Guest Editor-in-Chief

On behalf of the Journal Editorial Board,

Dr Vladimir Šiljkut, Dipl. El. Ing.
Editor-in-Chief and Responsible Editor

UDC: 621.314.52(497.11)

Dušan Joksimović[1], Đorđe Stojić[1], Nemanja Milojčić[1], Zoran Ćirić[1],
Slavko Veinović[1], Luka Ivanović[1], Ilija Klasnić[1], Miroslav Pavićević[2], Dušan Trišić[2]

Design and Dynamic Performance of Redundant Excitation Systems for Motor-Generators at Bajina Basta Pumped-Storage Hydro Power Plant

[1] Nikola Tesla Institute of Electrical Engineering JSC Belgrade, Serbia
[2] EPS JSC, Branch Drinsko-Limske HPPs, HPP Bajina Bašta, Serbia

Professional article

Highlights

- Revitalization of the units at PSHPP "Bajina Bašta" – crucial for system stability and the integration of renewable energy sources.
- Modern excitation regulators enable complete control of the units in all operating states, with high reliability ensured by a redundant (1+1) architecture of thyristor bridges and control units.
- Support for unit operation in all four quadrants of the capability diagram, including synchronous start and electrical breaking.

Abstract

The run-of-river and pumped-storage hydro power plants (PSHPP) "Bajina Bašta" in Perućac represent the largest hydroelectric facilities built on the Drina River. PSHPP "Bajina Bašta" is of immense importance to the Serbian power system due to its ability to operate in both generator and motor modes, which increases system flexibility in terms of production and consumption management. Additionally, due to its capability for rapid startup and quick transitions between generator and motor modes, this plant can react swiftly to system disturbances and replace any other unit within the "Elektroprivreda Srbije" system. Consequently, the revitalization of PSHPP "Bajina Bašta," aimed at extending the units' lifespan for several decades, is of great significance to the power system. During 2024, the first unit was revitalized, while the revitalization of the second unit was completed in 2026. As part of the revitalization, the entire excitation systems were replaced. High-performance components were installed within the power section of the excitation system: excitation transformers, circuit breakers, thyristor bridges, de-excitation equipment, etc. The core of the control section consists of certified digital excitation regulators, which feature integrated sequential automation for all operating modes: generator mode, motor mode, synchronous start, and electrical braking. The regulators enable various control modes: automatic stator voltage regulation, reactive power regulation, or power factor regulation, along with integrated limiter functions and a power system stabilizer. System reliability is further ensured by the redundant implementation of thyristor bridges and excitation regulators in a 1+1 configuration. Following the completion of installation and connection of all equipment, detailed tuning and testing of the excitation system were conducted, demonstrating high system performance. This guarantees reliable and stable operation of the units in all intended modes, with automatic operation limiting within the defined boundaries of the capability diagram.

Keywords

Excitation system, Motor-generator, Reliability, Revitalization

Notes:

**The full text of this article is available only in the Serbian language.
In the English version, only its Abstract (above) is available.**

This article represents an expanded, improved and additionally peer-reviewed version of the paper "*Excitation Systems for Motor-Generators in the Bajina Bašta Pumped-Storage Hydropower Plant*" (https://doi.ub.kg.ac.rs/doi/cigre37-a1-8/), awarded in the Expert Committee EC-A1 *Electrical Machines*, at the 37th CIGRE Serbia Conference, Zlatibor, 26-30 May 2025.

Received: April 6th, 2026 Reviewed: June 30th, 2026
Modified: July 9th, 2026 Accepted: July 14th, 2026
*Corresponding author: Dušan Joksimović, +381 64/82-59-741
E - mail: dusan.joksimovic@ieent.org

UDC: 621.311:502.131.1(497.11)

Jelica Janićijević[1], Danilo Vlahović[1], Aleksandar Latinović[1], Željko Đurišić[1]

Conceptual Design for Substituting Coal as Fuel in Units A1 and A2 of Nikola Tesla Thermal Power Plant Through the Application of Hydrogen Technologies Combined with Renewable Energy Sources

[1] University of Belgrade, School of Electrical Engineering, Belgrade, Serbia*

Original scientific research article

Highlights

- The key technological principles, limitations, and advantages of modern green hydrogen production methods were analyzed, with a focus on electrolysis.
- The challenges and solutions related to hydrogen storage were examined.
- Technological trends accelerating the adoption of hydrogen in energy systems were presented, including the growth of electrolyzer capacities, cost reductions, and improved integration with renewable energy sources.
- The paper highlights the importance of infrastructure optimization and the development of cost-effective solutions as prerequisites for the wider use of hydrogen in the decarbonization process.

Abstract

The integration of renewable energy sources (RES) into power systems (PS) represents a challenge due to their variable and non-dispatchable nature, which complicates the balancing of electricity generation and consumption. Stable operation of the power system requires dispatchable energy sources. On the other hand, the phase-out and shutdown of thermal power plants in the decarbonization process, as envisaged by the Integrated National Energy and Climate Plan, reduces the availability of dispatchable energy, thereby threatening balancing conditions and the energy independence of the power system. One of the proposed solutions is the utilization of surplus energy from renewable sources for the production of hydrogen and its derivatives, which can be stored and later used in gas-fired power plants as dispatchable energy sources.

This paper analyzes the conditions for establishing an energy complex for the production, storage, and utilization of hydrogen at the site of the existing Nikola Tesla A Thermal Power Plant . The basic concept is that the power plant would not be decommissioned in the future, but would instead transition from lignite to renewable fuel by replacing conventional boilers and steam turbines with gas turbine units adapted for hydrogen combustion. In this way, key infrastructure is preserved, particularly the grid connection facilities and the well-developed interconnection links of this important generation hub.

The potential for hydrogen production from photovoltaic power plants to be built in the area of the former Kolubara open-pit mines was also analyzed. A conceptual technological scheme of the process of hydrogen production, compression, storage, and utilization is presented, along with a calculation of the overall energy efficiency of the complete system. Based on available data, a preliminary estimate of the expected cost of generated electrical energy was carried out.

Note:

This article represents an expanded, improved and additionally peer-reviewed version of the student paper "*Conceptual Solution for the Decarbonization of Electricity Production at TPP 'Nikola Tesla' by Applying Hydrogen Technologies with Renewable Energy Sources*" (https://doi.ub.kg.ac.rs/doi/cigre37-c3-1/), awarded in the Expert Committee EC-C3 *Sustainability of Power System and Environmental Protection Performance*, at the 37th CIGRE Serbia Conference, Zlatibor, 26-30 May 2025.

Received: January 7th, 2026 Reviewed: July 1st, 2026
Modified: July 10th, 2026 Accepted: July 13th, 2026

*Corresponding author: Jelica Janićijević, +381 61/81-51-629
E - mail: jelicajanicijevic616@gmail.com

The concept assumes that during periods of low electricity market prices, energy from photovoltaic plants or the transmission grid is directed to electrolysis, while the produced hydrogen is stored and used during periods of high demand and insufficient energy from available primary sources in the system. Additionally, the heat generated during electrolysis and hydrogen combustion can be utilized for thermal energy storage and for supplying thermal consumers, thereby increasing the overall efficiency of the system.

Keywords

Decarbonization, Hydrogen, Nikola Tesla Thermal Power Plant, Renewable Energy Sources

1. INTRODUCTION

The depletion and declining quality of coal reserves, together with the aging of thermal power units in Serbia, pose significant challenges to the long-term sustainability of electricity generation in thermal power plants. Serbia also faces local air pollution in many cities, partly associated with electricity generation in thermal power plants and heat production in small-scale combustion installations. In addition to these local concerns, electricity generation from thermal power plants is not sustainable in the long term because of the contribution of CO_2 emissions to global warming and the resulting exposure of thermal power plants to carbon taxes. At the same time, the electrification of transport and continued industrial development require an increase in electricity generation.

Under these conditions, the global energy sector faces the challenges of decarbonization and the transition to renewable energy sources, with hydrogen and its derivatives emerging as promising options in this transition. The principal challenge associated with integrating renewable energy sources into power systems is power-system balancing, specifically matching RES generation profiles with electricity demand. Because RES generation is intermittent and non-dispatchable, dispatchable generation sources are required to ensure stable power-system operation and a reliable electricity supply. Conversely, the phase-out and shutdown of thermal power plants as part of the decarbonization process reduce the available dispatchable generation capacity, thereby jeopardizing power-system balancing and the energy independence of the power system.

Hydrogen has emerged as a potential solution for storing energy generated from RES through water electrolysis, enabling its subsequent conversion back into electricity in gas turbines or fuel cells, as illustrated in Figure 1. The use of green hydrogen in a power-to-power cycle represents an environmentally acceptable method of energy storage.

Hydrogen is already used across various sectors worldwide to support decarbonization and energy storage. In the energy sector, Denmark uses wind energy to produce green hydrogen as part of the H2RES project. Vienna is testing the use of hydrogen at the Donaustadt combined heat and power plant to reduce CO_2 emissions [2]. In the transport sector, Germany and Japan have developed hydrogen-powered trains, including the Alstom Coradia iLint [3] and the Hydrogen Hybrid Train, while South Korea uses hydrogen-powered buses in urban transport [4]. Hydrogen is also being deployed in the industrial sector. Shell is constructing Europe's largest green hydrogen production facility, while the Norwegian company Yara uses hydrogen to produce ammonia, thereby replacing natural gas in the production process [5]. Dubai has developed a solar-powered hydrogen production facility that enables surplus energy to be stored for subsequent use [6].

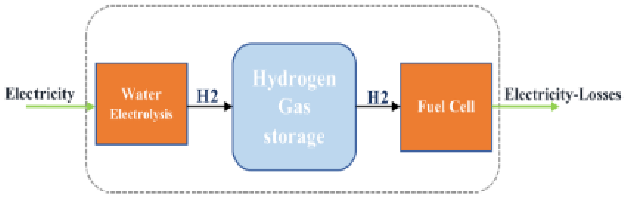

Figure 1. Schematic representation of a hydrogen production, storage, and fuel-cell conversion system, [1]

2. ENERGY CHARACTERISTICS OF HYDROGEN

Hydrogen was identified as a distinct substance by Henry Cavendish in 1766. The term "hydrogen" is derived from Greek words meaning "water-former." Water is the principal product of hydrogen oxidation. Hydrogen is the third most abundant element on the Earth's surface, after oxygen and silicon. Although it is one of the most abundant elements, molecular hydrogen (H_2) is rarely found freely in nature and must instead be extracted from chemical compounds, primarily water, which requires an energy input. For this reason, hydrogen is regarded as an energy carrier and a means of energy storage. Energy must first be supplied to produce hydrogen and can subsequently be recovered through hydrogen combustion or direct electrochemical conversion into electricity in fuel cells. Hydrogen has the highest gravimetric energy density of all conventional fuels: 1 kg of hydrogen contains approximately the same amount of energy as 2.8 kg of gasoline [7].

Its natural abundance, high energy content, and relatively favorable environmental characteristics when used as fuel are among the principal reasons why hydrogen strategies are being developed at both the global and national levels. These strategies examine the potential of hydrogen as a major energy carrier in the energy transition. Nevertheless, hydrogen production, storage, and utilization involve numerous challenges, attracting considerable attention from the scientific community, which has studied hydrogen as an energy carrier for several decades. Reference [8] provides a review and analysis of three decades of hydrogen-energy research, covering the period from 1990 to 2023, with particular emphasis on the development of renewable hydrogen production technologies. The study examines research trends, technological advances, and the interdisciplinary cooperation required to improve the performance of hydrogen systems to a level that would enable their widespread technical and economic viability. These developments could contribute to addressing some of the key challenges associated with sustainable energy systems.

2.1 Hydrogen Energy Density

The energy density of hydrogen is a key factor in its use as an energy carrier, particularly when it is compared with conventional fossil fuels. It can be considered in terms of two principal measures: gravimetric and volumetric energy density.

2.1.1 Gravimetric Energy Density (by Mass). Hydrogen has a high gravimetric energy density of approximately 142 MJ/kg, based on its higher heating value (HHV). This gives hydrogen a significant advantage over fossil fuels, particularly in transport applications such as aircraft and road vehicles, where fuel mass directly affects vehicle performance, including efficiency, acceleration, and range [9].

2.1.2 Volumetric Energy Density (HHV per Unit Volume). In contrast to its high gravimetric energy density, hydrogen has a relatively low volumetric energy density compared with most conventional fossil fuels. Consequently, substantially more storage volume is required to store an equivalent amount of energy. Typical volumetric energy-density values for hydrogen are as follows [9]:

- Under standard atmospheric conditions, gaseous hydrogen has a volumetric energy density of approximately 0.012 MJ/L.
- When hydrogen is compressed to 700 bar, its volumetric energy density reaches approximately 5.6 MJ/L.
- Liquid hydrogen has a volumetric energy density of approximately 10.1 MJ/L.

By comparison, conventional fuels have substantially higher volumetric energy densities: approximately 36.7 MJ/L for kerosene, 34.6 MJ/L for diesel fuel, and 34.2 MJ/L for gasoline [9].

Ammonia (NH_3) is also a potentially valuable hydrogen carrier with a favorable volumetric energy density. At ambient pressure, liquid ammonia has an energy density of approximately 11.5 MJ/L. This value is substantially higher than that of gaseous hydrogen under standard conditions and also exceeds the volumetric energy densities of compressed and liquid hydrogen.

Ammonia is therefore an attractive option for long-term energy storage and transport. The low volumetric energy density of hydrogen, particularly in its gaseous state, requires advanced storage technologies and represents one of the principal challenges to its efficient use as an energy carrier.

2.2 Classification of Hydrogen by Production Pathway

Separating hydrogen from naturally occurring chemical compounds requires an energy input. Hydrogen can be produced through several methods, each of which has a different environmental impact, particularly with respect to greenhouse gas emissions. The hydrogen "color" system is a classification framework used to categorize hydrogen according to its production pathway and the associated greenhouse gas (GHG) emissions. This terminology distinguishes between different types of hydrogen in terms of their environmental impact and sustainability in the context of the global energy transition. Figure 2 illustrates the principal hydrogen categories according to the energy source and production method used. It should be noted that this classification is not standardized. The literature may therefore include additional categories, such as black and brown hydrogen, as well as pink hydrogen, which refers to hydrogen produced using electricity generated by nuclear power plants.

2.2.1 Grey/Black Hydrogen. This category refers to hydrogen produced from fossil fuels without carbon capture. For example, "natural gas without carbon capture, utilization, and storage (CCUS)" and "coal gasification without CCUS" represent production pathways associated with substantial emissions. This is considered hydrogen production from unabated fossil fuels. These methods have a high carbon footprint and represent conventional hydrogen production methods that the energy transition seeks to replace.

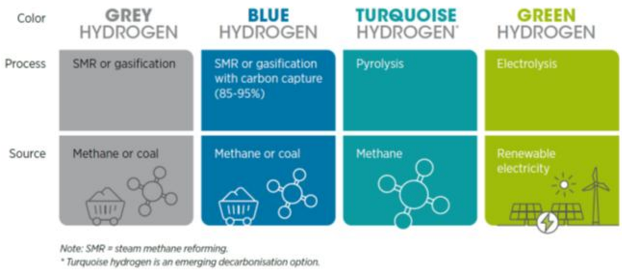

Figure 2. Classification of hydrogen according to the energy source and production method, [10]

2.2.2 Blue Hydrogen. Blue hydrogen is produced from fossil fuels, such as natural gas or coal, in combination with carbon capture, utilization, and storage (CCUS) technology. For example, hydrogen production through steam methane reforming (SMR) with CCUS or coal gasification with CCUS falls within this category. The objective of CCUS is to reduce the carbon footprint of hydrogen produced from fossil fuels. Certification criteria for "low-carbon" or "blue" hydrogen require substantial reductions in greenhouse gas emissions, typically of at least 30% and, in some cases, of 70% or 73%, relative to hydrogen production from unabated fossil fuels. These reduction levels may be used as quantitative thresholds for classifying hydrogen as blue [11].

2.2.3 Turquoise Hydrogen. Turquoise hydrogen is produced using natural gas as a feedstock. The principal production process is methane pyrolysis. Unlike conventional fossil-fuel-based hydrogen production methods, methane pyrolysis does not directly produce CO_2 emissions. Instead, the carbon contained in methane is converted into solid carbon, commonly referred to as carbon black. Solid carbon is substantially easier to store than gaseous CO_2.

2.2.4 Green Hydrogen. Green hydrogen is defined as hydrogen produced through water electrolysis using electricity generated from low-emission sources, particularly renewable energy sources such as photovoltaic power plants and wind power plants. Green hydrogen production therefore represents a pathway with no direct CO_2 emissions, making it the hydrogen category most extensively examined in hydrogen strategies for sustainable energy systems. Although green hydrogen is produced using renewable energy sources, completely eliminating CO_2 emissions is practically impossible because the manufacture of renewable-energy equipment used to generate electricity for hydrogen production also results in CO_2 emissions. No uniform certification standards for green hydrogen have been established. For example, the Indian green hydrogen standard specifies a maximum emissions intensity of 2 kg CO_2-eq/kg H_2, whereas the corresponding threshold in the European Union is 3.4 kg CO_2-eq/kg H_2.

2.2.5 Low-Emissions Hydrogen. In addition to color-based classifications, the International Energy Agency (IEA) frequently uses the broader term low-emissions hydrogen, which generally encompasses both green and blue hydrogen. According to the report cited in [11], low-emissions hydrogen includes hydrogen produced through water electrolysis using electricity from low-emission sources, including renewable or nuclear energy, as well as hydrogen produced from biomass or fossil fuels in combination with CCUS. This term serves as an overarching category that includes both green and blue hydrogen and emphasizes efforts to reduce greenhouse gas emissions associated with hydrogen production.

Uniform standards for classifying low-emissions hydrogen have likewise not been established. For example, the threshold in Brazil is 7 kg CO_2-eq/kg H_2, whereas the corresponding threshold in the United States is 4 kg CO_2-eq/kg H_2 [11].

Green hydrogen is an energy carrier that can be used in many different applications. However, its actual use remains very limited. Present-day hydrogen production is predominantly based on natural gas and coal, which together account for approximately 95% of total production. At present, hydrogen from renewable energy sources is not yet produced on a significant scale. Nevertheless, the subject is receiving considerable attention within the scientific community, both in terms of technological development and the integration of hydrogen systems into future power systems.

3. TECHNOLOGICAL TRENDS IN GREEN HYDROGEN PRODUCTION AND STORAGE

The development of hydrogen production and storage technologies is focused on improving efficiency and reducing process costs, thereby facilitating the wider commercial deployment of hydrogen as a sustainable energy solution. Several hydrogen production methods are currently available, among which water electrolysis is the most promising when electricity from renewable energy sources is used. Modern water electrolysis technologies convert electrical energy into the chemical energy of hydrogen and oxygen through electrochemical water-splitting reactions. In the context of large-scale energy systems and the integration of renewable energy sources, three principal technological platforms are currently used:

1. *Alkaline electrolysis (AEL – Alkaline Electrolysis)*
2. Proton exchange membrane electrolysis (PEM – *Proton Exchange Membrane Electrolysis*)
3. Solid oxide electrolysis (SOEC – *Solid Oxide Electrolysis Cell*)

Each of these technologies has specific technical characteristics, advantages, and limitations, as well as a different technology readiness level (TRL). Because the Nikola Tesla A Thermal Power Plant (TENT A) is a large-scale generation facility, a detailed understanding of the performance, limitations, and dynamic characteristics of PEM electrolysis, which was selected for this conceptual design, is essential [12].

Table I. Comparative characteristics of AEL, PEM, and SOEC technologies, [13]

Parameter	**AEL**	**PEM**	**SOEC**
Operating temperature	70–90°C	50–80°C	700–850°C
Operating pressure	1–30 bar	<30 bar	~1 bar
Efficiency (LHV)	50–68%	50–68%	75–85%
Start-up time to rated output	<50min	<20min	>600min
Technology maturity	High	High	Low
Capital cost	Lowest	High	Highest
Load-following capability	Poor	Excellent	Poor

For applications characterized by substantial power variability and dynamic operation, PEM electrolysis is currently the only technology capable of following the output profile of a photovoltaic (PV) power plant and responding to electricity-price signals. This is primarily due to its rapid response, wide operating range, and ability to operate under variable loading conditions [12].

Hydrogen storage represents a technological barrier to its integration into the global economy. Large-scale storage capacity is required to store energy in quantities measured in GWh and TWh. Geological formations, including salt caverns and depleted oil and gas reservoirs, offer considerable storage potential because of their capacity, safety, and favorable economic and technical characteristics [14]. In addition to underground storage systems, aboveground solutions include high-pressure compressed-hydrogen storage tanks and cryogenic storage tanks for liquid hydrogen. Alternative concepts under development include liquid organic hydrogen carriers (LOHCs), which enable hydrogen to be stored under moderate conditions and allow existing infrastructure to be used [14].

Although physical hydrogen storage methods, including compressed and liquid hydrogen and LOHC systems, are important for short- and medium-term balancing, chemical hydrogen carriers are receiving increasing attention for long-term energy storage. Among these, ammonia (NH_3) is particularly significant. Its high hydrogen storage density, well-developed global logistics infrastructure, and potential for direct combustion in gas turbines make it one of the most promising options for seasonal energy storage and energy conversion in large-scale power plants [15], [16]. For these reasons, ammonia plays an important role in the proposed conceptual design as a key component for seasonal power-system balancing as a means of supplementing the available hydrogen fuel supply.

Ammonia, which contains approximately 18% hydrogen by mass, has an approximately 50% higher hydrogen storage density than compressed or liquid hydrogen, while its energy density is almost three times greater. One of its principal advantages is the existence of well-developed global infrastructure for ammonia production, long-term storage, transport, and distribution [15]. Its main disadvantages are its toxicity, the potential hazards associated with leakage, and the additional capital costs associated with constructing an ammonia production plant. Ammonia has traditionally been produced primarily through the Haber–Bosch process, in which nitrogen and hydrogen react at elevated temperatures and pressures in the presence of a catalyst [16]:

$$N_2 + 3H_2 \rightleftharpoons 2NH_3 + \text{heat} \tag{1}$$

The conventional Haber–Bosch process relies on steam methane reforming (SMR) to produce hydrogen:

$$CH_4 + H_2O \rightarrow CO + 3H_2 \tag{2}$$

The carbon monoxide is subsequently converted into carbon dioxide through the water–gas shift reaction:

$$CO + H_2O \rightarrow CO_2 + H_2 \tag{3}$$

The principal disadvantage of the conventional Haber–Bosch process is its high level of CO_2 emissions, because most ammonia is produced using natural gas. An alternative method of reducing emissions is to produce ammonia from green hydrogen obtained through water electrolysis using surplus electricity from RES. The resulting product, commonly referred to as green ammonia, would be used in the proposed conceptual design [16]. Ammonia may also be synthesized directly through electrochemical processes in which electricity is used to combine nitrogen and hydrogen. This approach could reduce the need for high pressures and temperatures. Electrochemical ammonia synthesis remains at an early research and development stage and has not yet achieved technological maturity. However, it could potentially consume less energy than the conventional Haber–Bosch process [16]. Green ammonia is expected to become more economically viable than fossil-fuel-based alternatives by 2035. The overall energy efficiency of the ammonia production and combustion cycle ranges from approximately 30% to 48%. Ammonia combustion in power plants can achieve an efficiency comparable to that of conventional thermal power processes, indicating its potential as a carbon-free fuel [17].

In addition to compressed and liquid hydrogen, LOHC systems, and ammonia, solid-state hydrogen storage should also be considered. This approach is based on binding hydrogen within solid materials, most commonly metal hydrides such as MgH_2, $LaNi_5H_6$, TiFe-based hydrides, and high-entropy alloys [18]. The principal advantage of these systems is their greater safety, because hydrogen is not stored as a free gas under high pressure but is instead bound within the material structure, thereby reducing the risk of leakage and explosion. Nevertheless, because of the greater mass of storage materials, the need for temperature control, slower kinetics, and higher costs, this technology is not considered in this paper as the primary solution for large-scale seasonal storage. Instead, it is regarded as a promising option for future applications [18].

Hydrogen-capable gas-turbine technologies are becoming increasingly important. Modern gas turbines, including those developed by Siemens Energy and General Electric, can already use hydrogen–natural gas blends, while fully hydrogen-fired gas turbines are under development [19]. Their deployment at thermal power plants such as TENT A could substantially reduce CO_2 emissions while preserving existing power-generation capacity and infrastructure.

Despite considerable technological progress, key challenges remain. These include reducing equipment costs, increasing the efficiency of hydrogen production and storage, and developing infrastructure for hydrogen transport and distribution. These challenges raise important questions concerning the integration of hydrogen into existing thermal power systems, which will be analyzed in the following sections.

4. CONCEPTUAL DESIGN OF THE INTEGRATED ENERGY COMPLEX

The transition to environmentally sustainable energy generation as part of the decarbonization process requires a shift toward renewable energy sources. Since TENT A is an important generation hub within the Serbian power system, a conceptual design involving the construction of a photovoltaic power plant near TENT A is proposed to preserve the existing centralized infrastructure. This development would support the replacement of coal with green hydrogen-based fuel. The initial phase would involve implementing this change in Units A1 and A2, thereby initiating the transition toward environmentally sustainable generation sources. The underlying objective is to replace the electricity generated by these two oldest thermal power units with electricity from a photovoltaic power plant and hydrogen-fired gas-turbine systems, while maintaining the dispatchability of generation and improving overall system flexibility.

The low power density of solar radiation at the Earth's surface requires photovoltaic modules to cover large areas. To minimize adverse environmental effects, such power plants should be constructed on degraded or previously disturbed land. In this context, areas degraded by decades of coal extraction and the disposal of overburden and ash associated with thermal power generation represent suitable locations for photovoltaic installations.

The proposed concept envisages constructing photovoltaic power plants in these degraded areas, particularly within parts of the Kolubara open-pit mining region. Hydrogen and ammonia production and storage facilities would be installed within the existing thermal power complex. Another important advantage for hydrogen production is the already developed water-supply system drawing water from the Sava River. This would reduce costs and enable the existing infrastructure to be used. The new power plant would use gas-turbine systems instead of conventional boiler and steam-turbine systems. These systems would combust hydrogen and ammonia, thereby enabling the preservation of the existing infrastructure, including the power plant's grid connection and switchyard facilities, while also maintaining the existing power flows within the transmission grid.

The photovoltaic power plant would serve two functions. It would directly inject the electricity generated into the 400 kV transmission grid through the existing TENT A grid connection point, specifically the Mladost grid connection switchyard. It would also supply electricity to the hydrogen production system. Hydrogen storage capacity would be designed to balance daily and weekly variations in electricity generation and consumption. A portion of the hydrogen would be used for ammonia synthesis. Because ammonia has more favorable storage characteristics, it would provide a means of long-term energy storage. The proposed concept is illustrated in Figure 3.

4.1 Proposed Construction of a Photovoltaic Power Plant on Degraded Land in the Kolubara Mining Basin

To utilize degraded land, the photovoltaic power plant would be constructed within the Kolubara open-pit mining areas. The use of these locations represents an optimal solution because it would avoid the occupation of land of agricultural or infrastructural value, eliminate land-expropriation costs, and improve the environmental and social acceptability of the project.

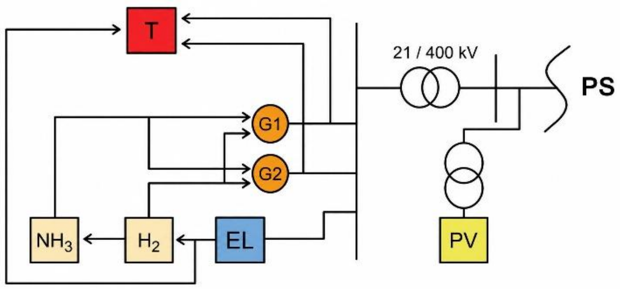

Figure 3. Schematic representation of the operation of the integrated energy complex based on a photovoltaic power plant and green hydrogen-based fuels

The Kolubara mining complex covers several thousand hectares of land that has become infertile or has low agricultural value because of coal extraction and overburden disposal. Considering these circumstances, the infertile land could be used for the construction of large-scale photovoltaic power plants. The proposed concept envisages a phased transition of TENT A to hydrogen-based fuels and a gradual reduction in coal production. During the initial stages, the construction of the photovoltaic power plants would therefore have to be coordinated so as not to interfere with existing and planned coal production. The currently available area, presented in Appendix 1, Figure A.1, is approximately 1,000 ha. This is more than sufficient for constructing the proposed photovoltaic power plant, which would be developed during the proposed phase of the decarbonization of electricity generation in the existing Units A1 and A2. Before construction begins, the terrain would have to be leveled and the area prepared for the installation of the PV modules and their support structures.

The proposed photovoltaic power plant would have a total installed capacity of 500 MWp. The modules would be ground-mounted using fixed, tent-shaped support structures arranged as a dual-pitch roof, with the two planes facing east and west and the module rows extending in a north–south direction. The modules would have a tilt angle of 15° toward the east and west relative to the ground. Calculations performed using the PVGIS tool indicate that a photovoltaic system with an installed capacity of 1 MWp and the proposed module configuration could generate an average of approximately 1,044 MWh annually. Accordingly, the proposed 500 MWp power plant would generate approximately 522 GWh of electricity per year.

This module configuration represents a favorable solution in terms of capital costs, installation requirements, and land-use efficiency. In addition, the temporal generation profile of this configuration is more favorable than that of south-facing modules. The sites of the proposed photovoltaic power plant are approximately 25 km from TENT A. The grid connection could be implemented by constructing a transformer substation and establishing a loop-in/loop-out connection to the existing 400 kV Overhead Transmission Line No. 436. The route of this line is located in the immediate vicinity of the open-pit mines and would directly connect the proposed photovoltaic power plant to the TENT A grid connection switchyard.

4.2 Development of a Green Hydrogen Production and Local Storage System at the TENT A Site

The proposed green hydrogen production technology, with PEM electrolysis assessed as the most suitable option, encompasses several processes integrated into a single system centered on the electrolyzer as the principal component of the facility. These processes may be divided into the following stages:

- water supply;
- electrolyzer;
- hydrogen storage.

4.2.1 Water Supply. TENT A has access to water resources from the Sava River, enabling an efficient and stable water supply for electrolysis. The theoretical specific water consumption of PEM electrolysis is approximately 9 L/kg of hydrogen produced. Under actual operating conditions, however, technological losses and auxiliary processes increase this figure to approximately 11–14 L/kg H_2. PEM electrolyzers require highly purified water with an electrical conductivity below 1 μS/cm to prevent membrane degradation and prolong system service life. To achieve the required water quality, the water first undergoes filtration, followed by reverse osmosis, while final purification is performed through deionization using ion-exchange resins. This multistage treatment produces the ultrapure water required for the uninterrupted operation of PEM cells.

Constructing the electrolysis system near TENT A would provide a significant advantage by allowing the existing infrastructure to be used. In particular, the existing water-filtration system could be upgraded, thereby optimizing both costs and resource use.

4.2.2 PEM Electrolyzer. The PEM electrolyzer (PEMEL) would form the central part of the hydrogen production facility. Its principal advantages are its relatively high energy efficiency at high power density and its pronounced operational flexibility, making it suitable for systems with a high share of renewable energy sources.

For modern industrial PEM electrolyzers, energy efficiency varies with the selected operating point and generally ranges from approximately 50% to 68%, calculated relative to the lower heating value of hydrogen. Increasing the current density increases the electrolyzer's hydrogen production capacity but reduces its efficiency. The selected operating regime therefore represents a compromise between maximizing hydrogen production and maximizing the overall energy efficiency of the system. The operational flexibility of a PEM electrolyzer is reflected in its broad dynamic operating range, extending from approximately 5% to 120% of rated capacity [13]. Owing to its very rapid response, with a response time or ramp rate on the order of seconds, an electrolyzer can adapt to changes in input power without adversely affecting system stability. Its cold-start time is less than 20 minutes, making it suitable for operation under conditions characterized by the pronounced intermittency and non-dispatchability of renewable energy sources.

Because of their favorable dynamic characteristics, electrolyzers may represent a significant centrally controlled demand-side resource capable of providing balancing services through the regulation of active power in the power system.

Hydrogen production under the proposed project would depend directly on electricity-price fluctuations in the market. The electrolyzers would be configured to operate at maximum capacity during periods when the electricity price falls below a predefined threshold, for example, below 25% of the annual average price. During periods when the electricity price ranges between 25% and 150% of the annual average, the electrolyzers would operate at reduced load only when electricity generated by the photovoltaic power plants cannot be delivered to the power system because of potential operational constraints in the transmission grid.

The initial phase of the project envisages the construction of a PEM electrolyzer with an installed capacity of 400 MW. It would partially provide the gaseous fuel required by the combined-cycle power plant intended to replace Units A1 and A2 at TENT A. At this installed capacity, expected hydrogen production would be up to approximately 8,000 kg/h, depending on the selected operating regime and the energy efficiency of the system.

The estimated service life of modern PEM electrolyzers is approximately 60,000–80,000 operating hours. During operation, system performance gradually deteriorates, most commonly through an increase in operating voltage and a decrease in energy efficiency. Typical degradation rates range from 0.5% to 2.5% annually [20]. These parameters substantially affect the project's overall economic viability and must be considered when planning plant operation.

The electrolyzer facility would require an area of approximately 8 ha. Ideally, the facility would be located in the immediate vicinity of the thermal power plant to reduce infrastructure costs and facilitate its integration into the existing energy system. The most suitable solution would involve using part of the existing ash-disposal site. In addition to hydrogen production, the system could subsequently be expanded to include oxygen storage if market demand for larger quantities of oxygen emerges. This could further increase the plant's overall utilization and the project's economic benefits. Appendix 1, Figure A.2, presents an example of the equipment layout for such a facility.

4.2.3 Hydrogen Storage. Hydrogen storage represents a particular challenge. As noted previously, because hydrogen has an exceptionally low volumetric energy density at atmospheric pressure and storage volume must be minimized as far as practicable, it must be stored under high pressure, potentially at pressures of up to 800 bar. Hydrogen, as the element with the lowest atomic mass, tends to permeate materials and cause embrittlement. Hydrogen leakage and material embrittlement therefore represent additional challenges in the construction of storage facilities. Nevertheless, the advantages of this storage method include rapid and straightforward operation and relatively simple infrastructure. Industrial compressors and storage tanks are already commercially available, while leakage-related challenges are expected to be addressed through continued research and rapid technological development.

This analysis assumes that hydrogen storage capacity would be dimensioned according to daily or weekly requirements, while long-term storage would be planned through ammonia production. Hydrogen production and compression release substantial quantities of heat; the integrated energy complex would therefore also include thermal energy storage. Figure 4 presents the proposed site for constructing the integrated energy complex for hydrogen production and storage, together with the infrastructure required for a pit thermal energy storage system. The proposed location is situated on part of the existing ash-disposal site. Before any construction begins, ash disposal at the site would have to cease, the disposal area would have to be stabilized, and sufficient time would have to be allowed for intensive settlement to stop. Considering that certain sections of the ash-disposal site have been closed for many years, areas suitable for the proposed purpose may already be available under the existing conditions. The designated area covers approximately 60 ha and is sufficient to accommodate all infrastructure components of the integrated energy complex. The existing ash-handling pipelines would have to be reorganized to use the remaining disposal cells. The site is particularly suitable for the installation of hydrogen production and storage systems and pit thermal energy storage. Its principal advantages include the following:

- The site is located only approximately 700 m from TENT A. It could therefore form part of the thermal power plant complex, and the electrical, thermal-energy, and road infrastructure required for the operation of all system components could be readily constructed.
- The site is located in the immediate vicinity of the Sava River, enabling the straightforward installation of heat-pump systems for thermal energy storage and water-supply systems for electrolysis.
- The site does not occupy land with agricultural value, and no adverse effects on the surrounding area are expected because it consists of infertile an artificial hill.
- The site is elevated approximately 30 m above the surrounding terrain, protecting it from flooding and from groundwater, the presence of which would be highly unfavorable for the construction of pit thermal energy storage. Consequently, the use of active ash-disposal cells would have to be planned so that they do not interfere with the thermal storage facility.
- Dry ash is an effective thermal insulator and could support efficient heat storage.
- The terrain is suitable for constructing underground hydrogen-storage tanks.
- The TENT A electrolyzer and generation units would be located close to the proposed pit thermal energy storage facility, making the construction of infrastructure for storing waste heat generated by these processes cost-effective and efficient.

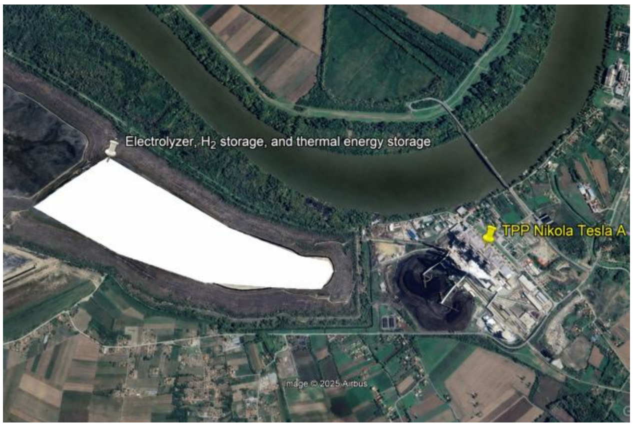

Figure 4. Proposed site for constructing the integrated energy complex for hydrogen production and storage and a pit thermal energy storage system at the TENT A site

4.3 Development of an Ammonia Synthesis and Local Seasonal Storage System

When the hydrogen storage facility is full but conditions remain favorable for continued hydrogen production, the surplus hydrogen would be used to produce ammonia. The ammonia would be stored over the long term and used primarily during winter, when electricity generation from photovoltaic power plants is reduced and market electricity prices are higher. This would enable seasonal balancing of the power system.

Ammonia would be produced by combining hydrogen with nitrogen separated from air using the Haber–Bosch process at temperatures of 400–500°C, pressures of 100–200 bar, and in the presence of an iron-based catalyst, as illustrated in Appendix 1, Figure A.3.

The ammonia synthesis and storage infrastructure would be installed at the hydrogen storage site to ensure the efficient use of space and existing infrastructure. Nitrogen, the second required process component, would be separated from air using a cryogenic air separation unit (ASU), which represents the most suitable solution for producing large quantities of high-purity nitrogen. The ASU system would be supplied continuously with electricity from the grid and would consist of compressor units, heat-exchange systems, and distillation columns for separating gaseous components.

Following preparation, hydrogen and nitrogen would be introduced into the synthesis loop, whose principal components would include compressors, heat exchangers, and ammonia-synthesis reactors. The final product would be liquid ammonia (LNH_3). Waste heat generated during the synthesis process would be partially reused within the process itself, while the remaining heat could be transferred to thermal energy storage, thereby further increasing the overall energy efficiency of the system.

Ammonia storage requires a specialized approach because of its toxicity and its potential to cause steel corrosion. Three principal ammonia storage methods are used in energy facilities: pressurized storage in steel tanks, refrigerated storage at atmospheric pressure and low temperatures, and combined systems operating at moderate temperatures and pressures. For storing large quantities of ammonia, refrigerated storage represents the most favorable option because, in the event of damage to a storage tank, ammonia is released more slowly than from a high-pressure storage system.

One of the significant challenges associated with using ammonia in energy systems is the emission of nitrogen oxides (NO_x), particularly during combustion at the high temperatures and pressures encountered in gas turbines. Selective catalytic reduction (SCR) is the most effective method of reducing NO_x emissions. This process uses catalysts and reducing agents, most commonly ammonia or urea, to convert nitrogen oxides into nitrogen and water vapor. The technology is compatible with modern gas-turbine plants and is already used in thermal power plants. Despite the application of NO_x-emission-control systems, the direct combustion of ammonia in gas turbines remains technologically challenging because of its unfavorable combustion characteristics. It is therefore considered preferable not to use ammonia directly as a fuel, but rather as a hydrogen carrier. Under the proposed concept, green ammonia would be decomposed into hydrogen and nitrogen in a dedicated ammonia-cracking facility, after which the recovered hydrogen would be used in the gas turbines. This approach would reduce NO_x emissions and enable the use of technologically mature gas-turbine solutions, while the direct combustion of ammonia would remain a prospective option for long-term development.

4.4 Construction of Gas-Turbine Power Plants at the Sites of the Existing Thermal Power Units

The existing Units A1 and A2 would be replaced with gas-turbine power plants. Instead of the existing coal-fired boiler systems and steam turbines, gas-turbine units could be installed at the same sites. During the initial development phases, these units would use a blend of natural gas and hydrogen, before gradually transitioning to the combustion of 100% green hydrogen and ammonia once such facilities become technologically mature and economically viable. From a spatial perspective, the new gas-turbine units could use the existing grid connection equipment, including the unit transformers and switchyard equipment. The condition of the generators in these units would have to be assessed; however, the installation of new generating units is recommended.

A gas-turbine system comprises three principal sections: multistage compression with intercooling, a combustion chamber, and an expansion turbine. Fuel-conversion efficiency depends on the turbine operating temperature. Higher temperatures produce greater efficiency and therefore more economical operation. Combustion products in a conventional gas turbine may reach temperatures of approximately 1,260°C. However, critical metal components within the turbine can withstand temperatures of only approximately 815–926°C. Compressor discharge air is therefore used to cool the principal turbine components, which ultimately reduces thermal efficiency. Advances in cooling technologies and high-temperature-resistant materials have enabled modern gas turbines to achieve turbine inlet temperatures of up to 1,427°C, approximately 167°C higher than those of previous turbine generations. A further method of improving efficiency is to install a recuperator or a heat recovery steam generator (HRSG), enabling energy to be recovered from the turbine exhaust gases. A recuperator captures waste heat from the turbine exhaust and uses it to preheat compressor discharge air before it enters the combustion chamber. An HRSG uses the waste heat contained in the gas-turbine exhaust gases to generate steam. These boilers are also known as heat recovery steam generators. The high-pressure steam generated in the HRSG can drive a steam turbine to produce additional electricity, creating a combined-cycle power plant. A simple-cycle gas turbine can achieve an energy-conversion efficiency of approximately 20–35%. Future hydrogen-fired combined-cycle gas turbines are expected to achieve efficiencies of 60% or more. If the waste heat generated by these systems is also used to supply the proposed thermal energy storage facility, the overall efficiency of the energy cycle could reach approximately 80%.

This analysis assumes that gaseous fuel is combusted in the presence of air and argon, which is used as an inert gas to reduce the flame temperature. The principal combustion products are nitrogen (N_2) and water (H_2O). Because the total installed capacity of Units A1 and A2 is approximately 400 MW, a gas-turbine capacity of 400 MW would also be required to use the existing infrastructure and maintain the same electricity injection capacity into the transmission grid. However, because this is an alternative facility, two or three lower-capacity gas-turbine generating units could be installed instead of a single large-capacity unit. This configuration could provide greater operational flexibility, more reliable operation, and easier system maintenance.

4.5 Development of a Waste-Heat Storage System for Heating Purposes

The efficient utilization of waste heat from energy facilities represents an important means of increasing energy efficiency and reducing overall system losses. A substantial quantity of waste heat is generated by the electrolyzer and, to a lesser extent, by the power plant. Gas-turbine power plants operating on a blend of natural gas and hydrogen, or on pure hydrogen, also generate substantial quantities of waste heat during combustion. This energy could be supplied to district-heating systems or industrial processes or stored in thermal energy storage systems for subsequent use.

This analysis proposes the use of pit thermal energy storage systems with water-filled surface reservoirs. Water as a thermal storage medium allows energy to be readily transferred to district-heating systems.

Because TENT A is located near urban areas with an established district-heating system, waste heat from the power plant could be used directly to heat the water stored in the pit thermal energy storage facility. The stored heat could subsequently be used to heat water within the district-heating network. This arrangement would reduce the need to combust additional fuels, thereby lowering greenhouse gas emissions and increasing the overall efficiency of the power plant. A particular advantage of this concept is the planned district-heating pipeline between Belgrade and TENT A, which would allow the thermal energy storage facility to be integrated into the Belgrade district-heating system.

With the introduction of a waste-heat utilization system, the overall efficiency of the gas-turbine power plant could increase from the standard range of 55–60% to more than 80%. This would simultaneously reduce heating costs and improve the economic viability of the energy facilities. Furthermore, using thermal energy storage in industrial or district-heating systems reduces the need for additional energy resources and contributes to the development of sustainable solutions in the energy sector.

5. Simulation of Energy Flows in the Proposed Integrated Energy Complex

To provide a more detailed analysis of the energy performance of the proposed system, energy flows through its principal components were simulated. The simulation provides insight into the distribution and efficiency of energy use, identifies potential losses, and enables the overall energy efficiency of the system to be assessed.

As previously stated, the electrolyzers would operate during periods of low electricity prices. For this analysis, a low-price period was defined as one in which the electricity price falls below 25% of the annual average price. In the graph presented in Appendix 1, Figure A.4, this threshold is indicated by the green line. The gas turbines would operate when the electricity price on the reference exchange exceeds 150% of the annual average price, corresponding to prices above the red line in the graph presented in Figure A.4. Based on this operating strategy and the hourly electricity prices in EUR/MWh recorded on the HUPX electricity exchange during 2024, the annual operating hours and threshold prices for both systems were calculated. The results are presented in Appendix 1, Figure A.4, and Table II.

Table II. Annual Operating Hours of the Electrolyzer and Gas Turbines

Average annual electricity price (HUPX-2024) [eur/MWh]	100.81
PEMel price threshold (H2 production) [eur/MWh]	25.20
Gas-turbine plant electricity price threshold (hydrogen consumption) [eur/MWh]	151.22
PEMel full-capacity operating hours (price below 25%)	785.00
Gas turbine operating hours (price above 150%)	1,058.00

This analysis assumes that a 400 MW electrolyzer would be installed within the integrated energy complex during the initial phase. The hydrogen produced would meet part of the gas turbine's fuel requirements, while the remaining fuel demand would be met by natural gas. With a PEM electrolyzer of this capacity operating according to the proposed strategy, approximately 340 GWh of electricity would be consumed annually, producing approximately 6,140 t of hydrogen. This amount represents slightly less than 50% of the hydrogen required to replace the entire blended fuel supply with pure hydrogen. Energy losses are unavoidable. Losses upstream of the electrolysis process are generally on the order of several percent, most commonly within the range of approximately 5–10% [21]. PEM electrolysis subsequently takes place at an efficiency of approximately 65%, while the remaining energy is converted into waste heat. A portion of this heat could be used to heat water in the thermal energy storage system. Hydrogen would therefore supply approximately half of the energy required to operate the gas turbines, while the remaining energy would be supplied by natural gas. Since the lower heating value (LHV) of natural gas is 13.894 kWh/kg, the required annual natural-gas quantity can be calculated as approximately 15,718 t. The hydrogen mass fraction in the fuel blend is 28%. The calculated fuel quantities, energy contents, and blending ratio are presented in Tables III and IV.

The efficiency of the combined-cycle power plant, comprising both gas and steam turbines, is approximately 60%. Accordingly, the final available electrical energy amounts to approximately 254 GWh.

During their operating cycles, both the gas turbine and the electrolyzer generate losses in the form of waste heat. A portion of this heat, available at a suitable temperature level, could be technically recovered and stored in thermal energy storage systems. Such thermal energy storage is primarily intended for short-term or immediate use because thermal storage systems inevitably experience heat losses. For this preliminary assessment, the technically recoverable waste heat from the PEM electrolyzer is assumed to equal 14–15% of the electricity supplied directly to the electrolyzer stack [22]. The amount of energy available for storage as heat is presented in Table V.

Table III. Required Fuel Quantities and Energy Parameters

Installed gas turbine capacity [MW]	400.00
Installed electrolyzer capacity [MW]	400.00
Specific system energy consumption [kWh/kg-H2]	55.30
Specific electrolyzer energy consumption [kWh/kg-H2]	51.10
Hydrogen energy content – LHV [kWh/kg]	33.33
Methane energy content – LHV [kWh/kg]	13.89
Gas turbine efficiency	40%
Additional energy recovery via the HRSG and steam turbine	20%
Total plant efficiency (combined cycle)	60%
Electrolyzer efficiency	65%
Natural gas required for gas turbines (100% methane) [t]	30,459.19
Hydrogen required for gas turbines (100% hydrogen) [t]	12,697.27
Hydrogen produced (fuel blend) [t]	6,144.81
Natural gas required for gas turbines (fuel blend) [t]	15,718.54

Table IV. Energy Content and Fuel Shares

Energy content of the total hydrogen produced [GWh]	204.81
Natural gas energy content [GWh]	218.39
Energy output from gas turbines [GWh]	253.92
Hydrogen energy share	48%
Natural gas energy share	52%
Hydrogen blending percentage (by mass)	28%

Table V. Waste Heat

Recoverable heat released during electrolysis [GWh\TJ]	47.10	169.56
Recoverable heat released during turbine operation [GWh\TJ]	84.64	304.70
Total energy that can be stored as heat [GWh\TJ]	131.74	474.26

When the complete annual energy cycle is considered from the electrical energy supplied for producing hydrogen as an energy carrier to the electricity subsequently regenerated by the gas turbines, the efficiency of the overall process can be determined. The annual energy flow and cycle efficiency are presented in Table VI. The cycle efficiency including heat recovery refers to a scenario in which part of the waste heat generated by the gas turbine and electrolyzer is recovered through thermal energy storage systems.

Under the stated assumptions, electricity generation by the gas-turbine power plants would occur during periods of very high electricity-market prices. Consequently, each MWh generated by these plants would have a high market value. Table VII presents the estimated gross annual revenue of the analyzed facility.

It should be noted that the estimated gross annual revenue does not include annual maintenance costs, which are currently difficult to assess. Evaluating the economic viability of the proposed project requires data on capital investment in equipment and system construction. Technologies for hydrogen production, storage, and utilization are developing rapidly. However, commercially available solutions remain limited, and their application is not yet widespread. Current research is therefore primarily focused on improving the energy efficiency of these systems and optimizing energy-conversion processes. The comprehensive economic viability of constructing hydrogen-based systems can be assessed more realistically once these technologies achieve a higher level of commercial maturity, with the anticipated reduction in capital costs and improvement in efficiency.

Table VI. Cycle Efficiency

Energy input into the PEMel system (including system losses) [GWh]	339.81
PEMel energy input used for electrolyzer operation [GWh]	314.00
Energy content of the total hydrogen produced [GWh]	204.81
Energy content of the total natural gas required [GWh]	218.39
Energy output from gas turbines [GWh]	253.92
Total energy that can be stored as heat [GWh]	131.74
Cycle efficiency without heat recovery	45%
Cycle efficiency (with short-term heat storage)	69%

Table VII. Gross Annual Revenue

Average electricity price (below 25% of annual average) [eur/ MWh]	0.71
Average electricity price (above 150% of annual average) [eur/ MWh]	254.62
Average gas price [eur/MWh]	45.00
Cost of purchased gas [eur]	9,827,700.59
Cost of electricity purchased for hydrogen production [eur]	242,428.27
Revenue from electricity generated using hydrogen [eur]	64,652,690.40
Gross annual revenue [eur]	54,582,561.54

6. CONCLUSION

This paper analyzed a conceptual design for converting Units A1 and A2 at TENT A from fossil-fuel-based thermal power units to gas-turbine systems using hydrogen as the primary fuel. Technological trends in green hydrogen production and storage were examined, together with the integration of renewable energy sources for the decarbonization of the electric power sector.

One of the principal challenges associated with this transition is the efficiency of converting electricity into hydrogen through electrolysis, as well as the losses incurred during combustion in gas turbines. The efficiency indicators for these processes were analyzed. The results indicate that significant energy losses occur, although the development of new technologies could contribute to the optimization of the overall system.

Particular attention was also given to the storage of hydrogen and its derivatives, including ammonia, as potential solutions for seasonal power-system balancing. The potential use of waste heat for heating purposes was also considered, as this could further improve the energy efficiency of the integrated energy complex.

The proposed design includes constructing a photovoltaic power plant with 500 MWp of installed PV-module capacity within parts of the Kolubara mining basin. The plant would generate approximately 522 GWh of electricity annually. Hydrogen would be produced during periods of low electricity prices on the regional market. Data from the HUPX electricity exchange were used to calculate hydrogen-production costs and the revenue that could be generated through the operation of the gas-turbine power plant. The results indicate that gross annual revenue could exceed EUR 50 million.

Overall, the results indicate that converting coal-fired thermal power plants into hydrogen-fired gas-turbine power plants is technically feasible. However, the process is currently very expensive and requires further investment in research and development to improve the efficiency of the entire energy production, storage, and conversion chain. Nevertheless, the proposed transition could be implemented in stages. During the initial phase, gas-turbine generating units could be constructed to operate on natural gas. As hydrogen technologies develop, hydrogen could then be introduced gradually through blending. The system should therefore be designed and technologically equipped to operate at any hydrogen blending ratio, including operation on 100% hydrogen. This approach would enable the transition to be completed using the same technological platform, contributing to the stability of the power system and the gradual decarbonization of electricity generation within the Serbian power system. In addition, this approach would strengthen Serbia's energy independence because, ultimately, all the electricity required for hydrogen production would be generated by photovoltaic and wind power plants located within Serbia.

The proposed approach would also enable the decarbonization of part of the thermal power sector, making a substantial contribution to addressing poor air quality. It would require only minimal changes to the overall energy concept and the construction of the missing transmission-grid infrastructure. Because it would use an existing energy hub, the proposed approach could substantially reduce the cost of integrating renewable energy sources into the Serbian power system.

REFERENCES

[1] „H2RES – Green Hydrogen Production“ [Internet]. [accessed 28 March 2026]. Available at: https://stateofgreen.com/en/solutions/h2res-green-hydrogen-production/

[2] „Share of green hydrogen in Vienna cogeneration plant reaches 15%“ [Internet]. [accessed 28 March 2026]. Available at: https://balkangreenenergynews.com/share-of-green-hydrogen-in-vienna-cogeneration-plant-reaches-15/

[3] Alstom, „Coradia iLint – World's first hydrogen-powered passenger train“ [Internet]. [accessed 28 March 2026]. Available at: https://www.alstom.com/solutions/rolling-stock/alstom-coradia-ilint-worlds-1st-hydrogen-powered-passenger-train

[4] „Hydrogen Economy Roadmap of Korea“ [Internet]. [accessed 28 March 2026]. Available at: https://h2council.com.au/wp-content/uploads/2022/10/KOR-Hydrogen-Economy-Roadmap-of-Korea_REV-Jan19.pdf

[5] Yara International, „Yara opens renewable hydrogen plant – a major milestone“ [Internet]. [accessed 28 March 2026]. Available at: https://www.yara.com/corporate-releases/yara-opens-renewable-hydrogen-plant-a-major-milestone/

[6] „Dubai's production of green hydrogen generates over 1 GWh of energy…“ [Internet]. [accessed 28 March 2026]. Available at: https://hydrogen-central.com/dubais-production-of-green-hydrogen-generates-over-1-gwh-of-energy-and-reduces-about-450-tonnes-of-co2-emissions/

[7] U.S. Department of Energy, „Hydrogen Fuel Basics“ [Internet]. [accessed 28 March 2026]. Available at: energy.gov/eere/fuelcells/hydrogen-fuel-basics

[8] S. H. Osman, N. S. M. Yatim, O. S. J. Elham, N. Shaari, Z. Zakaria, “Three decades of hydrogen energy research: A bibliometric analysis on the evolution of green hydrogen technologies”, *Sustainable Energy & Fuels*, Vol. 9, pp. 3182, 2025, DOI: 10.1039/d5se00254k.

[9] M. M. Hossain, B. Zahed Siddique, “Hydrogen as an alternative fuel: A comprehensive review of challenges and opportunities in production, storage, and transportation”, *International Journal of Hydrogen Energy*, Vol. 102, pp. 1026–1044, Feb. 2025.

[10] International Renewable Energy Agency, *Green Hydrogen: A Guide to Policy Making*, IRENA, 2020.

[11] *International Energy Agency. Global Hydrogen Review 2024, IEA, Sept. 2024.*

[12] V. A. Martinez Lopez, H. Ziar, J. W. Haverkort, M. Zeman, O. Isabella, “Dynamic operation of water electrolyzers: A review for applications in photovoltaic systems integration”, Renewable and Sustainable Energy Reviews, Vol. 182, Article 113407, 2023, DOI: 10.1016/j.rser.2023.113407.

[13] International Renewable Energy Agency, *Green Hydrogen Cost Reduction*, IRENA, 2020.

[14] Andersson, J., Grönkvist, S., “Large-scale storage of hydrogen”, International Journal of Hydrogen Energy, Vol. 44, No. 23, pp. 11901–11919, 2019, DOI: 10.1016/j.ijhydene.2019.03.063.

[15] M. Aziz, A. T. Wijayanta, A. B. D. Nandiyanto, “Ammonia as Effective Hydrogen Storage: A Review

on Production, Storage and Utilization”, Energies, Vol. 13, No. 12, Article 3062, 2020, DOI: 10.3390/en13123062.

[16] C. Smith, A. K. Hill, L. Torrente-Murciano, “Current and future role of Haber–Bosch ammonia in a carbon-free energy landscape”, Energy & Environmental Science, Vol. 13, pp. 331–344, 2020, DOI: 10.1039/C9EE02873K.

[17] A. Valera-Medina, H. Xiao, M. Owen-Jones, W. I. F. David, P. J. Bowen, “Ammonia for power”, Progress in Energy and Combustion Science, Vol. 69, pp. 63–102, 2018, DOI: 10.1016/j.pecs.2018.07.001.

[18] Hirscher, M., Yartys, V. A., Baricco, M., et al., “Materials for hydrogen-based energy storage – past, recent progress and future outlook”, Journal of Alloys and Compounds, Vol. 827, Article 153548, 2020, DOI: 10.1016/j.jallcom.2019.153548.

[19] Pashchenko, D., “Hydrogen-rich gas as a fuel for the gas turbines: A pathway to lower CO_2 emission”, Renewable and Sustainable Energy Reviews, Vol. 173, Article 113117, 2023, DOI: 10.1016/j.rser.2022.113117.

[20] „Technical targets for proton exchange membrane electrolysis“ [Internet]. [accessed 28 March 2026]. Available at: https://www.energy.gov/eere/fuelcells/technical-targets-proton-exchange-membrane-electrolysis

[21] „Hydrogen electrolysers – bridging the gap between manufacturer claims and real-world performance“ [Internet]. [accessed 28 March 2026]. Available at: https://www.h2cluster.rs/en/hydrogen-electrolysers-bridging-the-gap-between-manufacturer-claims-and-real-world-performance/

[22] E. van der Roest, R. Bol, T. Fens, A. van Wijk, “Utilisation of waste heat from PEM electrolysers”, *International Journal of Hydrogen Energy*, 2023

[23] Siemens Energy, „Hydrogen Solutions“ [Internet]. [accessed 28 March 2026]. Available at: https://www.siemensenergy.com/global/en/home/productsservices/productofferings/hydrogensolutions.html

[24] Pawar, N. D., Heinrichs, H. U., Winkler, C., et al., “Potential of green ammonia production in India”, International Journal of Hydrogen Energy, Vol. 46, No. 52, pp. 27247–27267, 2021, DOI: 10.1016/j.ijhydene.2021.05.180.

APPENDIX 1

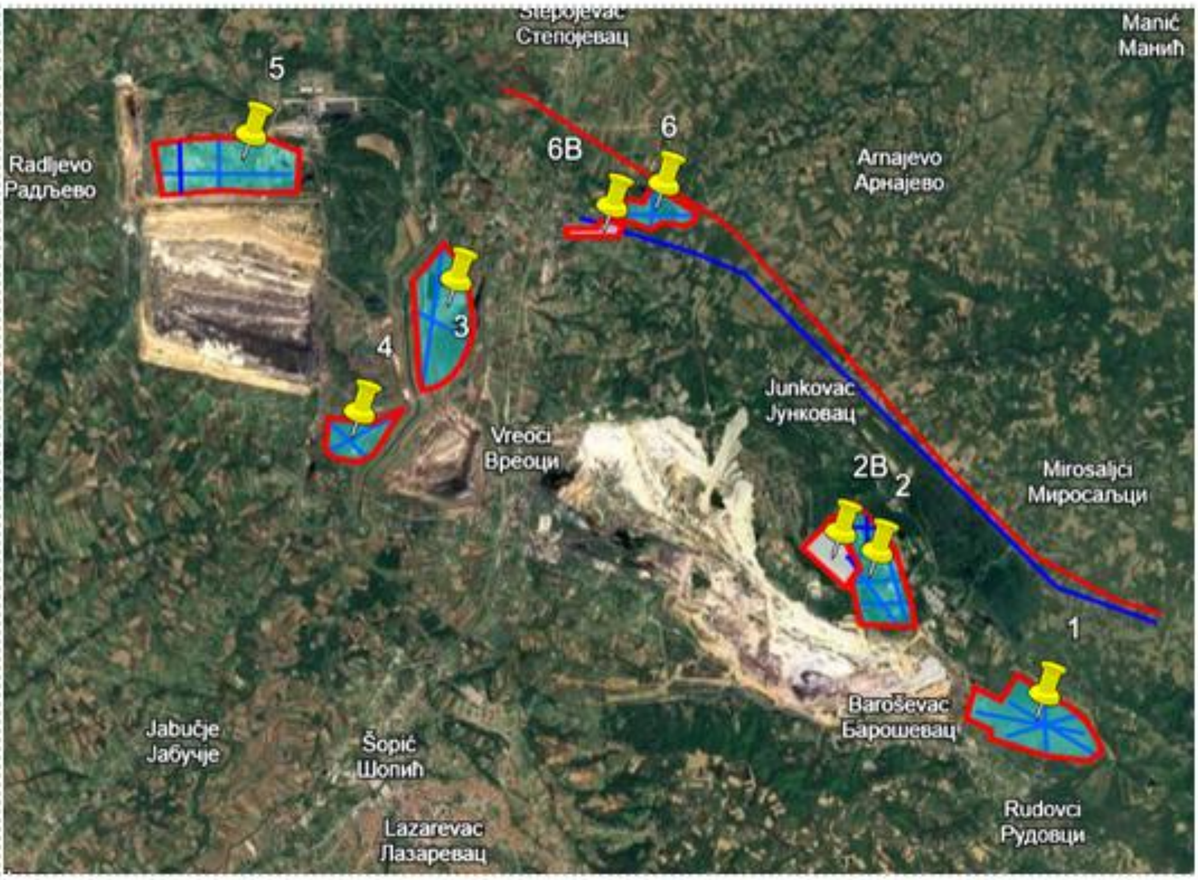

Figure A.1. Currently available areas in the Kolubara mining basin where the construction of a photovoltaic power plant could be planned

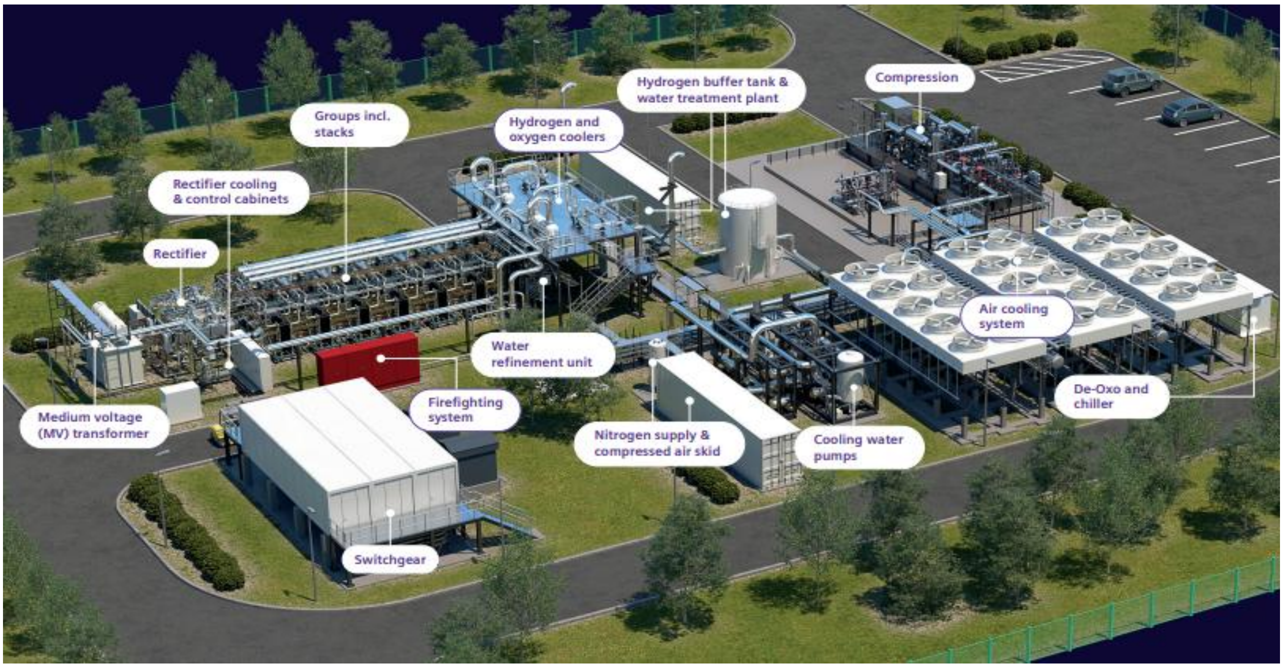

Figure A.2. Equipment layout of the hydrogen production system, [23]

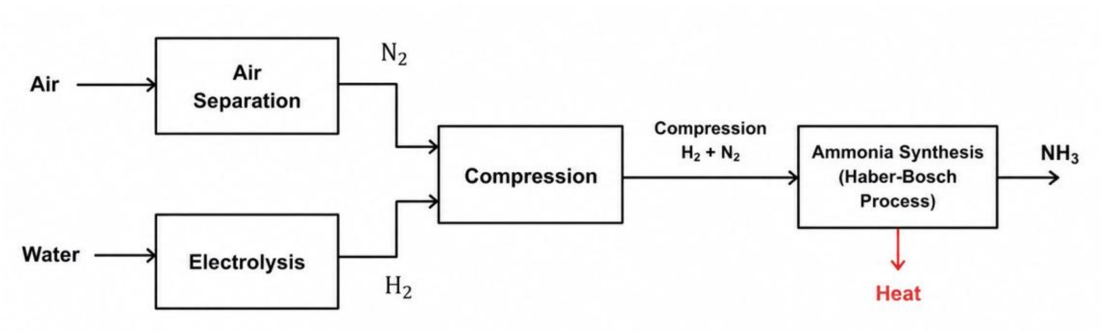

Figure A.3. Conceptual diagram of ammonia production using the Haber–Bosch process, [24]

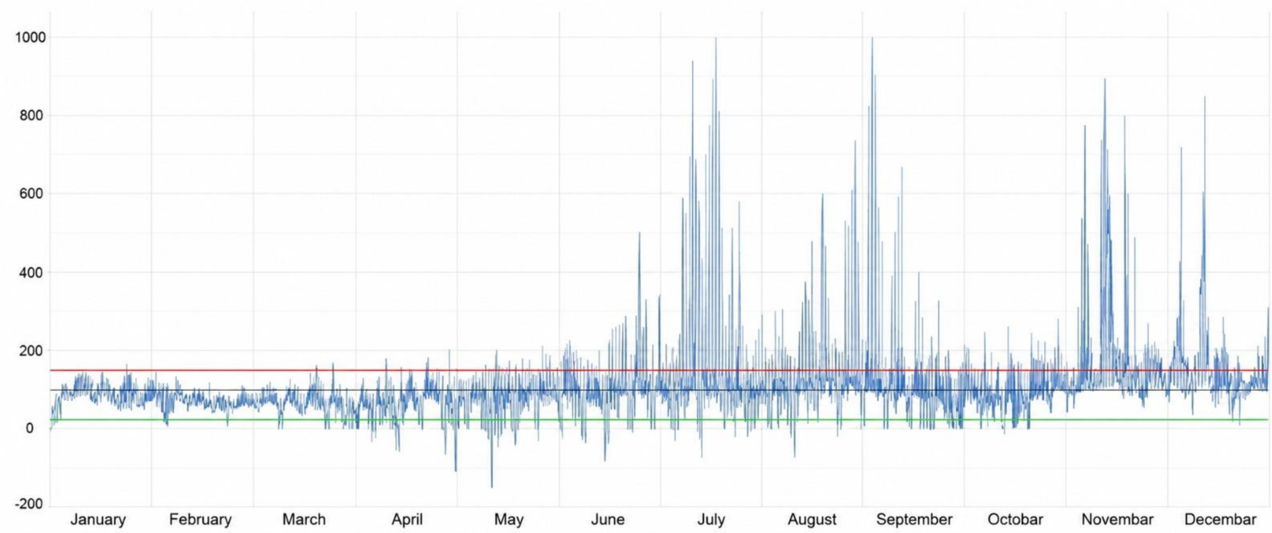

Figure A.4. Electricity prices on the HUPX electricity exchange in 2024, with the threshold values governing electrolyzer and gas-turbine operation indicated

BIOGRAPHIES

Jelica Janićijević was born in Belgrade, Republic of Serbia, in 2003. She completed the seventh and eighth grades of primary school and her secondary education in a specialized mentoring class at the Mathematical Grammar School in Belgrade. She is currently a fourth-year undergraduate student in the Power Engineering program at the University of Belgrade School of Electrical Engineering.

During her primary and secondary education, she participated in and received awards at national physics and mathematics competitions. She was also a member of the Petnica Science Center. During her university studies, she participated in projects involving the design of several power substations. She is the author of a student technical paper presented at the CIGRE Serbia 2025 Conference, where it received the award for the most outstanding student paper. She is also the author of a paper presented at the CIRED Montenegro 2026 Conference, which was likewise recognized as the most outstanding paper in its session. She received the Gordana Jokić Kašiković and Dragiša Kašiković Foundation Award for the best student paper of 2025. She is a recipient of a scholarship awarded by the Ministry of Education of the Republic of Serbia to gifted students. In recognition of her high academic achievement, she was also awarded a scholarship by Elektromreža Srbije. For her exceptional academic performance, she was also recognized as the best student in the Power Engineering program in both her third and fourth years of study.

ORCID: 0009-0002-6205-5587

Danilo Vlahović was born in Vršac, Republic of Serbia, in 2003. He completed his primary education at Jovan Sterija Popović Primary School as the highest-achieving student of his graduating class. He subsequently attended Borislav Petrov Braca Grammar School in Vršac. He is currently a fourth-year undergraduate student in the Power Engineering program at the University of Belgrade School of Electrical Engineering.

He is a recipient of a scholarship awarded by the Ministry of Education of the Republic of Serbia to exceptionally gifted pupils and students, a scholarship awarded by Elektromreža Srbije, and a scholarship from the Studenica Foundation. Throughout his education, he achieved notable results in national mathematics and physics competitions, including first prize at the national physics competition and qualification for the Serbian Physics Olympiad. He also participated in the international FYKOS team physics competition.

As part of his project activities, he completed a project entitled “Acoustic Levitator,” which was awarded second place at the national competition. He also authored a student paper presented at the CIGRE Serbia 2025 Conference, where it received the award for the most outstanding student paper. This paper also received the Gordana Jokić Kašiković and Dragiša Kašiković Foundation Award for the best student paper of 2025. He is also the author of a paper presented at the CIRED Montenegro 2026 Conference, which was recognized as the most outstanding paper in its session. His principal research interests include renewable energy sources, hydrogen, power systems, the energy transition, and energy storage.

ORCID: 0009-0007-9784-9084

Aleksandar Latinović was born in Bihać, Bosnia and Herzegovina, in 1986. He completed primary school in Lazarevo, a village near Zrenjanin, and subsequently graduated from Zrenjanin Grammar School. He completed his undergraduate and master’s studies at the University of Belgrade School of Electrical Engineering, Department of Power Engineering. From 2010 to 2025, he was employed by EPS AD, where his work included ancillary services, system software used to manage power-generation and maintenance processes, SCADA systems, and the development and construction of renewable energy projects. He is a member of the CIGRE C2 Study Committee. He also served on several working groups of the Ministry of Mining and Energy responsible for drafting and harmonizing technical regulations and legislation aimed at integrating renewable energy sources into the power system of the Republic of Serbia. Since 2025, he has worked as an independent consultant specializing in the technical aspects of power system balancing.

ORCID: 0009-0000-0194-4618

Željko R. Đurišić was born in the village of Babino, Berane, Montenegro, in 1972. He completed primary school in his native village and secondary electrical engineering school in Berane. He completed his undergraduate, master’s, and doctoral studies in the Power Systems program at the University of Belgrade School of Electrical Engineering.
He has been employed at the University of Belgrade School of Electrical Engineering since 2001, where he progressed through all academic and teaching ranks, and since 2023, he has held the rank of Full Professor. He is Head of the Laboratory for Power Plants. His research is primarily focused on the planning, integration, and operation of renewable energy sources in power systems. He is the co-author of four textbooks and approximately 300 scientific and professional papers, 40 of which have been published in international SCI-indexed journals. He has supervised seven doctoral dissertations and approximately 300 undergraduate and master’s theses at the Schools of Electrical Engineering in Belgrade and East Sarajevo.

ORCID: 0000-0003-2048-0606

UDK: 621.311:502.131.1(497.11)

Jelica Janićijević[1], Danilo Vlahović[1], Aleksandar Latinović[1], Željko Đurišić[1]

Idejno rešenje supstitucije uglja kao goriva u blokovima A1 i A2 TE „Nikola Tesla” primenom vodoničnih tehnologija sa obnovljivim izvorima energije

[1] Univerzitet u Beogradu – Elektrotehnički fakultet, Beograd, Srbija*

Originalni naučno-istraživački rad

Ključne poruke

- Analizirani su ključni tehnološki principi, ograničenja i prednosti savremenih metoda proizvodnje zelenog vodonika, sa fokusom na elektrolizu
- Sagledani su izazovi i rešenja u skladištenju vodonika
- Prikazani su tehnološki trendovi koji ubrzavaju primenu vodonika u energetskim sistemima: rast kapaciteta elektrolizera, pad troškova i unapređena integracija sa OIE
- Rad ističe značaj optimizacije infrastrukture i razvoja isplativih rešenja kao preduslova za širu upotrebu vodonika u procesu dekarbonizacije

Kratak sadržaj

Integracija obnovljivih izvora energije (OIE) u elektroenergetske sisteme (EES) predstavlja izazov zbog njihovog varijabilnog i neupravljivog karaktera, što otežava bilansiranje proizvodnje i potrošnje. Stabilan rad EES-a zahteva upravljive izvore energije. S druge strane, potiskivanje i gašenje termoelektrana u procesu dekarbonizacije, koja su predviđena integrisanim nacionalnim i klimatskim planom, smanjuje raspoloživu upravljivu energiju što ugrožava uslove bilansiranja i energetske nezavisnosti EES-a. Jedno od rešenja jeste korišćenje viškova energije iz OIE za proizvodnju vodonika i njegovih derivata, koji se mogu skladištiti i koristiti u gasnim elektranama kao upravljiv izvor energije.

U ovom radu analizirani su uslovi formiranja energetskog kompleksa za proizvodnju, skladištenje i upotrebu vodonika na lokaciji postojeće TE „Nikola Tesla A”. Osnovna ideja je da se elektrana u budućnosti ne ugasi, već da pređe sa lignita na obnovljivo gorivo, zamenom konvencionalnih kotlova i parnih turbina gasnoturbinskim postrojenjima prilagođenim sagorevanju vodonika. Na taj način zadržava se ključna infrastruktura, naročito priključno razvodno postrojenje i razvijena interkonektivna veza ovog važnog generatorskog čvorišta.

Analiziran je i potencijal proizvodnje vodonika iz fotonaponskih elektrana koje bi bile izgrađene na prostoru nekadašnjih Kolubarskih kopova. Prikazano je idejno rešenje tehnološke šeme procesa proizvodnje, kompresije, skladištenja i upotrebe vodonika, uz proračun energetske efikasnosti kompletnog sistema. Na osnovu dostupnih podataka izvršena je preliminarna procena očekivane cene proizvedene električne energije.

Napomena:

Ovaj članak predstavlja proširenu, unapređenu i dodatno recenziranu verziju studentskog rada „*Idejno rešenje dekarbonizacije proizvodnje električne energije u TE 'Nikola Tesla' primenom vodoničnih tehnologija sa obnovljivim izvorima*” (https://doi.ub.kg.ac.rs/doi/cigre37-c3-1/), nagrađenog u Studijskom komitetu STK-C3 *Održivost EES-a i performanse zaštite životne sredine,* na 37. Savetovanju CIGRE Srbija, Zlatibor, 26-30. maja 2025.

Primljeno: 7. januar 2026. Recenzirano: 1. juli 2026.
Izmenjeno: 10. juli 2026. Odobreno: 13. juli 2026.
* Korespondirajući autor: Jelica Janićijević, +381 61/81-51-629
Imejl: jelicajanicijevic616@gmail.com

Koncept podrazumeva da se u periodima niskih tržišnih cena električne energije energija iz fotonaponskih postrojenja ili prenosne mreže usmerava na elektrolizu, dok se proizvedeni vodonik skladišti i koristi u periodima visoke potrošnje i nedostatka energije iz raspoloživih primarnih izvora u sistemu. Dodatno, toplota dobijena tokom elektrolize i sagorevanja vodonika može se koristiti za skladištenje i snabdevanje toplotnog konzuma, čime se povećava ukupna efikasnost sistema.

Ključne reči

Dekarbonizacija, obnovljivi izvori energije, TE „Nikola Tesla", vodonik

UDC: 621.314.63:621.357.1
621.314.63:661.96

Nikola D. Kovačević[1], Sava M. Dobričić[1]

Powering Alkaline Electrolyzers with Twelve-Pulse Rectifiers without an Interphase Transformer

[1] Nikola Tesla Institute, Belgrade, Serbia*

Professional article

Highlights

- Twelve-pulse rectifiers without an interphase transformer have been successfully implemented for electrolyzer power supply and hydrogen
- The paper details the implementation method for the electrolyzer power supply, providing a display of measured electrical quantities during the commissioning of the new system
- The selected rectifier topology described in this work is not widely known, which represents an additional contribution and value to the paper
- The realization of this type of power supply for alkaline electrolyzers represents a unique step forward for the domestic industry in hydrogen production, which is considered the fuel of the future

Abstract

The paper presents the realization of a twelve-pulse rectifier without an interphase transformer, supplied via a transformer with two secondaries of different voltage amplitudes, intended for powering a hydrogen production electrolyzer with an output power of 40 kW. An analysis of the converter topology, theoretical considerations, and practical measurements during the commissioning of the device are provided. The chosen solution is compared with other currently popular solutions from the aspects of reliability, immunity to grid disturbances, and efficiency. Viewing hydrogen as a significant energy source of the future, its production is predicted to become widespread in our country in the coming years. Therefore, the possibility for a wide application of converters and electrolyzers is discussed here, as well as the concepts of hydrogen application in the electrical power system.

Keywords

Electrolysis, Green energy, Hydrogen production, Special converters, Twelve-pulse rectifier

Notes:

The full text of this article is available only in the Serbian language.
In the English version, only its Abstract (above) is available.

This article represents an expanded, improved and additionally peer-reviewed version of the paper "*Implementation of a Twelve-Pulse Rectifier Without an Interphase Transformer for Supplying Hydrogen Generating Electrolyzer*" (https://doi.ub.kg.ac.rs/doi/cigre37-b4-12/), awarded in the Expert Committee EC-B4 *HVDC and Power Electronics*, at the 37th CIGRE Serbia Conference, Zlatibor, 26-30 May 2025.

Received: February 11th, 2026 Reviewed: June 9th, 2026
Modified: July 19th, 2026 Accepted: July 21st, 2026

* Corresponding author: Nikola Kovacevic , +381/64-82-43-858
E - mail: nikola.kovacevic@ieent.org

UDC: 621.314.24

Miroslav Popovic[1], Aleksandar Milic[1], Nikola Mirkovic[2]

Loss Modeling of GaN Transistors Using Datasheet Data

[1] University of Belgrade – School of Electrical Engineering, Belgrade, Serbia*
[2] University of Belgrade – Institute Nikola Tesla, Belgrade, Serbia

Original scientific research article

Highlights

- Development of a loss-estimation algorithm for GaN power transistors
- Comparison of hard, soft, and semi-soft switching processes, with separation of channel current and parasitic capacitance contributions
- Validation of the model through a 1 kW synchronous buck converter prototype

Abstract

Transistors based on modern wide-bandgap semiconductors, such as Gallium Nitride (GaN), are increasingly used in power electronics devices. Due to their specific structure and ability to rapidly switch states, standard calculations used for determining losses in silicon transistors are not applicable in this case. Therefore, an analytical model has been developed to estimate losses in GaN transistors in a half-bridge configuration, relying on data from technical documentation. The model considers different types of switching, including hard, soft, and semi-soft switching. A comparison of losses during soft and hard switching of transistors in a synchronous buck converter under the same operating conditions has been conducted. Finally, the proposed model has been verified through the design of a 1 kW buck converter.

Keywords

GaN transistors, loss model, synchronous buck converter

Received: December 16th, 2025 Reviewed: July 3rd, 2026
Modified: July 8th, 2026 Accepted: July 22nd, 2026
* Corresponding author: Miroslav Popovic
E - mail: miroslav@etf.bg.ac.rs

Note:
This article represents an expanded, improved and additionally peer-reviewed version of the student paper "*Analytical Loss Model of GaN Transistors Based on Datasheet Data*" (https://doi.ub.kg.ac.rs/doi/cigre37-b4-05/), awarded in the Expert Committee EC-B4 *HVDC and Power Electronics*, at the 37th CIGRE Serbia Conference, Zlatibor, 26-30 May 2025.

1. INTRODUCTION

Decades of progress in development of power electronics devices have resulted in almost full exploitation of the potential of power transistors based on silicon (Si) technology. Therefore, further development of converters that rely on this type of semiconductors has become much more complex. However, development of transistors using wide band gap semiconductors, such as gallium nitride (GaN) and silicon carbide (SiC), has paved the way for the design of new topologies, as well as reaching higher efficiency and smaller converter dimensions [1]. As shown in Figure 1, GaN semiconductors, compared to Si and SiC, are characterized by higher electronic mobility, higher maximum electron velocity, and a larger breakdown field, [1].

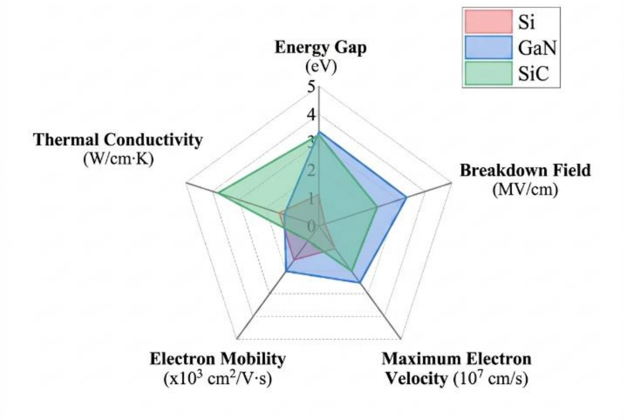

Figure 1. A comparative analysis of semiconductors technology, [1]

Considering that the GaN material has a significantly wider band gap and breakdown field compared to silicon semiconductors, it is possible to design a shorter conducting channel within a transistor for the same breakdown voltage value. A shorter conduction channel, coupled with a higher packing density of GaN transistor, results in lower conducting channel resistance and reduced parasitic capacitances. These properties provide lower power losses during switching on and off processes, which enables significantly higher switching frequencies to be achieved, [2].

To exploit the full potential of GaN transistors, it is necessary to create a reliable physical model that describes the switching process, in order to determine the total power losses and the maximum switching frequency. The switching models developed so far for Si transistors are not applicable to GaN devices, since the chemical and physical structure of these transistors is different, [2], [3]. The switching processes of GaN and Si transistors, although similar at first glance, differ considerably. Gallium nitride technology allows for a higher switching rate, whereby the influence of nonlinear parasitic capacitances becomes significant and cannot be disregarded. In addition, the conduction principles and the establishment of the conduction channel differ compared to silicon transistors. In [4], a piecewise linear model of losses is shown. This approach provides quick and easy estimation of losses but does not take into account the nonlinear dependence of parasitic capacitances on the corresponding voltages, which leads to significant errors in the estimation of switching losses in the band of several hundred kilohertz. A more detailed model of losses is presented in [5] and takes into account the nonlinear dependence of parasitic capacitances but disregards the nonlinear transconductance dependence of GaN power transistors. Considering these limitations, in this paper, an analytical switching model of GaN transistors has been developed, which at the same time takes into account the nonlinear dependencies of parasitic capacitances and transconductances, and enables precise determination of the total power losses on the transistor compared to currently available solutions in literature. The developed model is based on non-approximate data from the manufacturer's technical documents and takes into account the physical structure of the transistor.

Chapter 2 describes the model of GaN transistor and the physical dependencies between the modeled elements. During modeling, for a more precise determination of losses, the total current of the transistor was grouped into two contributions – the current of the conductive channel and the current of parasitic capacitances. Namely, during switching, not all current flows only through the conduction channel of the power transistor. A significant portion of the current, especially in the transition phases, goes to charging and discharging of the parasitic capacitance of the device, which directly affects the dynamic behavior of the transistor and affects the overall switching losses. Therefore, this classification, in addition to taking into account the nonlinear capacitances and transconductance of GaN power transistors, is crucial for realistic modeling and accurate estimation of power losses during a transistor operation. Also, switching on and off of switches is divided into phases and is described in detail for transistors in a half-bridge configuration. For the selected transistor in Chapter 3, there is an extraction of relevant data from the datasheet and an algorithm for estimating losses is given. Finally, the experimental results, confirming the reliability of the model, are given in Chapter 4.

2. MODEL OF THE TRANSISTOR AND SWITCHING PROCESS

Power transistors based on GaN technology, although their structure resembles the Si MOSFET (*Metal Oxide Semiconductor Field Effect Transistor*) devices, have certain characteristics that significantly affect their switching behavior. This chapter describes in detail the electrical model of GaN transistors with an emphasis on key differences compared to classic silicon MOSFET transistors. For the purpose of analytical modeling and calculation of transistor power losses, theoretical and analytical switching processes are described in detail in case of switching the transistors on and off in a half-bridge configuration. As a result, a system of differential equations is obtained, with which it is possible to determine the time forms of channel current $I_{ch}(t)$ and channel voltage $v_{ds}(t)$ required to calculate losses during the process of switching the transistors on and off. The GaN transistor model is shown in Figure 2 and largely corresponds to the Si MOSFET transistor model.

The main difference is the absence of a built-in diode for conducting current in the opposite direction. Due to their symmetrical structure, when conducting current in the opposite direction, the drain and source electrodes change their role. The drain electrode potential is now lower than the gate potential, so now the voltage v_{gd} dictates the conductivity of the channel and allows the transistor to conduct current. Further in the paper, this conduction mechanism will be called the inverse conduction of GaN transistors.

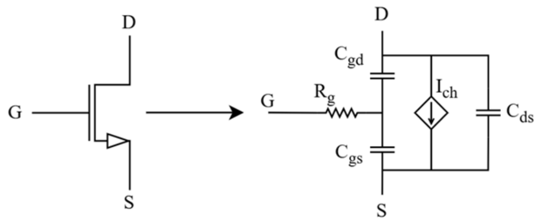

Figure 2. GaN transistor model

2.1 Switching process of power transistors in half-bridge configuration

Two transistors in a half-bridge configuration represent a universal switching cell in modern power converters, [1]. Although this configuration is not present in virtually every topology, most practical power converter architectures can be decomposed into cells in a half-bridge configuration or into some of their extended variants, [6]. In this subchapter, the switching process of two GaN transistors in a half-bridge configuration will be presented and explained in detail. Based on the derived model, an algorithm for estimating transistor power losses will be designed in Chapter 3.

Transistor switching in a half-bridge configuration is the process of changing current path from one transistor to another. To prevent a shoot-through between the upper and lower transistors in the half-bridge, the concept of dead time is introduced. This is the short time interval between the moment when one transistor is switched off and the moment the other transistor is switched on. Dead time ensures that the first transistor is completely switched off before a signal is sent to switch on the second transistor, effectively preventing the current conduction through both transistors at the same time. The switching process in the half-bridge configuration is conditioned by the operating mode of the inverter, that is, the direction of current through the transistor to be switched off. Two different types of switching can be distinguished, where the main difference between them is reflected in the direction of the current through the transistor channel I_L at the time of switching, as shown in Figure 3.

Switching type I is shown in Figure 3a and indicates that the current was present prior to switching, in the direction from the drain to the transistor source. Figure 3a shows an example of turning-off the upper switch in the half-bridge. After the conductive transistor is switched off, the current passes to the opposite transistor in the half-bridge. This type of switching off is known in literature as hard switching. Since the current cannot be switched instantaneously, in parallel with the described process, the opposite transistor marked with number 2 in Figure 3 takes over the current through its parasitic capacitance, since the direction of the current allows it. After the parasitic capacitance C_{ds} is completely discharged, transistor 2 conducts current by an inverse conduction mechanism, and this process continues until the rest of the dead time expires. When the dead time expires, this transistor can be switched on under zero-voltage conditions. This phenomenon is called soft switching, since the flow of the load current has naturally discharged the parasitic capacitance C_{ds}, [1]. We conclude that the switching type I is determined by the direction of the current from the drain to the transistor source and is characterized by a sequence of hard switching off – soft switching on.

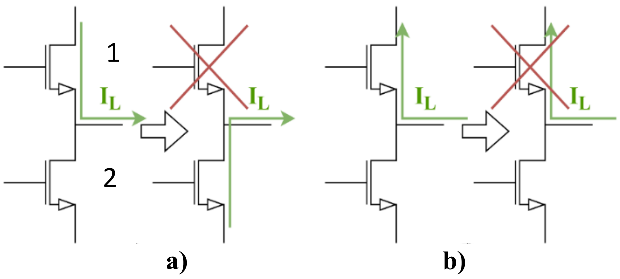

Figure 3. Types of switching for different current directions: a) "positive" current direction; b) "inverse" current direction

Switching type II (Figure 3b) indicates that the current through the semiconductor device has a direction from the source to the drain, whereby the current after the switching off continues to pass through the same transistor with the inverse conduction of the GaN transistor. This type of transistor switching off is known in literature as soft switching. Only the transition from a regular conduction mechanism to an inverse conduction mechanism is considered to be a lossless or soft process, but nevertheless conduction losses increase due to voltage increase v_{sd}. In this case, the capacitance C_{ds} of the second transistor is not discharged during dead time because there is no necessary current to make this possible, as in the first case. Switching on of the transistor that follows after the remaining dead time has elapsed is called hard switching on. We conclude that the switching type II is determined by the direction of the current from the source to the drain of the transistor and is characterized by a sequence of soft switching off – hard switching on.

Both types of switching process are given for the example of switching off the upper transistor – switching on the lower transistor in the half-bridge, but the same conclusions may be made for the opposite sequence without losing generality, by following the direction of the current through the conductive transistor.

For both cases, the GaN model shown in Figure 2 is considered. During the switching process, the transistor operates in ohmic mode. In this mode, the conduction channel can be modeled as a controlled current source I_{ch}, where the peak value of the current I_{ch} is related to the voltage v_{gs} via transconductance g_m. In all the described switching processes, it is assumed that the output current of the half-bridge I_L does not change and remains constant for the duration of the switching process. The following sections will describe in detail both the switching on and switching off processes of the power transistor.

2.2 Transistor switching off

Switching off process of the GaN transistor is described separately for switching types I and II. Each of these switching off processes is separated into specific stages to provide an accurate analysis of transistor behavior and transient losses. In this way, it is possible to understand the dynamics of the device and later optimize the control signals to achieve maximum efficiency.

2.2.1 Switching type I – hard switching off

As explained in Section 2.1, transistor switching off during the switching type I means that the switching current I_L is taken by the second transistor in the half-bridge. This case is divided into three phases as shown in Figure 4. This type of switching occurs when the current I_L is positive, that is, it has a direction from the drain to the source of the conductive transistor.

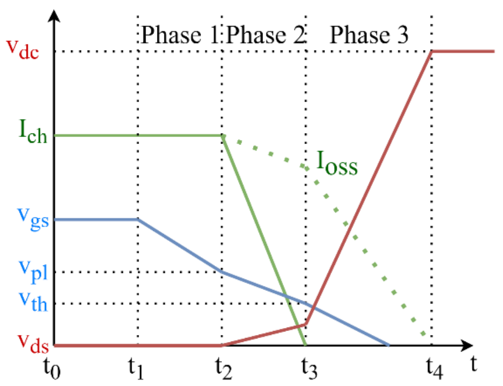

Figure 4. Switching type I – hard switching off

During phase I, the driver received a switching off command and began to reduce the voltage v_{gs}. Voltage v_{gs} changes its value according to the following law:

$$v_{gs} = v_{dr\_on} \cdot e^{-\frac{t}{R_e C_{gs}}}, \quad (1)$$

where v_{dr_on} is the switching on voltage of the transistor provided by the driver, and R_e the total resistance of the gate loop circuit and is the sum of the self-resistance of the transistor gate, the external resistor of the driver circuit, and the driver output resistance.

During this phase, a constant current $I_{ch} = I_L$ passes through the conduction channel of the transistor. The transistor is saturated all the time during phase I, so the current of the channel does not depend on the voltage v_{gs}. At the time when the voltage v_{gs} is equal to the Miller plateau voltage v_{pl}, where the v_{pl} voltage corresponds to the current I_L at the transfer characteristic of the transistor shown in Figure 5, phase I ends. At that time, the transistor exits the saturated operating mode and begins to operate in the ohmic region where the channel current I_{ch} is directly proportional to the gate voltage, v_{gs}.

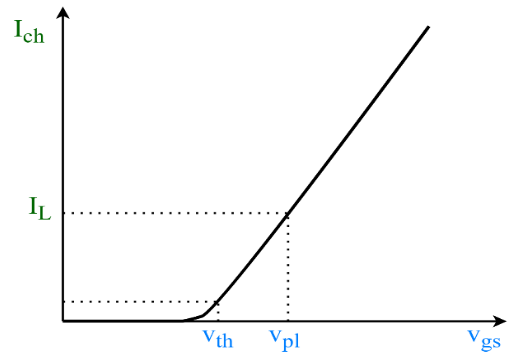

Figure 5. Current-voltage characteristic of GaN transistor

During phase II, the voltage v_{gs} continues to drop but its drop is slowed down because the driver at this point begins to charge the parasitic capacitance, as shown in Figure 6.

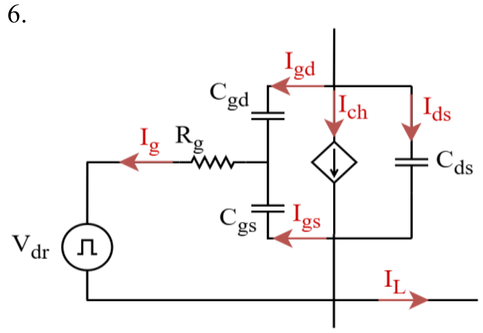

Figure 6. Current directions in GaN transistor model during phase II

The differential equation describing the change v_{gs} is given by (2), [7]:

$$\frac{dv_{gs}}{dt} = \frac{I_g}{C_{gd}+C_{gs}} - \frac{C_{gd}}{C_{gd}+C_{ds}} \cdot \frac{(I_L - I_{ch})}{2} \cdot \frac{1}{(C_{gd}+C_{gs})}, \quad (2)$$

while the current of the channel I_{ch} changes non-linearly with the change of v_{gs}, according to the transfer characteristic shown in Figure 5. It is important to note that all parasitic capacitances of transistors, such as C_{gs}, C_{gd} and C_{ds}, are not constant, but represent nonlinear functions of the corresponding voltages. Therefore, for an accurate analysis at any time, it is necessary to know the actual values of voltages v_{gs}, v_{ds} and v_{gd} to accurately determine the values of these capacitances. Since the value of v_{gs} is known at any time, it is necessary to determine both v_{ds} and v_{gd}. The voltage $v_{ds}(t)$ can be determined by solving the following differential equation, [1]:

$$\frac{dv_{ds}}{dt} = \frac{I_L - I_{ch}}{C_{oss1}+C_{oss2}}, \quad (3)$$

where both C_{oss1} and C_{oss2} are the output capacitances of the transistor and represent the sum of C_{ds} and C_{gd}. Voltage v_{gd} is obtained as the difference of the voltage v_{gs} and v_{ds}.

Phase II lasts until the channel current I_{ch} drops to zero, more precisely until the voltage v_{gs} reaches the conduction threshold voltage v_{th}.

During phase III, the conduction channel of the transistor is closed, but the total current through the transistor is non-zero until the parasitic capacitances C_{ds} and C_{gd} are loaded. The equations given for phase II are still valid for phase III with the fact that now $I_{ch} = 0$.

2.2.2 Switching type II – soft switching off

During the switching type II (Figure 3b), the active transistor switches off, but all current continues to flow through it due to the process of inverse conduction of the GaN transistor. This process represents the transition of the transistor from saturated mode to inverse conduction mode, is shown in Figure 7 and is divided into two phases.

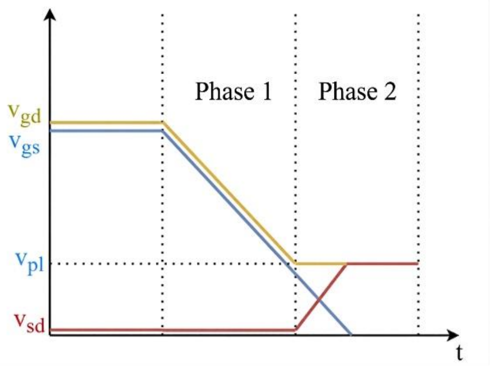

Figure 7. Switching type II – soft switching off

This type of switching can occur only if the current I_L is negative, that is, if the current direction is from the source to the drain of the conductive transistor (Figure 3b). In this type of switching, the voltage v_{sd} does not rise to the voltage v_{dc} but to the voltage of the inverse conduction of the GaN transistor. For low-power devices, this voltage is several volts.

Phase I is identical to the first switching type, and its phase I described in Subchapter 2.2.1, so that the voltage v_{gs} varies according to the law described in equation (1). The voltage v_{gd} during this phase is equal to the sum of the voltage v_{gs} and v_{sd}. The voltage drop across the conduction channel v_{sd} during this phase is constant and is equal to the product of the resistance of the conduction channel R_{ds_on} and the channel current I_{ch}.

Phase II begins when the voltage v_{gd} reaches the Miller plateau v_{pl}, that is, the voltage corresponding to the current I_L at the transfer characteristic given in Figure 3. After that time, the voltage v_{gd} remains constant. The voltage v_{gs} continues to change according to equation (2). Since the voltage v_{gd} is constant and the voltage v_{gs} drops, the voltage drop across the conduction channel of the transistor v_{sd} during this phase will increase and can be determined by the following equation:

$$v_{sd} = v_{gd} + v_{sg} \; . \tag{4}$$

2.3 Transistor switching on

When switching on the power transistor, two types of switching are again distinguished – when the current I_L has a positive (from the drain to the source) and when it has an inverse (from the source to the drain) direction (Figure 2). Each of these processes, similar to switching analysis, is divided into phases. The division into phases provides a precise understanding of the dynamics of the device during the transition from the off to the on state, which will later be necessary for an accurate estimation of switching losses and performance optimization.

2.3.1 Switching type I – soft switching on

During the transistor switching on during the switching type I (Figure 3a), it is normal that its parasitic capacitances C_{ds} and C_{gd} are both discharged (during switching off the opposite switch) and that a current I_L passes through the transistor by inverse conduction. This case is divided into two phases as shown in Figure 8.

During phase I, the voltage v_{gd} is constant and corresponds to the voltage of the Miller plateau for current I_L, while the voltage v_{gs} rises according to the equation:

$$v_{gs} = v_{dr_{on}} \left(1 - e^{-\frac{t}{R_e C_{gs}}}\right). \tag{5}$$

At the time instant when the voltage v_{gs} reaches the Miller plateau voltage for current I_L, the inverse conduction of the GaN transistor stops and now the active area is fully conductive and allows current to pass in both directions. During phase II, the voltage continues to rise according to the dynamics shown in (5) and reaches the value of v_{dr_on}.

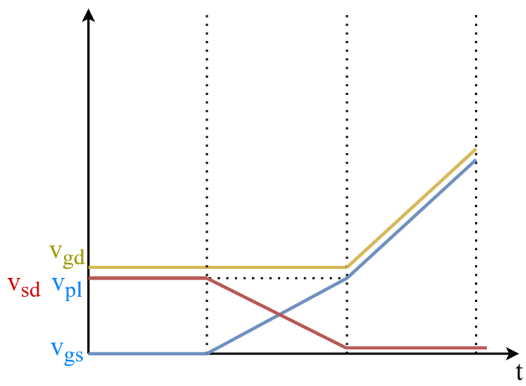

Figure 8. Switching type I – soft switching on

2.3.2 Switching type II – hard switching on

While transistor is switching on during the switching type II, Figure 3b, the parasitic capacitance C_{ds} and C_{gd} are not pre-discharged, as in the previous case, so they need to be discharged during the switching process. In this case, the switching on takes place in three phases, shown in Figure 9.

During phase I, the voltage v_{gs} rises to the voltage of the transistor conduction threshold v_{th}. During both phase

I and phase II, the voltage v_{gs} changes according to equation (5). When the current through the active area of the transistor begins to rise, phase II begins.

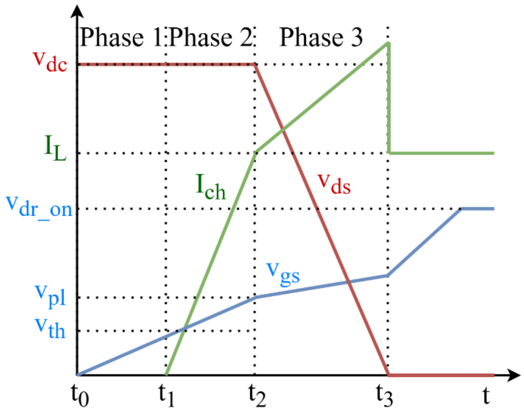

Figure 9. Switching type II – hard switching on

During phase II, the voltage v_{gs} rises from the conduction threshold voltage v_{th} to the Miller plateau voltage v_{pl} corresponding to the current I_L, while the current rises from zero to I_L. The relationship between voltage v_{gs} and current I_L is given in Figure 2. Until the transistor that switches on takes all the current from the transistor that is in the inverse conduction mechanism, there can be no change in voltage v_{ds}. The reason why this phenomenon develops is hidden in the inverse conduction mechanism itself, which does not allow the voltage drop in its active area to change as long as there is an inverse current flowing through the channel.

During phase III, the parasitic capacitances C_{ds} and C_{gd} are discharged by current through the active channel of the transistor, as shown in Figure 10.

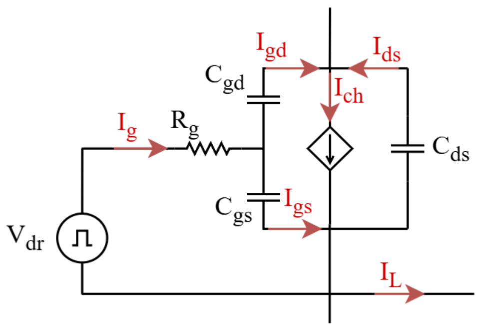

Figure 10. Current directions in the GaN transistor model during the switching type II process – switching on

During this phase, there is a significant increase in the current of the transistor active area I_{ch}, so that the stress that the semiconductor suffers is significantly higher than the stress of the steady state operating mode. The current through the active region I_{ch} is related to the voltage v_{gs} via the graph given in Figure 10.

The rate of voltage v_{gs} change is now significantly slowed down because the current provided by the driver not only charges the capacitance C_{gs} but also discharges the capacitance C_{gd}. The change in voltage v_{gs} is given, [7] by:

$$\frac{dv_{gs}}{dt} = \frac{I_g}{C_{gd}+C_{gs}} - \frac{C_{gd}}{C_{gd}+C_{ds}} \cdot \frac{(I_{ch}-I_L)}{2} \cdot \frac{1}{(C_{gd}+C_{gs})}, \qquad (6)$$

while the change in voltage v_{ds} is given by the equation:

$$\frac{dv_{ds}}{dt} = \frac{I_{ch}-I_L}{C_{oss1}+C_{oss2}}. \qquad (7)$$

By solving the system of differential equations (1) - (7) and taking into account that the values of all parasitic capacitances are a function of their corresponding voltages, the time-domain waveforms of current $I_{ch}(t)$ and voltage $v_{ds}(t)$ are obtained. Current $I_{ch}(t)$ and voltage $v_{ds}(t)$ time waveforms are needed to accurately determine the losses at transistors.

3. LOSS CALCULATION

The key performance indicators of a power converter are efficiency, size, and price. Efficiency can be increased by selecting GaN semiconductor components with better static and dynamic characteristics than conventional Si transistors. Better dynamic characteristics provide operation at higher frequencies, which leads to a reduction in the required dimensions of passive components such as transformers, inductors, and capacitors. To take full advantage of GaN transistors, it is essential to develop a reliable model for calculating losses. Based on such a model, it is possible to determine which GaN transistor is most suitable for a specific application, whether additional cooling is required, which type of cooling is adequate, as well as the maximum operating switching frequency. In this chapter, a model for estimating losses based on previously derived equations and information collected from the transistor datasheet, will be developed.

Losses in transistors during a single switching cycle include losses in switching on, losses in switching off, losses in gate loop, losses during current conduction, and losses due to the reverse conduction mechanism. Figure 11 shows the waveforms of power losses during transistor hard switching on and switching off. It is important to note that the overlap of current and voltage is significantly more pronounced during transistor switching on, which is why the energy of losses during switching on is higher than when switching it off. In certain topologies, in which two switching transitions of the type I can be realized (Figure 3a), and which are characterized by a sequence of soft switching on and hard switching off within a single switching period, it is possible to greatly reduce the overall switching losses. In this case, during one period, two soft switching ons and two hard switching offs are obtained. This sequence is characteristic of LLC resonant converters, which can achieve very high efficiencies compared to other isolated DC/DC topologies by using GaN transistors. Although this mode of operation is common for LLC converters, it is also possible to implement it in a synchronous buck converter, under the conditions that will be discussed in detail in Chapter 3.2.

Total switching and conduction losses can be expressed as the product of the current flowing through the conduction channel of the transistor and the voltage drop across it:

$$P_{total} = \frac{1}{T_{PWM}} \int_0^{T_{PWM}} I_{ch}(t) \cdot v_{ds}(t) \cdot dt. \qquad (8)$$

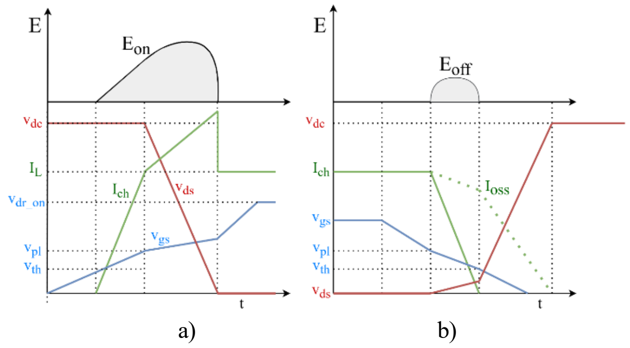

Figure 11. Losses energy during hard (a) switching on (b) switching off

In order to evaluate the power of the losses at the transistor, it is necessary to determine the time waveforms of quantities of importance in the function of operating modes. In order to determine the time waveforms of the channel current $I_{ch}(t)$ and the channel voltage drop $v_{ds}(t)$, it is necessary to solve the system of differential equations resulting from Chapter 2. In order for a system of equations (1) (7) to be solvable, it is necessary to know the following dependencies:

$I_{ch}(v_{gs})$ – dependence of the current of the transistor active area on the voltage v_{gs};

$I_{ch}(v_{gd})$ – dependence of the current of the transistor active area on the voltage v_{gd} during inverse conduction of current;

$C_{ds}(v_{ds})$ – dependence of the drain-source capacitance on the voltage drop in the transistor active area v_{ds};

$C_{gd}(v_{gd})$ – dependence of gate-drain capacitance on voltage v_{gd};

$C_{gs}(v_{gs})$ – dependence of gate–source capacitance on voltage v_{gs}.

The above dependencies can be precisely determined by experimental methods, such as the *double-pulse test*. However, this approach is often not practical because it involves purchasing a component and doing all measurements to verify its suitability for a particular application. Alternative ways include use of approximation expressions, the adjustment of curves, or, in the case of parasitic capacitances, the application of a charge-based model. Although experimental measurements are the most reliable source of data, they are the most difficult to obtain, while approximation methods often lead to significant discrepancies.

Therefore, a different approach is taken in this paper. Based on the curves given in the transistor datasheet, discrete values of the required quantities are determined using the *Automeris* software package. From these discrete dependencies and differential equations obtained by discretizing the expression (1) - (7), it is possible to determine the waveforms $I_{ch}(t)$ and $v_{ds}(t)$.

3.1 Acquisition of data from the datasheet

The data in the transistor datasheet is most often presented in the form of graphics, which are obtained based on measurements done by the manufacturer and then presented in the datasheet. If the manufacturer does not have tabular values of the required dependencies or is not willing to share them, it is necessary to extract the data directly from the graphics from the datasheet. In this paper, this procedure is done using a software package [8]. An example of how to use this tool is shown in Figure 12.

This software package is intended for the digitization of graphic data, i.e. the extraction of numerical values from graphic figures. This tool enables for the user to easily obtain tabular data suitable for further analysis and calculation from existing diagrams.

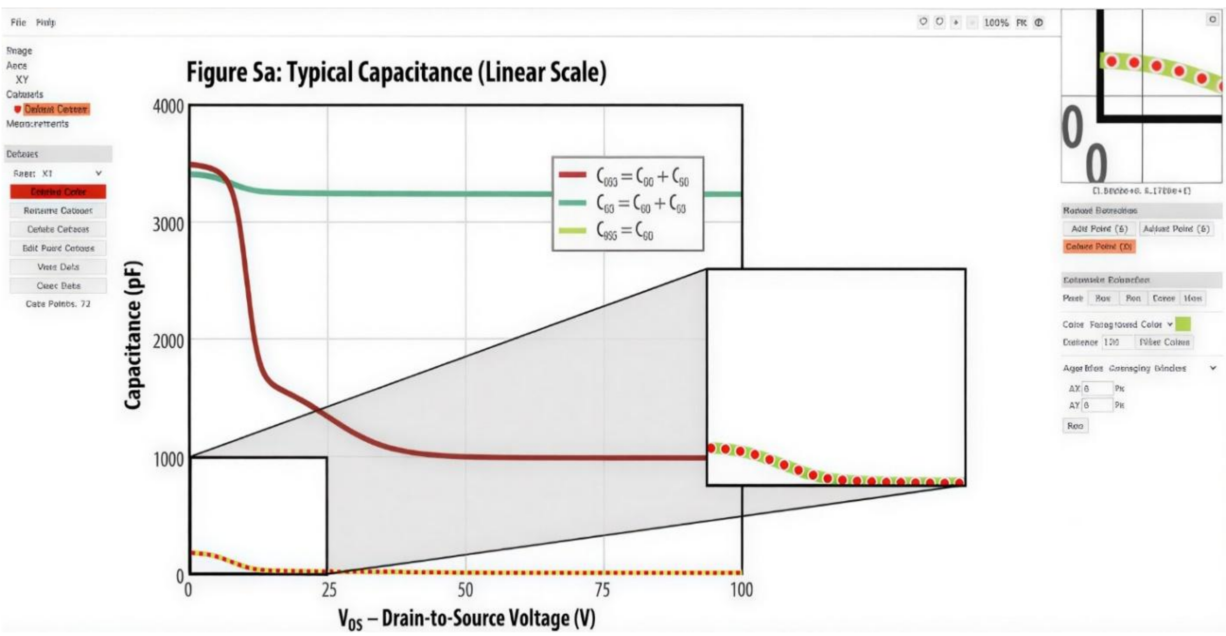

Figure 12. Using tools to extract data from the datasheet

The figure shows the change in parasitic capacitances extracted from the datasheet of a commercially available GaN transistor depending on the drain–source voltage v_{ds}. The software package was used to estimate discrete capacitance values at more than 100 points, which are marked with red dots, thus ensuring high accuracy of the dependencies shown.

3.2 Algorithm for estimating losses

Based on the differential equations derived in Chapter 2 and the data collected from the datasheet, it is possible to estimate the losses dissipated at the transistors. To determine the operating state of the transistor and the type of switching process that is currently being executed, it is necessary to know the current of the half-bridge I_L at any time. The current I_L does not depend directly on the type of transistor, but on the external parameters of the electrical circuit, such as the voltage of the DC link and the values of the passive elements and active load. By knowing the current I_L based on the algorithm shown in Figure 13, it is possible to determine the states through which the transistor passes during a single period of switching. The positive direction of the current means the current that has the direction from the drain to the source, while the negative direction of the current is from the source to the drain.

The result of the algorithm is the discrete values of the voltage drop on the conduction channel $v_{ds}(k)$ and the current of the conduction channel $I_{ch}(k)$, and the losses on that transistor over a switching period are determined based on the discretized equation (9).

$$P_{total} = \frac{1}{N}\sum_{k=0}^{N-1} I_{ch}(k) \cdot v_{ds}(k) \tag{9}$$

3.3 Loss analysis

This chapter evaluates switching losses for the selected GaN transistor in the half-bridge configuration. The losses were determined and intercompared for two different values of current waves, in order to have an overview of the effect of different sequences of switching states on the overall power dissipation. For this purpose, scripts were developed in the software package [9], which enabled solving the system of differential equations obtained by discretizing expressions (1) – (7) using Euler's first-order discretization method. The states of the system were determined by applying the algorithm shown in Figure 13, which enabled study of the transistor losses in different operating modes of the converter.

The analysis of losses was made under the following conditions. The power of the converter is determined to be $P = 1$ kW, the input voltage is $V_{in} = 60$ V and the duty cycle $d = 0.75$, while other parameters of importance are given in Table I. The total losses on both transistors in the half-bridge configuration are given in Figure 14, for the case when the current ripple is higher than its mean value.

From the graphs, it is directly noticeable that the switching losses are negligible compared to the conduction losses. In this operating mode, the output current is approximately $I_L = 22$ A, while the amplitude of the ripple of the current is 27 A. Due to such a high ripple when the lower transistor is switched off, the current is negative and it is $I_{L\_min} = -5$ A. Then this switching off takes place according to the scenario described in 2.2.1.

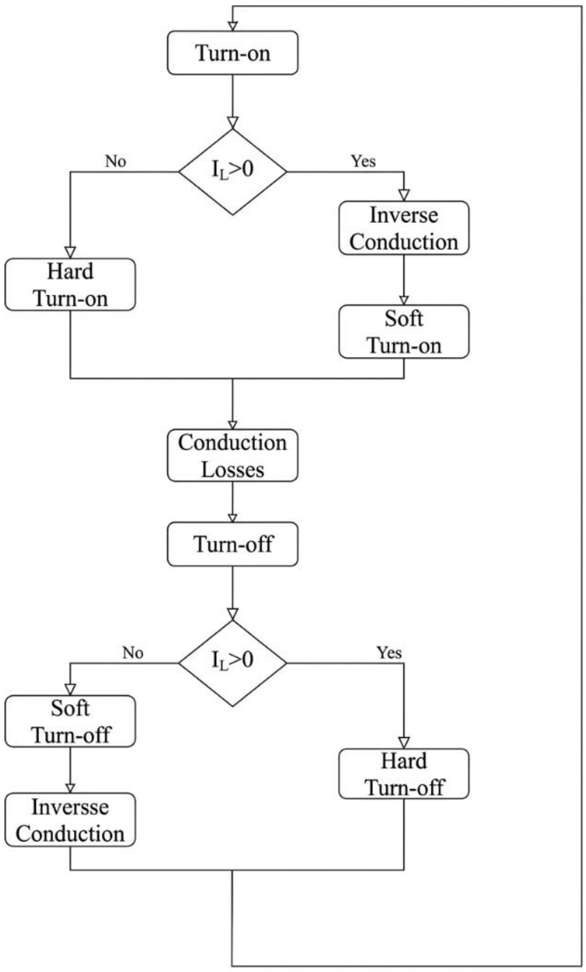

Figure 13. States that a transistor in a half-bridge passes through during a single switching cycle

Table I Parameters of the designed buck converter

Parameter	Value	Unit
Input voltage	10–72	V
Output voltage	5–70	V
Nominal power	1	kW
Switching frequency	125	kHz
Dead time	25	ns
Inductor	1,5	µH
Transistor	GaN [10]	/
Driver	[11]	/

From Figure 3, it can be seen that the overlap between the current I_{ch} *(t)* and the voltage v_{ds} *(t) is* very small, and the losses defined by equation (8) are very small. After the lower transistor is switched off, there is a period of dead time and switching on of the upper transistor. Switching on the upper transistor takes place according to the scenario described in 2.3.1 and also generates minimal losses. It is important to note that when this type of commutation occurs, switching off of the upper and the switching on of the lower one, it is realized according to scenario 2.2.1, then 2.3.1 and it results in minimum switching losses. The combination of switching 2.2.1 and 2.3.1 can be achieved twice during one period only if the current when the upper transistor is switched on is negative, that is, if the ripple of the current is greater than the mean current of the consumer I_L. The total losses at both transistors in the case where the current ripple is less than the mean current I_L are shown in Figure 15. The loss in this case is now 10% higher.

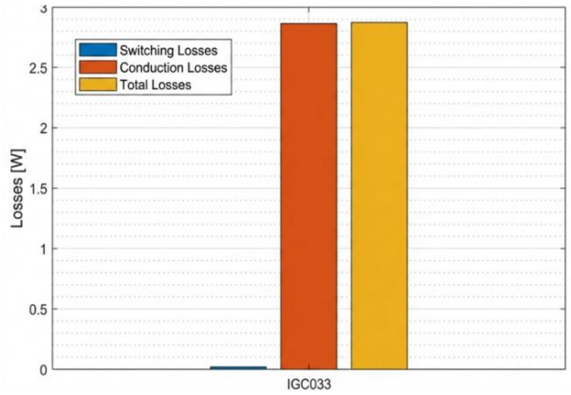

Figure 14. Total losses in both transistors in the half-bridge configuration

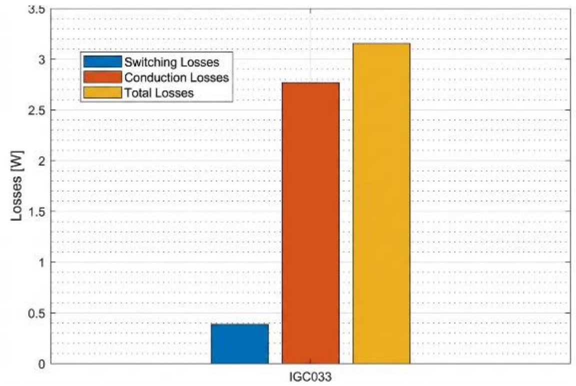

Figure 15. Total losses in both transistors in the half-bridge configuration at hard switching

4. EXPERIMENTAL RESULTS

In order to test and verify the analytical model, a 1 kW buck converter was designed (Figure 16). While designing and prototyping, special attention was paid to the arrangement of components on the printed circuit board to minimize the parasitic elements of the driver circuit and their impact on the switching process. Key data describing the converter prototype are given in Table I. Validation of the described commutation model was experimentally done on the setup given in Figure 17.

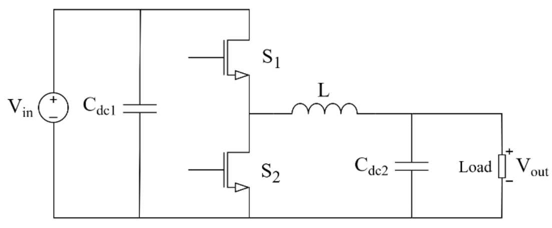

Figure 16. Topology of the designed power converter

The setup consists of:
(1) a laptop to communicate with the converter in real time;
(2) power supply;
(3) voltage and current probes with a bandwidth of up to 150 MHz;
(4) developed converter prototype;
(5) oscilloscope;
(6) passive resistance consumer $R_L = 2\ \Omega$.

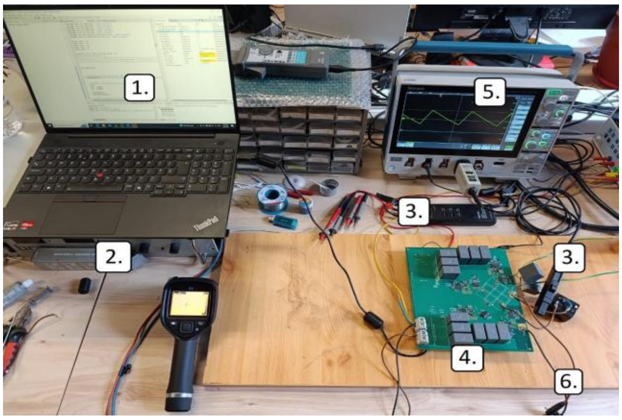

Figure 17. Experimental setup in the Laboratory for Digital Control of Converters and Drives, Faculty of Electrical Engineering, University of Belgrade

There are several methods to verify the switching model and the algorithm for estimating losses. One approach is to measure the total losses at the level of the entire converter, after which they are grouped into losses in copper conductors, reactive elements and auxiliary electronics. By subtracting these components from total dissipation, it is possible to indirectly estimate the losses at the transistors. However, in the converter designed, switching losses account for a relatively small proportion of the total losses, which makes this method subject to significant errors and deviations.

Therefore, the other approach was applied – direct assessment of the accuracy of the switching model by comparing the waveforms of voltage $v_{ds}(t)$ and current $I_{ch}(t)$. As these two quantities are closely related, a good matching of voltage waveforms implies good matching of the current, and therefore an adequate estimation of switching losses.

A series of experiments were conducted in which the input voltage was changed in the range of $V_{in} \in [10, 60]\ V$10 V, while at the same time the duty cycle took values of $d \in$ [0,25; 0,5; 0,75]. The resistance of the passive load was fixed during all experiments and was 2 Ω.

The key parameter for verifying the developed model is the duration of the switching. The duration of the switching was tested on the setup shown in Figure 16 under different operating modes and further compared with the results of the analytical-numerical model. With an oscilloscope, the time it takes for the voltage $v_{ds}(t)$ to change from 0 V to V_{dc}, when the lower switch is switched off (Figure 18), is measured.

Duration of switching for the lower and upper transistors for six different input voltages were measured. The experimental results were compared with the durations of switching obtained from the models over the entire operating range of the voltage converter. The results are shown in Figure 19.

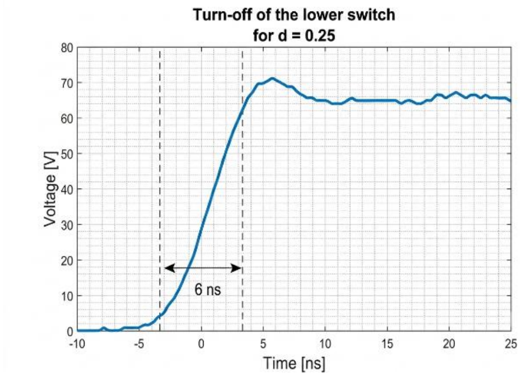

Figure 18. Changing the voltage of the v_{ds} when the lower transistor is switched off

From Figure 19, it can be concluded that the developed model follows the experimental values quite well, especially in the case of the lower transistor. At 10 V voltage, the model shows an almost perfect match with the measurements, with an accuracy of 99%.

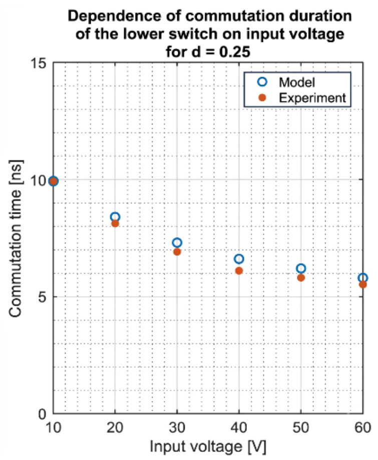

a)

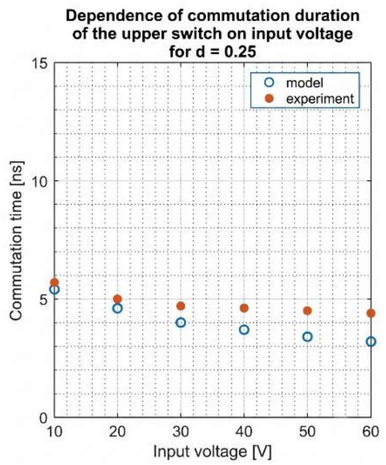

b)

Figure 19. The dependence of the switching duration on the input voltage: a) the lower transistor; b) the upper transistor in the half-bridge

However, as the input voltage increases, some deviation of the model is observed, with the largest difference observed at 40 V, where the accuracy drops to 92%.

On the other hand, the results for the upper transistor show a slightly poorer match with the experiment. The accuracy of the model decreases with increasing input voltage, reaching 75% at 60 V. This may indicate additional nonlinear effects or asymmetry in the influence of parasitic elements that are not fully covered by the actual model. Despite the discrepancies, the model demonstrates satisfactory accuracy, making it a useful tool for estimating switching times and estimating losses at transistors.

5. CONCLUSION

The paper describes in detail the processes of switching GaN transistors in the half-bridge configuration. A physical model of commutations is derived, which output parameters are the waveform of the current of the channel $I_{ch}(t)$ and the waveform of the voltage drop on the channel $v_{ds}(t)$. The parameters of interest are described in the function of operating modes. In order for the derived equations to be solvable without any introduction of approximations, with an appropriate software package, the relevant data were extracted from the datasheet of the specific transistor. The data extracted in this way were used to discretely solve the equations of the previously described physical model. For verifying the formed analytical-numerical model, a prototype of a buck converter based on GaN technology was developed and tested. The tests were done over the entire operating voltage range and the durations of the switching times resulting from the model and the experimental setup were compared. The model shows a very good match of over 92% with experimental tests of the switching duration of GaN transistors. The greatest deviations between the results obtained by the analytical-numerical model and the experimentally measured switching times on the prototype reach up to 25% for the upper transistor, which indicates the presence of certain effects that are not fully covered by the model and leaves room for further research.

LITERATURE

[1] Lidow A., De Rooij M., Glaser J., “GaN Power Devices for Efficient Power Conversion”, fourth edition, Wiley, Hoboken, 2025.

[2] Spaziani L., Lu L., “Silicon, GaN and SiC: There's |Room for All: An Application Space Overview of Device Considerations”, *2018 IEEE 30th International Symposium on Power Semiconductor Devices and ICs (ISPSD)*, Chicago, IL, USA, 2018, pp. 8-11, DOI: 10.1109/ISPSD.2018.8393590.

[3] Ding X., Zhou, Y., Cheng, J., “A Review of Gallium Nitride Power Device and its Applications in Motor Drive” *Proceedings of the CSEE*, vol. 41, no. 4, pp. 1386–1397, April 2021.

[4] Klein J., “Synchronous Buck MOSFET Loss Calculations with Excel Model” [Internet]. Sunnyvale: Fairchild Semiconductor; 2006 [cited 5. 1. 2026]. Available at:

https://www.bdtic.com/datasheet/fairchild/AN-6005.pdf.

[5] Huang X., Li Q., Liu Z., Lee F. C. "Analytical Loss Model of High Voltage GaN HEMT in Cascode Configuration" *IEEE Energy Conversion Congress and Exposition*, Denver, CO, USA, 2013, pp. 3587-3594, DOI: 10.1109/ECCE.2013.6647173.

[6] Erickson R., Maksimovic D,. "Fundamentals of Power Electronics", Springer Science & Business Media, New York, 2007.

[7] Qin, H., Zheng, X., Zhu Z., and Gong, C., "Analytical Power Loss Model for GaN Transistors Based on Temperature and Parasitic Parameters", *Proceedings of 7th International Conference on Electrical Engineering and Green Energy (CEEGE)*, Los Angeles, CA, USA, 2024, pp. 119-124, DOI: 10.1109/CEEGE62093.2024.10744178.

[8] Automeris Rohatgi, A. (2025). WebPlotDigitizer. [Software tool]. https://automeris.io.

[9] The MathWorks, Inc. (2024). MATLAB (R2024a) [Software tool]. https://www.mathworks.com.

[10] Infineon Technologies, "IGC033S101 Datasheet", Rev. 1.0, 2025. [Semiconductor component]. Available at: https://www.infineon.com/assets/row/public/documents/24/49/infineon-igc033s101-datasheet-en.pdf

[11] Infineon Technologies, "2EDB8259F Datasheet", Rev. 1.0, 2024. [Semiconductor component]. Available at: https://www.infineon.com/assets/row/public/documents/24/49/infineon-2edb8259y-datasheet-en.pdf

BIOGRAPHY

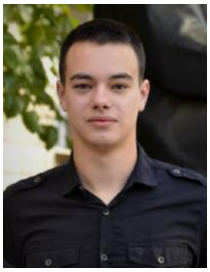

Miroslav Popovic was born in 2001 in Belgrade, Serbia. He completed his graduate and master's studies at the Faculty of Electrical Engineering, University of Belgrade in 2024 and 2025, respectively. He is currently a PhD student at the same university. In 2023, with the H-Bridges team, he won second place at the IFEC (*International Future Energy Challenge*) in Hannover, Germany. His areas of research include large energy gap semiconductors and power converter design.

ORCID: 0009-0009-5388-8932

Aleksandar R. Milić was born in Smederevo, Yugoslavia, in 1993. He obtained his bachelor's and master's degrees in electrical engineering at the University of Belgrade in 2016 and 2017, respectively. He is currently employed at the Department of Energy Converters and Drives at the Faculty of Electrical Engineering, University of Belgrade. His research interests include digital control of electric drives and grid converters. From 2017 to 2025, as a mentor to the H-Bridges student team, he received six awards at the IEEE *International Future Energy Challenge*.

ORCID: 0000-0003-2675-4292

Nikola Mirković was born in Belgrade, Serbia, in 1997. He obtained his bachelor's and master's degree in electrical engineering at the Faculty of Electrical Engineering, University of Belgrade in 2020 and 2021, respectively. He defended his PhD in Industrial Electronics at the *Centro de Electrónica Industrial, Universidad Politécnica de Madrid*, Madrid, Spain, in April 2025. Since 2021, he has been a member of the *Centro de Electrónica Industrial, Universidad Politécnica de Madrid* (UPM). His areas of research include inductive energy transfer and power converters.

ORCID: 0000-0003-0018-4682

UDK: 621.314.24

Miroslav Popović[1], Aleksandar Milić[1], Nikola Mirković[2]

Modelovanje gubitaka GaN prekidača na osnovu kataloških podataka

[1] Univerzitet u Beogradu – Elektrotehnički fakultet, Beograd, Srbija*
[2] Univerzitet u Beogradu – Elektrotehnički institut „Nikola Tesla" AD, Beograd, Srbija

Originalni naučno-istraživački rad

Ključne poruke

- Izvođenje algoritma za ocenu gubitaka GaN prekidača snage
- Poređenje tvrdih, mekih i polumekih prekidačkih procesa i izdvajanje strujnog doprinosa kanala i parazitnih kapacitivnosti
- Verifikacija modela kroz prototip sinhronog spuštača napona snage 1 kW

Kratak sadržaj

Prekidači zasnovani na savremenim poluprovodnicima velikog energetskog procepa, kao što je galijum-nitrid (GaN), sve češće se koriste u uređajima energetske elektronike. Zbog specifične strukture i sposobnosti da brzo menjaju radno stanje, standardni proračuni koji se koriste za određivanje gubitaka u silicijumskim prekidačima nisu primenljivi u ovom slučaju. Stoga je razvijen analitički model za procenu gubitaka kod GaN prekidača u konfiguraciji polumosta, koji se oslanja na podatke iz tehničke dokumentacije. Model uzima u obzir različite tipove komutacija, kao što su tvrdo, meko i polumeko komutovanje. Izvršeno je poređenje gubitaka pri mekom i tvrdom komutovanju prekidača u sklopu sinhronog spuštača napona. Na osnovu predloženog modela određena su vremena trajanja komutacija, koja su iskorišćena kako bi se verifikovao predloženi model na pretvaraču spuštaču napona snage 1 kW.

Ključne reči

GaN prekidači snage, model gubitaka, sinhroni spuštač napona

Primljeno: 16. decembar 2025. Recenzirano: 3. jul 2026.
Izmenjeno: 8. jul 2026. Odobreno: 22. jul 2026.
* Korespondirajući autor: Miroslav Popović
Imejl: miroslav@etf.bg.ac.rs

Napomena:
Ovaj članak predstavlja proširenu, unapređenu i dodatno recenziranu verziju studentskog rada „*Analitički model gubitaka GaN tranzistora na osnovu podataka iz tehničke dokumentacije*" (https://doi.ub.kg.ac.rs/doi/cigre37-b4-05/), nagrađenog u Studijskom komitetu STK-B4 *HVDC i energetska elektronika,* na 37. Savetovanju CIGRE Srbija, Zlatibor, 26-30. maja 2025.

UDC: 621.311.1:621.318.43
621.316.542:621.3.015.3

Uroš N. Njegovan[1,2], Zoran N. Stojanović[1], Aleksandar D. Marjanović[1,3]

Mitigation of Switching Transients Using Point-on-Wave Controlled Circuit Breaker Closing

[1] University of Belgrade – School of Electrical Engineering, Belgrade*
[2] Siemens Energy d.o.o. Beograd – Belgrade, Serbia
[3] Siemens d.o.o. Beograd – Belgrade, Serbia

Original scientific research article

Highlights

- Effects of switching transients caused by the connection of different loads are presented
- The technique of controlled circuit breaker switching is described
- The effects of applying the technique were tested on a real-time simulator
- Compared controller and conventional shunt reactor circuit breaker switching

Abstract

Transmission lines loaded below their surge impedance present a significant source of reactive power in the network, that can lead to local voltage increase. Transmission system operators around the world turn to shunt reactors in combination with a conventional high-voltage circuit breakers to cope with voltage issues. Implementation of such solution introduces a significant increase in the number of switching transients. Using controlled switching technology (Point-on-Wave), through individual switching of each breaker pole at optimal time, it is possible to limit reactor inrush current when shunt reactor is energized and the recovery voltage when it is de-energized. The paper presents the negative effects of uncontrolled switching of shunt reactor on transmission system. The technique of controlling the timing of circuit breaker switching is presented as a tool to mitigate the negative effects of switching transients. The algorithm for controlled switching of the circuit breaker has been tested in the laboratory. The test setup consists of a Point-on-Wave Intelligent Electronic Device (IED) and HIL (Hardware-in-the-Loop) device used to simulate 400 kV shunt reactor and circuit breaker. The devices exchange information using IEC 61850 Sampled Values and GOOSE protocol. Experimental results confirm limitation of inrush current magnitude when shunt reactor is energized by controlled switching device.

Keywords

Controlled switching, Hardware-in-the-Loop, Point-on-Wave, Reactor inrush, Shunt reactor

Received: December 26th, 2025 Reviewed: March 19th, 2026
Modified: May 6th, 2026 Accepted: May 12th, 2026

*Corresponding author: Uroš N. Njegovan, +381 60/81-70-242
E - mail: uros.njegovan@siemens-energy.com

Note:
This article represents an expanded, improved and additionally peer-reviewed version of the paper "*Application of Controlled (Point-on-Wave) Switching for 400 kV Shunt Reactor*" (https://doi.ub.kg.ac.rs/doi/cigre37-b5-08/), awarded by Expert Committee EC-B5 *Protection and Automation* at the 37th CIGRE Serbia Conference, Zlatibor, May 26-30, 2025

1. INTRODUCTION

Switching transients are a leading cause of excessive stress on power system equipment. For instance, the energization of a shunt reactor may lead to voltage waveform distortion and the occurrence of high-amplitude inrush currents, whereas capacitor bank energization may be accompanied by excessive overvoltages. Point-on-Wave controlled switching of CBs is employed to mitigate or eliminate switching transients arising from the energization and de-energization of shunt reactors, power transformers, and capacitor banks. In recent years, the application of this technique has expanded to both high-voltage overhead transmission lines and cable systems.

The combination of high-voltage (HV) circuit breakers (CB) with stable operating characteristics and modern microprocessor-based devices has led to the refinement of CB controller algorithms, simplified their integration into primary and secondary circuits, and enabled their application across a wide range of load types. Owing to the substantial increase in its deployment over the past years, controlled switching has become recognized as a reliable means of mitigating the effects of switching transients.

The controller optimizes the operating instant of the HV circuit breaker by introducing an appropriate command delay depending on the type of load being switched. Consequently, the adverse effects of switching operations within the power system are reduced. The main advantages of modern controlled switching are [1]:

- increased power system reliability through reduced voltage variations and lower harmonic distortion;
- improved power quality;
- extended equipment service life;
- mitigation of switching overvoltages and transformer magnetizing inrush currents.

1.1 Shunt reactor circuit breaker closing

Busbar voltage levels, together with frequency and the degree of harmonic distortion, are the key indicators of power quality. In transmission lines loaded below their surge impedance, the capacitances of long high-voltage transmission lines become increasingly significant, acting as substantial sources of reactive power and consequently causing local voltage rises above allowed limits. The operation of 400 kV and 220 kV transmission lines below their surge impedance loading (SIL) is a common occurrence both in Serbia and throughout the region.

Across the power system, voltage conditions are local in nature and, in many cases, cannot be regulated on a system-wide basis without the use of additional reactive power compensation devices.

A wide range of reactive power compensation technologies is currently available. These include synchronous condensers, Shunt Reactors, Static VAR Compensators (SVC), Static Synchronous Compensators (STATCOM), combined series-shunt FACTS controllers such as the Unified Power Flow Controller (UPFC) and the Interline Power Flow Controller (IPFC), as well as FACTS controllers including the Thyristor Controlled Phase Shifting Transformer (TCPST) and the Thyristor Controlled Voltage Regulator (TCVR).

The shunt reactor is one of the most widely employed reactive power compensation devices used by transmission system operators worldwide. It is used at selected grid nodes to maintain the desired voltage profile within the power system. Shunt reactors are manufactured as either single-phase or three-phase units, with or without tap changers (variable or fixed reactors). They are connected either directly to the HV substation busbar system through conventional CBs (Fig. 1) or to the tertiary winding of power transformers.

During periods of heavy power system loading and increased power transfer over high-voltage transmission lines, shunt reactors are typically disconnected from the network. Depending on voltage variations and the frequency of switching operations performed by shunt reactor CBs, a significant increase in the number of switching transients may occur at the point of connection. Such transients are one of the major sources of excessive stress on transmission system equipment, particularly on CBs. Furthermore, they adversely affect power quality and may lead to unnecessary responses of protective relays.

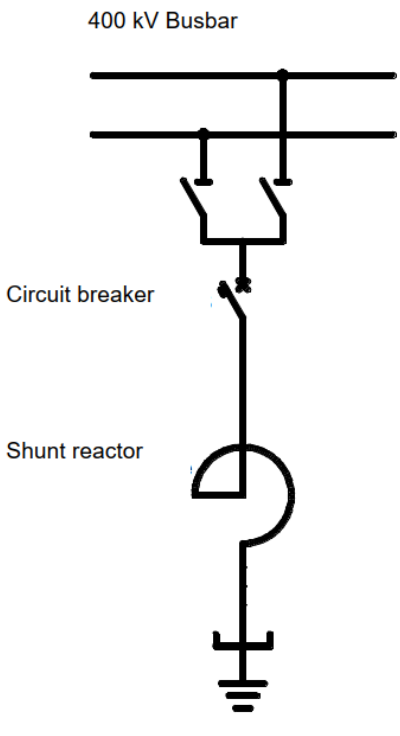

Figure 1. Direct connection of the shunt reactor to HV substation busbars

1.2 Power transformer circuit breaker closing

Power transformers are key components in ensuring the reliable operation of power systems. Owing to the significant increase in the demand for uninterrupted electricity supply over recent decades, high reliability requirements have been imposed on power transformers (hereinafter referred to as transformers).

Transformer magnetizing inrush current (Fig. 2), [2] is a phenomenon that occurs during the energization of an unloaded transformer. Under certain conditions, it may approach fault-current levels [3]. Although its impact is less severe than that of a fault current, the frequency of its occurrence and its duration may adversely affect the service life of HV equipment. In addition to the high magnitude of the inrush current, transformer energization may generate higher-order harmonics, adversely affect power quality, and lead to unnecessary responses of protection relays.

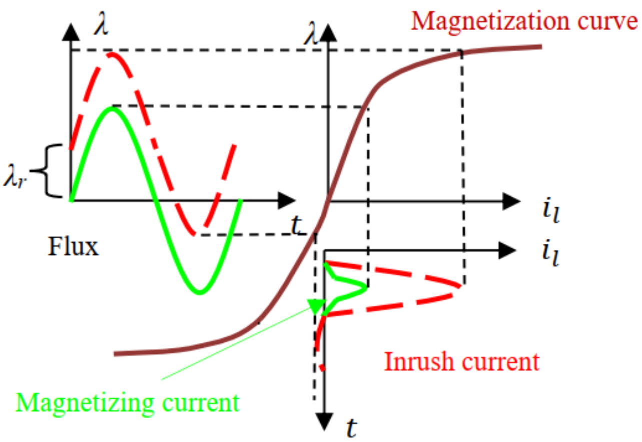

Figure 2. Transformer magnetizing current

Under steady-state no-load conditions, the flux is confined to the transformer magnetic core. Consequently, only a small magnetizing current is required, as shown in Fig. 2. It typically amounts to 1–2% of the transformer's rated current. For economic reasons, transformers are designed with the operating flux value close to the knee point of the magnetization curve.

Conventional energization of a transformer at a random instant may result in an asymmetric magnetic flux and core saturation. It is important to note that, following transformer de-energization, a portion of the magnetic flux remains in the core. This flux, referred to as remanent or residual flux (λ_r), may affect the amplitude of the magnetizing inrush current during subsequent transformer energization, depending on the voltage value at the instant of energization.

As transformers are an important component of the power system and their outage may be harmful during periods of heavy system loading, controlled switching can make a significant contribution to extending transformer service life.

1.3 Capacitor bank circuit breaker closing

When a capacitor bank or harmonic filter is de-energized, a certain amount of time is required for the residual energy stored in the bank to be discharged. In order to prevent re-energization of the capacitor bank before its complete discharge, a time-delay relay is typically applied to block the CB mechanism for a specified period. The built-in discharge resistors ensure that the capacitor bank is fully discharged before the blocking interval expires. A typical relay setting is 10 minutes from the instant of CB opening to the earliest possible subsequent closing operation.

A discharged capacitor bank effectively appears as a short circuit at the instant voltage is applied to its terminals, i.e., during CB closing. If energization occurs at voltage peak, voltage and current variations may be significant.

Depending on the grid configuration, overvoltages during capacitor bank energization may result in damage or even insulation failure of individual power system components such as transformers, insulators, cables, etc. For certain capacitor bank configurations, energization may lead to high-amplitude and high-frequency currents, which in extreme cases may compromise the mechanical integrity of both the capacitor bank and the CB.

These transients can be significantly mitigated by controlled switching of capacitor bank CBs such that energization occurs at a voltage zero crossing (Fig. 3), [4].

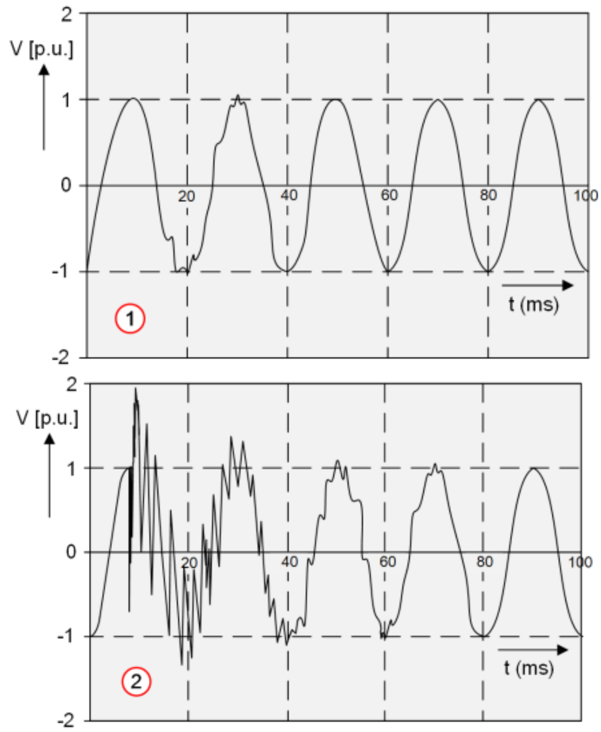

Figure 3. Voltage waveforms during controlled (top) and uncontrolled (bottom) capacitor bank switching

2. POINT-ON-WAVE CONTROLLED SWITCHING

One of the most widely used CB control techniques is based on selecting the optimum instant on the voltage waveform (Point-on-Wave). Such controlled switching can significantly reduce the adverse effects of switching transients that may occur during conventional random switching. The algorithm that determines the optimal switching instant for each phase based on the input parameters is implemented in the CB controller. The CB controller's characteristics are similar to those of modern microprocessor-based protection and control devices.

Upon receiving a CB closing command, the controller evaluates the optimum switching instant based on the measured voltage waveform and accordingly calculates the required command execution delay. In this way, each breaker pole closes independently at the optimum instant. The expected controller repeatability and the accuracy of current establishment relative to the optimum point on the voltage waveform are within ±1 ms. The controller monitors variations in the reference voltage frequency by detecting voltage zero crossings and, based on this information, determines the execution instant.

The principle of controlled closing, including all key time instants, is illustrated in Fig. 4, [5]. It can be observed that, before mechanical closing occurs, dielectric breakdown of the insulating medium occurs as the CB contacts approach one another, resulting in the establishment of an electric arc. This corresponds to the establishment of electrical contact between the CB poles, i.e., the electrical closing of the CB. The mechanical closing time ($T_{CLOSING}$) is a characteristic of the CB and can be measured. Arc initiation time (T_m) is an input parameter of the controller used to calculate the total time interval between issuing the command and establishing current, i.e., the electrical closing of the CB (T_{MAKING}).

The total delay introduced by the controller between the detection of the closing command and its execution (T_{total}) is equal to the sum of the voltage zero-crossing detection time (T_W) and the synchronization delay calculated by the controller (T_{cont}). The synchronization delay is used to ensure that current is established at the optimum instant on the voltage waveform, taking into account the calculated electrical closing time of the CB (T_{MAKING}).

Accordingly, the controller is designed to ensure the establishment of electrical rather than mechanical contact between the CB poles at the optimum instant, which is calculated as (1):

$$T_{MAKING} = T_{CLOSING} - T_m \quad (1).$$

The effectiveness of controlled switching is strongly influenced by the consistency of the CB's mechanical performance and its dielectric properties. Another significant factor is the controller's ability to accurately predict CB behavior throughout its service life.

Required CB characteristics for application in controlled switching schemes are:

- independent pole operation;
- stable closing time with high mechanical reliability;
- excellent dielectric properties, i.e., a steep Rate of Decrease of Dielectric Strength (RDDS).

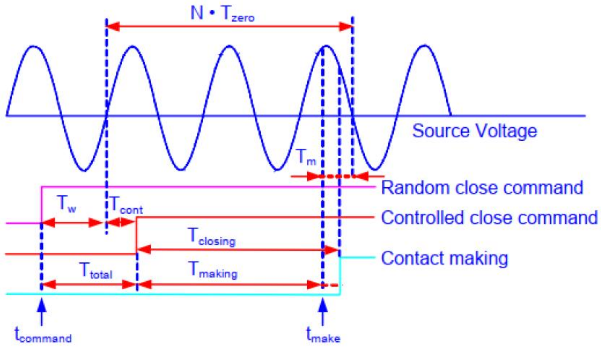

Figure 4. Key time instants of controlled circuit breaker switching

The operating times of CBs vary considerably depending on the breaker type as well as operating and ambient conditions. A portion of the total variation in CB operating time can be predicted. In addition to predictable variations, there are also variations that cannot be predicted because they are purely statistical in nature. The CB operating time can be expressed as (2):

$$T_{Oper} = T_{Nom} + \Delta T_{Comp} + \Delta T_{Drift} + \Delta T_{Statistic} \quad (2),$$

where:

- T_{Oper} – CB operating time;
- T_{Nom} – CB operating time under nominal conditions;
- ΔT_{Comp} – predictable variation that can be compensated for by the controller;
- ΔT_{Drift} – variation caused by CB aging and wear throughout its service life;
- $\Delta T_{Statistic}$ – statistical variation.

Therefore, there is a variable component of the CB operating time that can be predicted and accounted for within the controller (ΔT_{Comp}). Variations in CB operating time are caused by changes in control voltage and ambient temperature and, in the case of pneumatic CBs, by variations in pressure. Consequently, these variations can be predicted and their impact on CB operating time can be compensated for using sensor data available to the controller.

3. CONTROLLED CLOSING STRATEGIES FOR DIFFERENT LOAD TYPES

The following sections provide an overview of CB closure control strategies for the three principal load types. Depending on user requirements and the available controller functionalities, the controller can be configured for one of the standard load types and, if required, for both operating modes – closing and opening.

3.1 Controlled closing of shunt reactor circuit breakers

For an ideal shunt reactor, the current waveform lags the voltage at its terminals by approximately 90° [6]. Consequently, the instantaneous voltage reaches its maximum value when the current passes through zero, as shown in Fig. 5.

The magnitude of the reactor inrush current and the degree of voltage waveform distortion depend on the value of the system voltage at the instant the closing command is issued, as well as on the CB operating time.

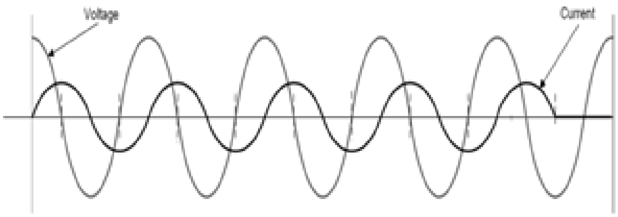

Figure 5. Shunt reactor current and voltage waveforms

Conventional shunt reactor energization at a random instant results in asymmetric currents and increased electromechanical stresses on both the CB and the reactor windings. In extreme cases, it may lead to saturation of current transformers and unnecessary trip of the earth-fault protection (50N/51N), which operates based on the current measured in the reactor neutral grounding conductor. If energization occurs when the voltage of one phase is close to zero, the switching transient will be most pronounced.

In three-phase systems, the phase-voltage peaks always occur in the inverse sequence (L1–L3–L2) relative to the phase sequence of the system voltages (L1–L2–L3) and are displaced by one-third of a cycle, corresponding to 6.66 ms in a 50 Hz system (Fig. 6).

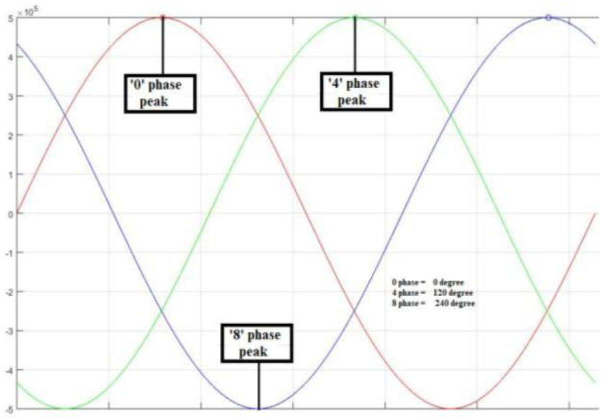

Figure 6. Three-phase voltage waveforms and their peak values

The optimal reactor energization strategy is based on closing each CB pole at voltage peak. Since the reactor is an inductive element, closing at voltage peak theoretically results in the minimum magnetic flux and, consequently, minimizes the inrush current. The reference instant is defined as the zero crossing of the phase L1 voltage waveform. The controller is designed to close the L1 pole with a phase shift of 90° relative to the reference instant, i.e., when the phase L1 voltage reaches its peak [7].

Phase L3 reaches its negative peak value next, at 90° + 60° = 150°, corresponding to a delay of 3.33 ms relative to phase L1. The final step is the closing of phase L2, with a theoretical delay of 90° + 120° = 210°, corresponding to 6.66 ms.

Although beyond the scope of this paper, it should be noted that shunt reactor CB opening may also be challenging. The difficulty arises not from the magnitude of the interrupted current, but from the energy stored in the reactor. Current chopping before the natural current zero crossing may result in pronounced high-frequency oscillations due to the energy stored in the reactor as an inductive element, together with the effect of parasitic capacitances. A sudden rise in the transient recovery voltage across the CB contacts may lead to arc re-ignition. It should be emphasized that modern SF_6 CBs are designed such that the probability of current chopping is minimal.

During shunt reactor de-energization, the controller initiates mechanical separation of the CB contacts immediately after current zero crossing. Following contact separation, the arc is stretched and current continues to flow until the dielectric strength becomes sufficient to extinguish the arc at the next current zero crossing. Once the arc is extinguished, the contact gap should be large enough for the dielectric strength to withstand the transient recovery voltage and prevent arc re-ignition.

3.2 Controlled closing of power transformer circuit breakers

In three-phase transformers assembled from three single-phase units, there is no magnetic coupling between the phases of a given winding. Consequently, from the perspective of the closing strategy, such transformers can be treated similarly to shunt reactors, with each phase being energized at the maximum value of its respective phase voltage.

Three-phase transformers with a common magnetic core and tank are commonly used throughout the region. Their primary and secondary windings may be connected in either wye (with grounded or isolated neutral) or delta configuration. In some cases, transformers are also equipped with a tertiary winding. When a transformer is equipped with a tertiary winding or is constructed as a three-phase unit with a common magnetic core, magnetic coupling exists between its phases, which affects the optimal energization strategy.

Table I presents the optimum closing instants of individual transformer CB phases depending on the winding connection and neutral grounding arrangement of the primary winding. The desired closing instant is expressed as the phase angle of each individual phase relative to the reference instant, or by the zero crossing of the phase L1 voltage waveform. The energization strategy specifies that the winding listed first in Table I is energized first.

The described closing technique is based on measurement of the reference voltage and does not take the transformer remanent flux into account.

Table I Optimum closing instant depending on the transformer winding connection

Winding connection	Phase L1 [°]	Phase L2 [°]	Phase L3 [°]
YNd; YNyn	90	180	180
Yd; Yy; Dd; Dyn; Dy	60	60	150

3.2.1 Transformer with grounded neutral (YNd; YNyn). The following strategy applies to transformers whose energized winding is wye-connected with a grounded neutral point. In this configuration, phase L1 is energized first at the voltage peak, when the flux reaches its minimum value. Magnetizing current is established in this phase and flows through the grounded neutral of the winding. The magnetizing current in phase L1 induces a symmetrical flux in phases L2 and L3, whose magnitude is equal to one half of the flux in phase L1 and has the opposite polarity. As a result, the magnetizing current established in phase L1 is 1.5 times higher than the steady-state magnetizing current when all three phases are energized.

The remaining two phases should be energized simultaneously with a 90° phase shift relative to the first phase. At this instant, the magnetic flux in phase L1 reaches its maximum value, while the flux induced in phases L2 and L3 reaches the level corresponding to the flux that would be produced in those phases by the system voltage at that instant. Although phases L2 and L3 are not energized at the peak of their respective system voltages, the switching instant corresponds to the maximum magnetic flux induced in those phases by phase L1.

3.2.2 Transformer with isolated neutral (Yd; Yy; Dd; Dyn; Dy). For transformers with an isolated neutral point, energizing a single phase cannot establish magnetizing current due to the isolated neutral or the delta-connected winding configuration (D). Therefore, phases L1 and L2 are energized simultaneously at the maximum value of the phase-to-phase voltage $U_{L1\text{-}L2}$, corresponding to a 60° phase shift relative to the reference instant (the zero crossing of phase L1 voltage).

At the instant of energization, the flux amplitude in phases L1 and L2 is zero. The voltage of phase L3 reaches its peak with a 90° delay (60° + 90° = 150° relative to the reference instant). Energizing phase L3 at this instant ensures that switching occurs at minimum flux.

3.3 Controlled closing of capacitor bank circuit breakers

When voltage is applied to a discharged capacitor bank, which is a low-impedance element, at the instant of voltage maximum, a pronounced transient process occurs, which is characterized by overvoltages and high-amplitude inrush currents.

To minimize the potential difference during controlled closing, energization should take place as close as possible to the voltage zero crossing of each phase. Table II presents the optimal closing instants of the individual CB poles depending on the grounding arrangement of the capacitor bank neutral point.

Table II Optimum closing instant depending on the capacitor bank grounding

Capacitor bank neutral point	Phase L1 [°]	Phase L2 [°]	Phase L3 [°]
Grounded	0	120	60
Isolated	180	90	90

3.3.1 Capacitor bank with grounded neutral. For capacitor banks with a grounded neutral point, each phase is energized independently at its respective voltage zero crossing (Fig. 7). The zero crossing instants of the phase-voltage waveforms are mutually displaced by 60°.

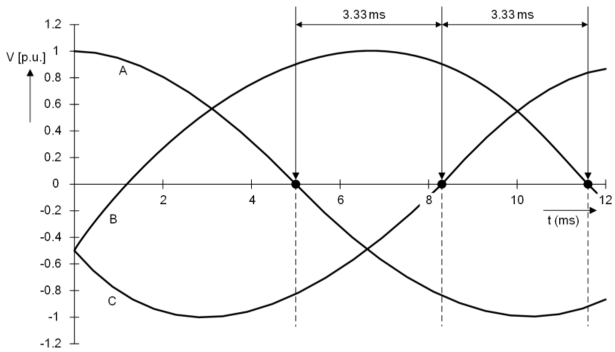

Figure 7. Optimal switching instants for a capacitor bank with grounded neutral

The closing sequence of the CB poles shown in Fig. 7 is L1–L3–L2, with a time shift of 3.33 ms for a 50 Hz system and 2.77 ms for 60 Hz systems.

3.3.2 Capacitor bank with isolated neutral. For capacitor banks with an isolated neutral point, zero-voltage closing is interpreted differently from that used for capacitor banks with a grounded neutral point. Instead of energizing each phase independently at its phase-voltage zero crossing, two phases are energized simultaneously (Fig. 8) at the instant when their phase voltages are equal. This corresponds to the instant when the phase-to-phase voltage $U_{L2\text{–}L3}$ is equal to zero, resulting in zero-voltage energization of phases L2 and L3. A quarter of a cycle later, phase L1 is energized at the instant its phase voltage passes through zero.

The key instants identified in Fig. 8 are:

1. controller reference instant – zero crossing of the phase L1 voltage;
2. energization instant of phases L2 and L3;
3. energization instant of phase L1.

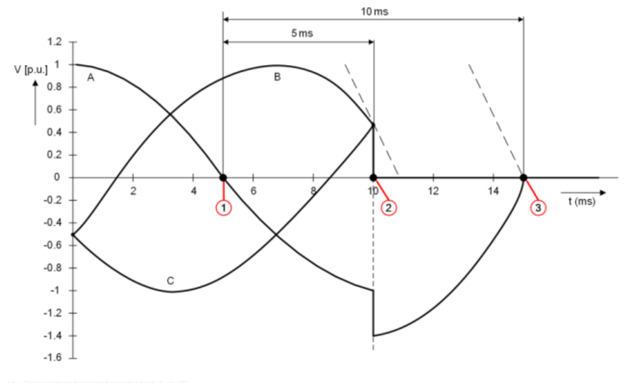

Figure 8. Optimal switching instants for a capacitor bank with isolated neutral

4. LABORATORY SETUP

The effects of controlled CB closing were tested under laboratory conditions using a 400 kV shunt reactor as a case study. A laboratory setup (Fig. 9) was assembled for this purpose, consisting of a microprocessor-based protection and control device acting as the CB controller, a network communication switch, and a Hardware-in-the-Loop (HIL) device implementing models of a 400 kV shunt reactor, a high-voltage (HV) circuit breaker, and a portion of the surrounding power system.

The process bus network (implemented in accordance with the IEC 61850 standard) was simplified and configured using a star topology with a single network switch. In addition to the information exchange function, the switch provides time synchronization via the IEEE 1588 Precision Time Protocol (PTP). which is required for generating valid Sampled Values.

4.1 Shunt reactor model

Within the HIL device, a 400 kV bay was modeled, comprising a shunt reactor, a CB, current transformers, and other relevant HV equipment. The shunt reactor is a nonlinear, wye-connected unit with a solidly grounded neutral. Its technical characteristics are summarized in Table III. The magnetic circuit is of a five-limb design and incorporates an air gap.

Table III Shunt reactor technical characteristics

Rated voltage	420 kV
Rated frequency	50 Hz
Rated power	250 Mvar
Rated current	343.66 A
Winding connection	Yn
Winding inductance	2.25 H (per phase)

The reactor CB was modeled as a switching device with independently controlled poles. Its technical characteristics are provided in Table IV.

Table IV Circuit breaker technical characteristics

Mechanical closing time of the circuit breaker	50 ms
Mechanical opening time of the circuit breaker	30 ms

The network was modeled as a Thevenin equivalent derived from the short-circuit power at the reactor point of connection. The magnitude and damping of reactor inrush currents are primarily determined by the reactor parameters and the CB closing instant. By contrast, network strength and electrical distance to the source are secondary and mainly affect the overvoltage magnitude rather than the effectiveness of controlled closing.

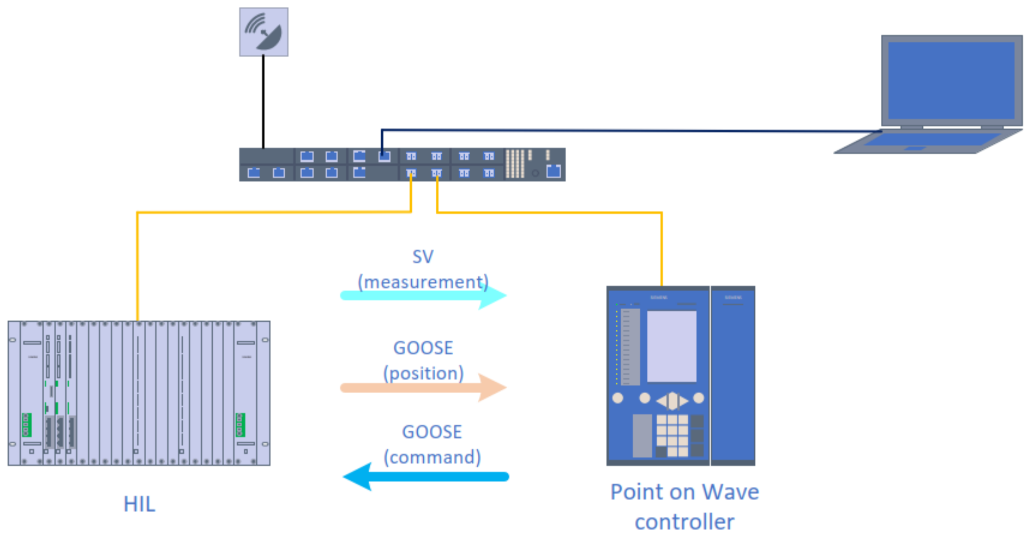

Figure 9. Block diagram of the laboratory setup

Including circuit resistance introduces additional transient damping and a slight shift of the optimum closing instant. However, it has no significant impact on the controlled switching strategy, nor does it significantly increase the error in determining the optimum closing instant.

The primary equipment model implemented on the HIL device was developed subject to the following limitations:

- there are no variations in operating times between individual CB poles, they always correspond to the predefined values in all three phases;
- a communication delay exists between the instant a command is issued by the controller and its reception by the HIL device. Since information exchange between the controller and the HIL device is performed via GOOSE messages, the maximum delay is limited to 1 ms;
- there is no time delay between electrical and mechanical contact establishment of the CB poles, as confirmed by the absence of arcing in the oscillographic records.

4.2 Circuit breaker controller

The controller functionality was implemented within a microprocessor-based protection and control device (Fig. 10). By analyzing the reference voltage waveform and taking into account configured parameters, such as the selected switching strategy and CB timing characteristics, the controller calculates and applies the optimum delay for energizing the CB closing coil.

The reference signal is obtained from a voltage transformer connected to the 400 kV busbars. It is generated by the HIL platform acting as an SV publisher, while the controller receives it as an SV subscriber through the process bus network. Instantaneous voltage values are transmitted as IEC 61850-9-2 Sampled Values (SV) streams.

Table V summarizes the SV stream contents. Each measurement stream contains samples of the three phase voltages and the residual voltage, together with the phase currents measured at the shunt reactor terminals and the calculated neutral current.

Information regarding the status of the switching equipment is generated by the HIL device in the form of GOOSE messages, while the controller transmits GOOSE messages to the HIL device containing commands for individual CB poles.

Table V Content of Sampled Values stream

IEC 61850-9-2 Sampled Value stream							
Busbar voltage				Shunt reactor current			
U_{L1}	U_{L2}	U_{L3}	$3U_0$	I_{L1}	I_{L2}	I_{L3}	$3I_0$
Pos 1	Pos 2	Pos 3	Pos 4	Pos 5	Pos 6	Pos 7	Pos 8

Monitoring functions are enabled in the controller. Following each closing operation, the controller collects and analyzes the recorded data and issues an alarm if abnormal conditions are detected. The following functions have been implemented:

- recording the measured inrush current and comparing it against a predefined threshold, which in this case is set to twice the rated current of the reactor;
- measuring the mechanical closing time of the CB using information from the breaker auxiliary contacts modeled in the HIL device and recording any deviation from the configured value;
- measuring the electrical CB closing time by detecting current establishment and recording any deviation from the calculated value.

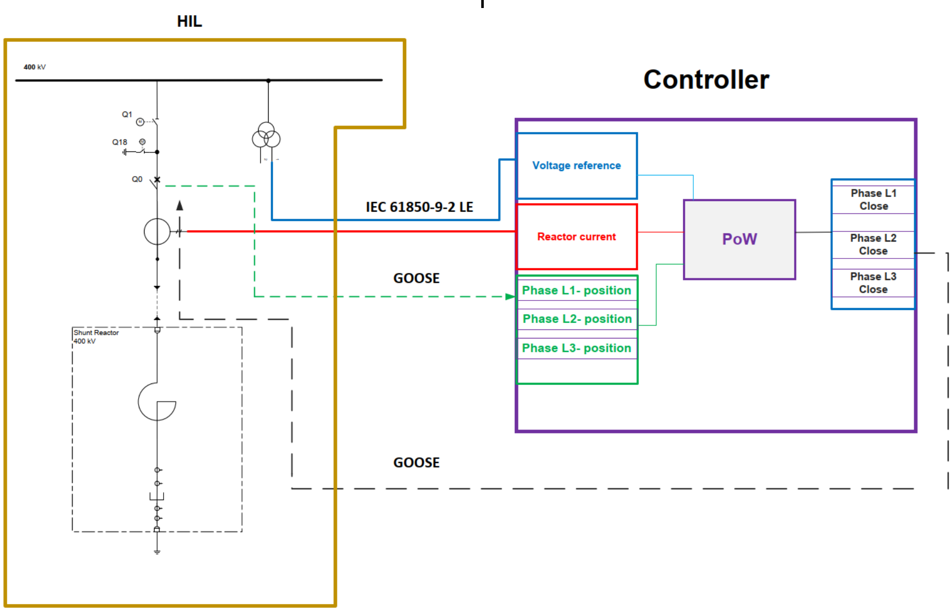

Figure 10. Logical diagram of information exchange between the HIL device and the controller

5. TEST RESULTS

The effectiveness of the proposed technique was evaluated by comparing three different shunt reactor CB closing strategies using the laboratory model:

1. Conventional closing – simultaneous random closing of all three CB poles;
2. Controlled closing with each pole closed at the most unfavorable instant;
3. Controlled closing with each pole closed at the optimum instant.

Following each closing, oscillographic records and event logs were retrieved from the controller. These data were used to evaluate and compare the voltage and current waveforms of the shunt reactor, as well as the status indications of the CB auxiliary contacts.

5.1 Conventional circuit breaker closing

Conventional closing is characterized by the simultaneous issuance of closing commands to all three CB poles. In this case, the controller acts as a passive element and introduces no intentional delay between the receipt of a closing command from the control system and its execution. Since the command may be issued at any point, both the degree of asymmetry and the magnitude of the inrush currents depend on the instant at which the command is issued, as well as on the CB operating time. The oscillographic record (Fig. 11) confirms the simultaneous closing of all three CB poles.

The record clearly shows the dependence of the inrush current value on the instantaneous value of the system voltage at the moment of closing. A pronounced inrush transient of long duration is observed. This leads to noticeable distortion of voltage and current waveforms, as well as high inrush currents.

In this case, the peak values were $I_{L1} = 1.63\ kA$, $I_{L2} = 2.88\ kA$ and $I_{L3} = 955\ A$. The peak current value in the reactor neutral conductor was $I_N = 1.86\ kA$.

5.2 Controlled closing of each circuit breaker pole at the most unfavorable instant

Since the shunt reactor is an inductive element, controlled closing of each CB pole at the voltage zero crossing in each phase represents the most unfavorable case. Under these circumstances, waveform distortion is most pronounced.

Although the controller aims to mitigate energization transients, improper parameter settings may lead to closing conditions under which adverse effects are maximized.

The voltage waveforms are shown in Fig. 15, while the current waveforms are presented in Fig. 16.

This switching condition produces exceptionally high peak inrush currents of $I_{L1} = 3.47\ kA$, $I_{L2} = 3.64\ kA$ and $I_{L3} = 3.80\ kA$. The asymmetry of the inrush currents becomes particularly pronounced, causing the reactor grounding conductor current to reach a peak value of $I_N = 3.33\ kA$ (Fig. 12).

Due to the duration of the inrush transient, unnecessary responses of the earth-fault protection may occur, depending on its operating time delay.

In addition, the high X/R ratio causes the DC component of the current to decay slowly, increasing the likelihood of current transformer saturation.

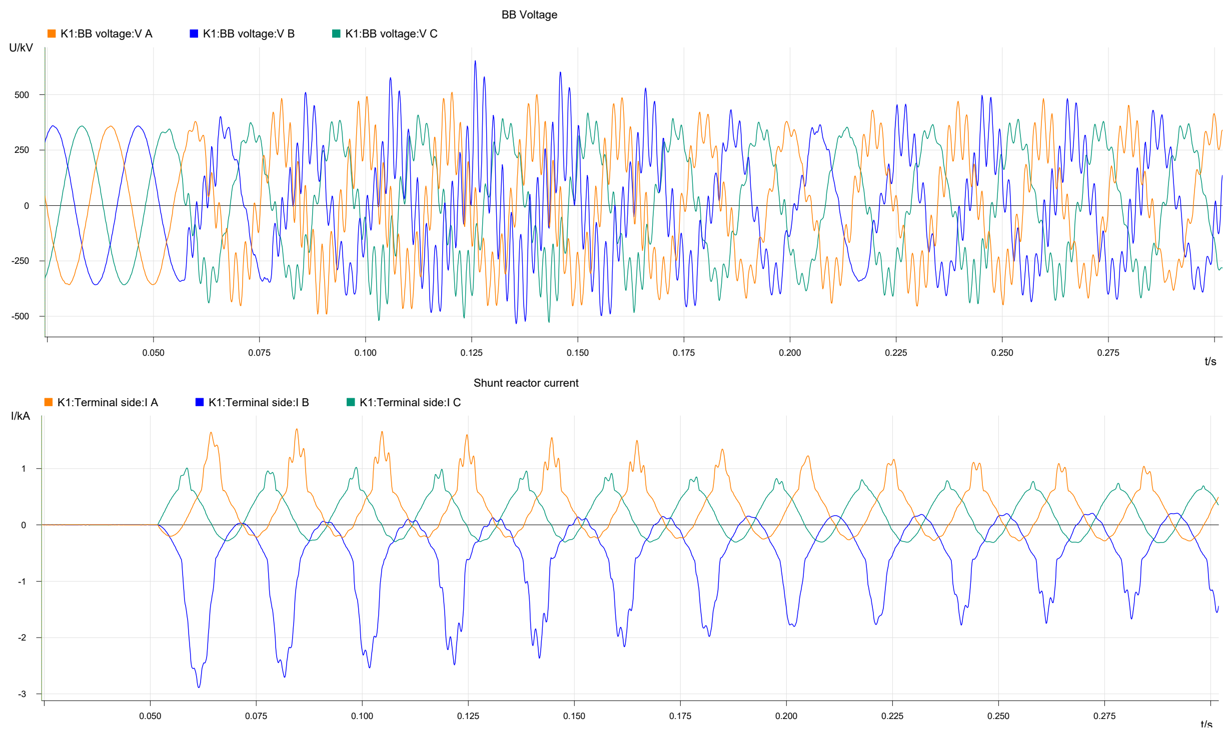

Figure 11. Voltage and current waveforms during conventional switching

5.3 Optimum circuit breaker closing

The optimum shunt reactor energization strategy is based on closing each CB pole at the voltage peak. The reference instant is defined as the zero crossing of the phase L1 voltage waveform. The controller is intended to close the L1 pole with a phase shift of 90° relative to the reference instant, i.e., when the phase L1 voltage reaches its maximum value.

The next voltage peak is reached by phase L3, with negative polarity, at 90˚ + 60˚ = 150˚, with a delay of 3.33 ms relative to phase L1. The final step is the closing of phase L2 with a theoretical delay of 90º + 120º = 210º, corresponding to 6.66 ms.

Fig. 13 shows the sequential issuance of pole-closing commands. Analysis of the event records confirms that no deviations from the theoretically calculated controller operating times were observed.

Analysis of the oscillographic records shows timely closing of each pole. This is illustrated by the phase L1 record shown in Fig. 14, where current establishment occurs at the voltage peak.

By comparing the voltage waveforms (Fig. 15) and current waveforms (Fig. 16), it can be concluded that controlled switching completely eliminates the inrush transient. With optimum switching, voltage waveform distortion is hardly noticeable, while higher harmonics are effectively eliminated.

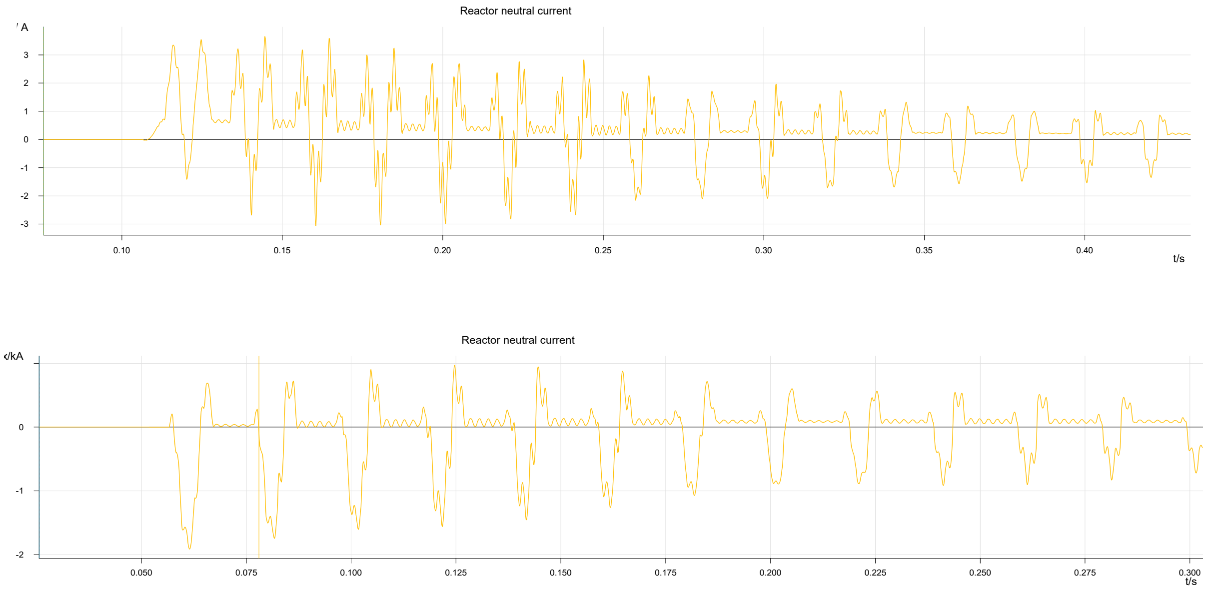

Figure 12. Reactor neutral current waveform under the most unfavorable (top) and conventional (bottom) switching conditions

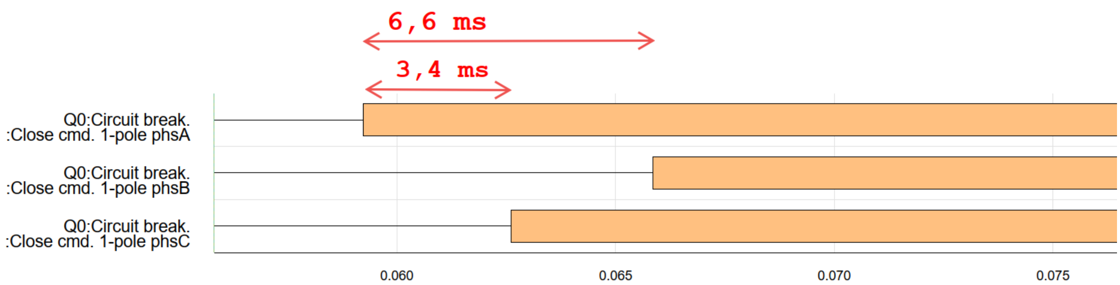

Figure 13. Sequence of circuit breaker pole closing commands

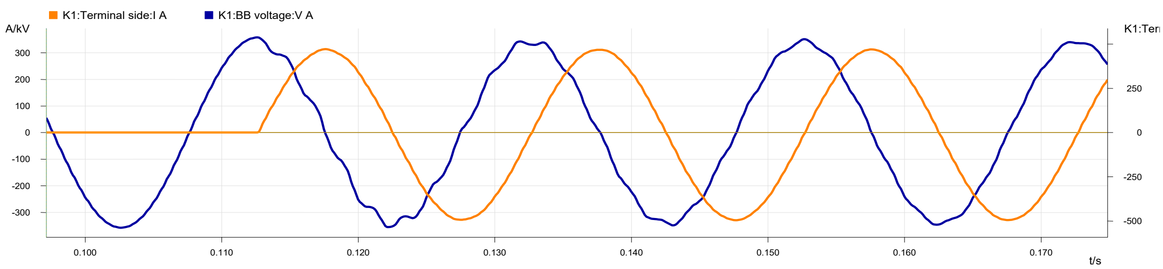

Figure 14. Current establishment instant relative to the voltage waveform

Controlled closing limits the peak inrush currents to $I_{L1} = 469\ A$, $I_{L2} = 523\ A$ and $I_{L3} = 488\ A$. The RMS current during the first cycle is approximately 340 A, corresponding to the rated current of the shunt reactor.

The controlled-closing results exhibit symmetrical current waveforms and no observable DC component. By eliminating the transient period, the peak current in the reactor grounding conductor is limited to $I_N = 358\ A$ (Fig. 17).

The oscillographic records indicate that the transient impulse of the neutral current lasted approximately 6 ms under optimum switching conditions, whereas in the most unfavorable case it exceeded 500 ms. The exact duration could not be determined because the recording window was limited.

The effectiveness of controlled closing in limiting reactor inrush currents can be evaluated by comparing the measured results obtained for all three switching strategies investigated on the laboratory model (Table VI).

The maximum measured inrush current was 3.80 kA, while controlled closing limited this value to a maximum measured current of 0.52 kA. Similarly, the suppression of current asymmetry reduced the peak current in the reactor grounding conductor from $I_N = 3.33$ kA to $I_N = 0.36$ kA.

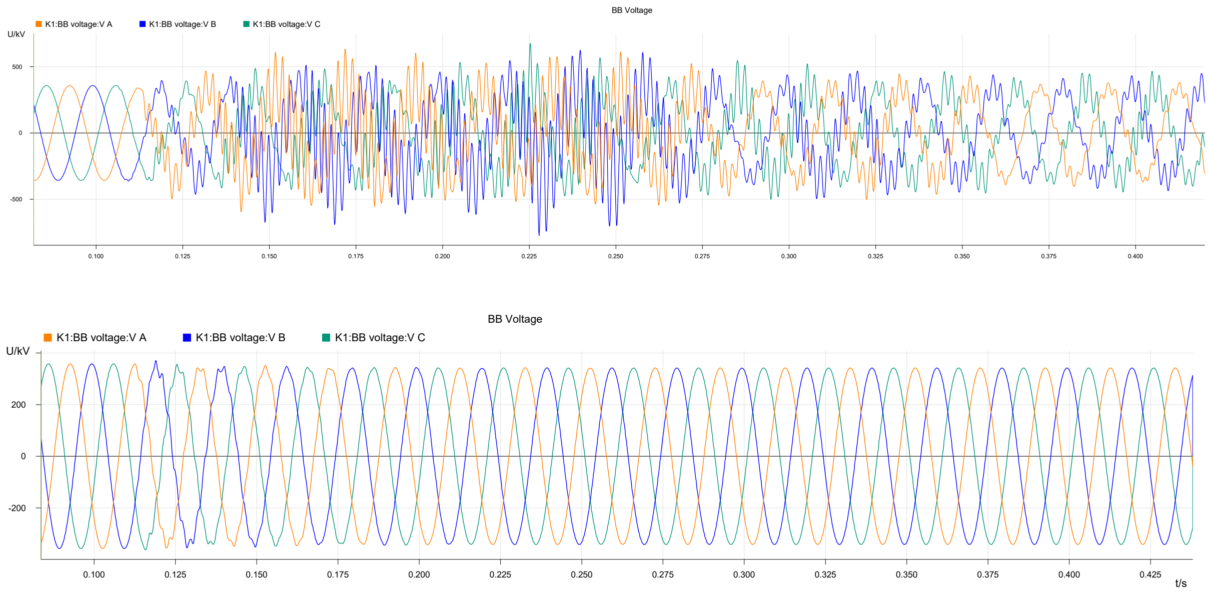

Figure 15. Voltage waveforms under the most unfavorable (top) and optimum (bottom) reactor switching conditions

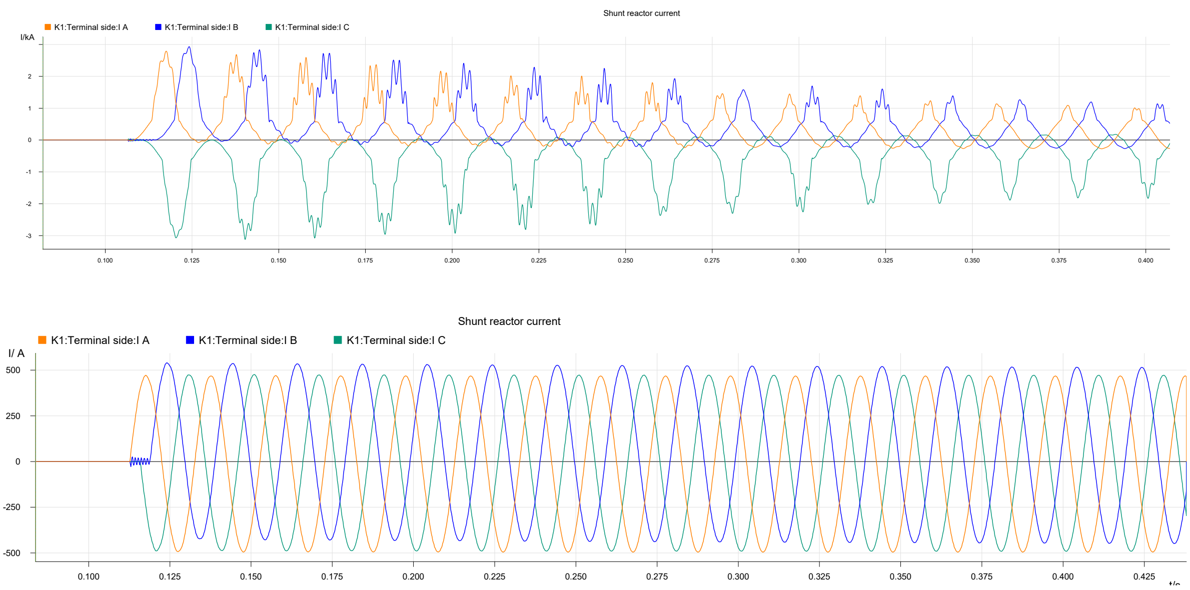

Figure 16. Current waveforms under the most unfavorable (top) and optimum (bottom) reactor switching conditions

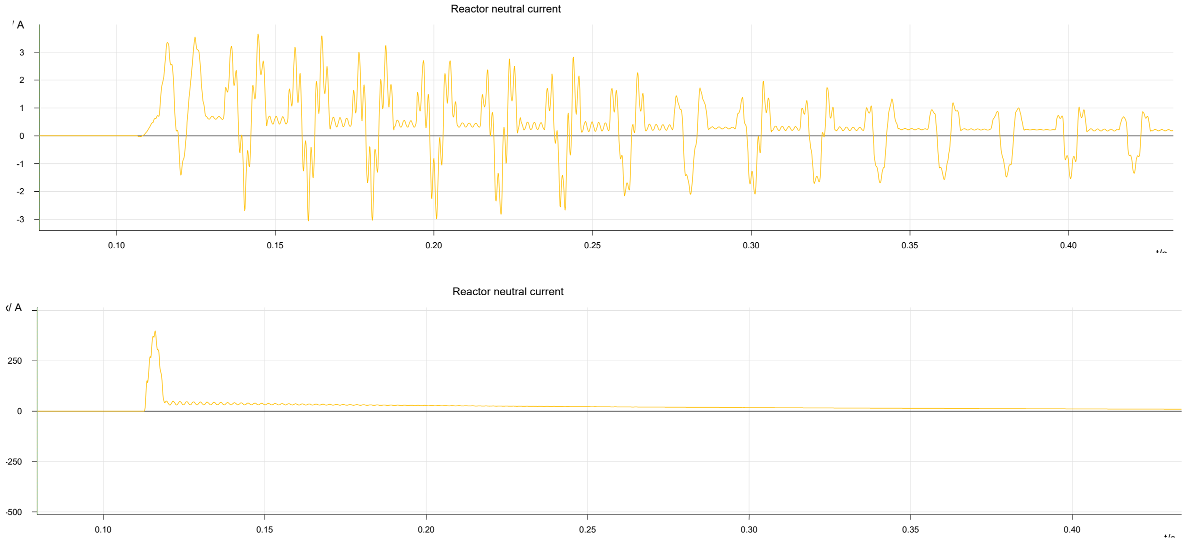

Figure 17. Reactor neutral current waveform under the most unfavorable (top) and optimum (bottom) switching conditions

Table VI Shunt reactor inrush current

Shunt reactor inrush current	Phase L1 [kA]	Phase L2 [kA]	Phase L3 [kA]	I_N [kA]
Conventional – uncontrolled circuit breaker closing	1.63	2.88	0.95	1.86
Controlled - closing at the most unfavorable instant	3.47	3.64	3.80	3.33
Controlled - closing at optimal instant	0.47	0.52	0.42	0.36

6. CONCLUSION

Conventional (uncontrolled) CB closing is inherently random, meaning that the waveforms depend on the voltage at the moment of closing. In general, uncontrolled closing results in significant voltage waveform distortion accompanied by a long-lasting transient process and high inrush currents, which may reach up to ten times the rated current. Neutral grounding conductor currents of up to 1.86 kA were observed and, due to the prolonged duration of the inrush transient, may lead to unwanted operation of protection functions.

Testing controlled switching at the most unfavorable instant proved particularly valuable. This approach provided consistent results, enabling an assessment of the benefits of optimum Point-on-Wave switching. The test results enabled the authors to gain insight into the critical importance of accurate coordination between controller parameters and CB timing. Each 1 ms deviation between the set and actual CB closing time corresponds to approximately 18° deviation from the optimum switching instant. The use of a controller with incorrectly configured parameters results in more severe switching transients compared to those resulting from random closing.

Analysis of the oscillographic records obtained for the three investigated 400 kV shunt reactor CB closing strategies, including a comparison of current and voltage waveforms as well as measured inrush current values, confirmed that controlled switching can completely eliminate the inrush transient.

Continued technological advances are increasing the flexibility, reliability, and ease of application of controlled switching systems while simultaneously reducing implementation costs. This enables their broader deployment across power systems.

Finally, it should be noted that shunt reactor de-energization also presents several technical challenges, including current chopping, transient recovery voltage control, and arc re-ignition. These issues will be addressed in the authors' future research.

ACKNOWLEDGEMENT

This work was financially supported by the Ministry of Science, Technological Development and Innovation of the Republic of Serbia under Contract No. 451-03-137/2025-03/200103.

REFERENCES

[1] European Network of Transmission System Operators for Electricity: „Controlled Switching Device: Application, Use And Maintenance Problems”, Final 16 November 2022.

[2] Yahiou A., Mellaha H., Bayadib A., „Inrush Current Reduction by a Point-on-Wave Energization Strategy and Sequential Phase Shifting in Three-Phase Transformer”, *International Journal of Electrical Engineering,* Vol. 35 No. 12, p.p. 2321-2328, December 2022.

[3] Dhotre D., Rajguru G., Belhekar V., Kulkarni P., „Reduction of Transient Inrush Current in Transformer Using Point-on-Wave Switching Method”, *International Journal of Scientific Development and Research,* Vol. 2 No. 5, p.p. 433 – 436, May 2017.

[4] SIPROTEC 5 Point-On-Wave Switching Manual V9.90, document reference C53000-H5040-C082-7, edition 11. 2024.

[5] Goldsworthy D., Roseburg T., „Controlled Switching of HVAC Circuit Breakers: Application Examples and Benefits”, *34th Annual Western Protective Relay Conference*, Spokane, Washington, October 2007.

[6] Faiz M., Chang, A. Q., Mirjat, B. A., Memon N., „The Simulation Analysis of Shunt Reactor Controlled Switching at 500 kV Network”, *International Journal of Electrical Engineering & Emerging Technology*, Vol. 05, No. 02, p.p. 31-37, December 2022.

[7] Kumar A., Perveen R., Parikh U., „Controlled Switching of Power Transformer and Shunt Reactors for Minimization of Switching Transients: A Review”, *Journal of The Institution of Engineers* (India), Vol. 103, p.p. 1013–1024, October 2021.

BIOGRAPHIES

Uroš Njegovan was born in Pančevo, Serbia, in 1990. He completed high school in his hometown. He continued his education at the School of Electrical Engineering, University of Belgrade, where he obtained his Bachelor's and Master's degrees. In 2024, he enrolled in PhD studies at the Department of Power Systems at the same faculty. He is currently employed at Siemens Energy d.o.o. Belgrade. His professional interests include power system protection and the digitalization of power substations.

ORCID: 0009-0000-5626-0969

Zoran Stojanović was born in Požarevac, Serbia, in 1979. He completed general secondary school in Svilajnac. He received his B.Sc., M.Sc., and Ph.D. degrees from the School of Electrical Engineering, University of Belgrade, in 2003, 2009, and 2012, respectively. He was appointed Full Professor at the same faculty in 2022. He is also a visiting professor at the Faculty of Electrical Engineering, University of Banja Luka, the Faculty of Technical Sciences, University of Novi Sad, and the Faculty of Electronic Engineering, University of Niš. His research and professional interests include power system protection, substations, digital signal processing, monitoring and diagnostics of high-voltage equipment.

ORCID: 0000-0003-2432-394X

Aleksandar Marjanović was born in Belgrade, Serbia, in 1991. He completed primary and secondary education in Valjevo. He continued his studies at the School of Electrical Engineering, University of Belgrade, where he obtained his Bachelor's and Master's degrees. In 2024, he enrolled in PhD studies at the Department of Power Systems at the same faculty. He is currently employed at Siemens d.o.o. Belgrade. His professional interests include power system and substation control, digitalization of power substations, integration of renewable energy sources and energy storage systems, as well as microgrid management.

ORCID: 0009-0004-3318-8967

UDK: 621.311.1:621.318.43
621.316.542:621.3.015.3

Uroš N. Njegovan[1,2], Zoran N. Stojanović[1], Aleksandar D. Marjanović[1,3]

Ograničenje sklopnih tranzijenata primenom tehnike kontrolisanog uključenja prekidača (Point-on-Wave)

[1] Univerzitet u Beogradu – Elektrotehnički fakultet, Beograd, Srbija*
[2] Siemens Energy d. o. o. Beograd – Beograd, Srbija
[3] Siemens d. o. o. Beograd – Beograd, Srbija

Originalni naučno-istraživački rad

Ključne poruke

- Predstavljeni efekti sklopnih tranzijenata usled priključenja različitih vrsta opterećenja
- Opisana tehnika kontrolisanog uključenja prekidača
- Efekti primene tehnike testirani na simulatoru u realnom vremenu
- Izvršeno poređenje sa konvencionalnim uključenjem prekidača kompenzacione prigušnice

Kratak sadržaj

Podopterećena prenosna mreža, odnosno vodovi opterećeni ispod svoje prirodne snage, značajan su izvor reaktivne snage sa posledicom lokalnog povećanja napona. Kao sredstvo regulacije naponskih prilika operatorima prenosnog sistema širom sveta nametnula se upotreba paralelno priključene prigušnice (engl. Shunt Reactor) u kombinaciji sa konvencionalnim visokonaponskim prekidačem. Implementacija ovakvog rešenja dovodi do značajnog porasta broja sklopnih tranzijenata. Primenom tehnike kontrolisanih operacija prekidača (Point-on-Wave), kroz pojedinačno uključenje/isključenje svakog pola prekidača u najpovoljnijem trenutku, u velikoj meri se mogu ograničiti vrednosti udarne struje uključenja prigušnice i povratnog napona pri isključenju. U radu su predstavljeni negativni efekti nekontrolisanog priključenja paralelnih prigušnica na prenosni sistem. Opisana je tehnika kontrole trenutka uključenja prekidača kao mera ograničavanja negativnih uticaja sklopnih tranzijenata. Funkcija kontrole prekidača i potencijalni efekti primene u prenosnoj mreži su testirani u laboratorijskim uslovima. Laboratorijska postavka se sastoji od mikroprocesorskog uređaja za zaštitu i upravljanje kao kontrolera i simulatora u realnom vremenu (HIL – Hardware-in-the-Loop) na kome je realizovan model 400 kV paralelne prigušnice i prekidača. Uređaji komuniciraju korišćenjem IEC 61850 Sampled Values i GOOSE protokola. Dobijeni rezultati potvrđuju skoro potpunu eliminaciju udarnog perioda prilikom uključenja kompenzacione prigušnice.

Ključne reči

Kompenzaciona prigušnica, kontrolisano uključenje prekidača, simulacija *Hardware-in-the-Loop*, udarna struja prigušnice

Primljeno: 26. decembar 2025. Recenzirano: 19. mart 2026.
Izmenjeno: 6. maj 2026. Odobreno: 12. maj 2026.

* Korespondirajući autor: Uroš N. Njegovan, +381 60/81-70-242
Imejl: uros.njegovan@siemens-energy.com

Napomena:
Ovaj članak predstavlja proširenu, unapređenu i dodatno recenziranu verziju rada „*Primena tehnike kontrolisanog uključenja prekidača (Point-on-Wave) na primeru kompenzacione prigušnice 400 kV u mreži*" (https://doi.ub.kg.ac.rs/doi/cigre37-b5-08/), nagrađenog u Studijskom komitetu STK-B5 *Zaštita i automatizacija,* na 37. Savetovanju CIGRE Srbija, Zlatibor, 26-30. maja 2025.

UDC: 621.311.1(497.11)
621.311:351.824.11(497.11:4-6EU)

Marija Đorđević[1], Srđan Mladenović[1], Ivana Stamenić[1], Branko Šumonja[1]

Implementation of European Processes in the Operational Activities of EMS JSC

[1] Joint Stock Company Elektromreza Srbije Belgrade, Serbia*

Professional article

Highlights

- This paper examines the coordinated processes taking place at the level of European Transmission System Operators, as well as the key changes currently being implemented in the operational activities of EMS JSC
- Particular emphasis is placed on the two most important processes, namely coordinated security analysis and coordinated transmission capacity calculation
- A technical framework has been established for defining a region for coordinated capacity calculation in South-Eastern Europe
- The paper also assesses the ability of the Serbian Transmission System Operator to fulfil its regulatory obligation to allocate transmission capacity in accordance with the MACZT methodology

Abstract

At the level of ENTSO-E and across Europe, processes are under way that directly impact the Serbian power sector and the day-to-day operations of the Transmission System Operator. Two key ENTSO-E processes — coordinated security analysis and coordinated transmission capacity calculation — are implemented in a coordinated manner. Within the framework of transmission capacity calculation, two methodological approaches are applied: the Net Transfer Capacity (NTC) method and the flow-based method. This paper presents the regulatory process of EMS JSC joining the European capacity calculation regions — CORE and the South-Eastern Europe (SEE) region — with particular emphasis on the challenges faced by EMS JSC in this context. Furthermore, the fundamental concepts of coordinated processes are outlined, which will be implemented partly within the Transmission System Operator and partly through the regional coordination centres. Irrespective of the transmission capacity calculation methodology applied at different stages, compliance with the rule requiring the allocation of 70% of the capacity of critical network elements is mandatory. The paper presents preliminary results regarding compliance with this requirement, bearing in mind that its implementation is obligatory under the Energy Law.

Keywords

ENTSO-E, MACZT (*Margin Available for Cross-Zonal Trade*), RCC (*Regional Coordination Centre*), TSO (OPS)

Note:
This article represents an expanded, improved and additionally peer-reviewed version of the paper "*Coordinated Processes in EMS AD in Compliance with the Latest European Regulations*" (https://doi.ub.kg.ac.rs/doi/cigre37-c5-08/), awarded by Expert Committee EC-C5 *Electricity Market and Regulation* at the 37th CIGRE Serbia Conference, Zlatibor, May 26-30, 2025

Received: December 19th, 2025 Reviewed: (Editor's input)
Modified: (Editor's input) Accepted: (Editor's input)
* Corresponding author: Marija Đorđević, +381 64 840 86 69
E - mail: marija.djordjevic@ems.rs

1. REGULATORY FRAMEWORK

The new legislative framework, through which European regulation has been transposed, has introduced a new reality in operational planning and management of the transmission system.

According to the decision of the Ministerial Council of the Energy Community (Energy Community, EnC), adopted on 15 December 2022 regarding the transposition of European regulations related to the electricity sector into the legislative frameworks of all Energy Community members, EnC countries undertook the obligation to complete the transposition into national legislation by the end of 2023.

The regulations in question include the CEP (Clean Energy Package) regulations: 2019/942, 2019/943 and 2019/941, as well as five network codes (SOGL, ER, CACM, FCA and GL EB). This represents a significant step towards integrating the Republic of Serbia into the single European electricity market.

In this way, European network codes have become a binding obligation, unlike the earlier "early implementation" of network codes which allowed a certain degree of discretion.

One of the key obligations of the contracting parties of the Energy Community within the process of transposing European regulation is the definition of regions for the implementation of coordinated activities such as security analyses and capacity calculations.

The main provisions relating to the daily activities of Transmission System Operators include the establishment of operational security regions and regions for the calculation of transmission capacities.

Another important element in coordinated transmission capacity calculations is related to the fulfilment of the criterion of "allocation of 70% of transmission capacity" or the MACZT criterion. This requirement may lead to situations where security issues must be resolved over shorter time horizons such as the intraday timeframe and the timeframe close to real time.

In addition, congestion management is expected to be addressed through redispatching and counter-trading mechanisms, which may have significant operational and financial implications.

2. COORDINATED REGIONAL PROCESSES

This paper does not address the political connotations related to the definition of regions, but rather focuses solely on technical parameters.

The definition of operational security regions (Security Operational Region – SOR) has existed for several decades in South-Eastern Europe, primarily as a response to the need for coordinated planning of outages on annual, monthly and weekly time horizons.

This practice arose from the necessity of mutual coordination of activities among the Transmission System Operators, particularly with regard to key 400 kV, 220 kV and interconnection transmission lines.

Later, this approach became institutionalised through the establishment of Regional Coordination Centres (RCC), which expanded the scope of coordination to other planning activities, such as:

1. System modelling across various time horizons: intraday, day-ahead, two-days-ahead, weekly, monthly and yearly horizons. These activities include the preparation of individual models as well as a common grid model of the interconnected system, which represents the basis for all planning activities.
2. Coordination of operational security and verification of compliance with the security criteria N-1 and N-x, where security coordination centres play the dominant role.
3. Coordination of regional and ENTSO-E short-term adequacy assessments (Short-term Adequacy – STA).
4. Coordination of operational outage planning for all relevant network elements at the ENTSO-E level (Operational Planning Coordination – OPC).

JSC EMS participates in the creation of the Common Grid Model (CGM), which serves as the basis for all calculations related to transmission system security and transmission capacity calculations.

The creation of a common pan-European model is carried out on a rotational basis by all European regional coordination centres. The unified model is used throughout Europe and within our region.

Such a jointly generated model is used in analyses at the level of the entire ENTSO-E network, including the region in which JSC EMS operates, thereby ensuring coordinated planning and operational security of the system.

When it comes to regional coordination of security in South-Eastern Europe, which includes both European Union member states and non-EU countries, a European approach and a dynamic scheduling of activities are applied. The objective is to identify potential critical situations already during the day-ahead planning stage and to take corrective measures in a timely manner.

Countries within European security regions have implemented a highly complex coordinated security process that is carried out within precisely defined time intervals.

Transmission System Operators are required to submit their network models (IGM) for the following day by 18:00. The creation of the common grid model (CGM) is completed within the following hour, after which a regional operational security analysis (Cross-Regional Operational Security Assessment – CROSA) is performed. If overloads are identified, corrective measures must be applied and new network models created, followed by another coordinated operational security analysis, known as CCROSA (Coordinated Cross-Regional Operational Security Assessment).

This operational regime requires planning activities to extend into the afternoon shift, often until 22:00. Each phase of the process is accompanied by teleconferences in which both Transmission System Operators and regional coordination centres actively participate.

In our region, in cooperation with SCC (Security Coordination Centre), the most important activities are carried out, representing an introduction to the full implementation of the CROSA process, as described below.

The preparation of the D-1 models is performed by 18:00, followed by the merging of the common grid model and the execution of security analyses.

Coordination teleconferences are organised on a daily basis between 20:00 and 22:00, based on the conducted security analyses, in order to review and, if necessary, apply corrective measures ("remedial actions"). These actions may have no financial impact, but may also include measures that entail operational financial costs.

A prerequisite for the full implementation of the CROSA process is the definition of Operational Security Regions (SORs). At the ENTSO-E level, SOR frameworks have been defined (Figure 1), within which all functionalities prescribed by regulation are carried out in a coordinated manner in cooperation with other TSOs and Regional Coordination Centres: Central, Baltic, Nordic, IU, South West (SW), GRIT and South East (SE).

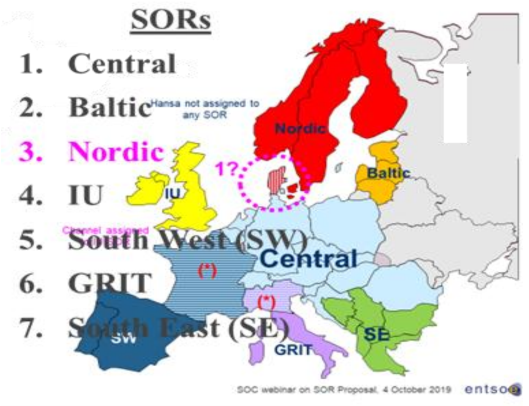

Figure 1. Initial definition of Operational Security Regions

The transposition of European Union regulation is currently ongoing. In the case of the Energy Community region, the SOR is in the process of being redefined. It is expected that the future definition of SOR will be aligned with the definition of regions for transmission capacity calculation.

3. CAPACITY CALCULATION REGIONS

In Europe, regions for coordinated transmission capacity calculation, known as Capacity Calculation Regions (CCR), have already been defined. Each of these regions has developed its own methodologies adapted to the specific characteristics of the region.

Currently defined CCRs include: Baltic region, Central Europe, CORE region, Greece–Italy region, Hansa region, Northern Italy region, Nordic region, SEE region (South-Eastern Europe), SWE region (South-Western Europe).

Within the Energy Community countries, the process of regulatory transposition is ongoing, and the regions for transmission capacity calculation are being defined at the level of Energy Community member states.

As an alternative to the so-called "default" solution, which was initially proposed by the Ministerial Council, and due to the atypical characteristics of certain Energy Community countries, an alternative solution is being implemented. This solution envisages the integration of trading zones into two existing European regions or CCRs.

Figure 2 shows the Central Europe region and the South-Eastern Europe region, to which Serbia is expected to be connected in the near future. Under this arrangement: JSC EMS, the Serbian Transmission System Operator, CGES, the Montenegrin Transmission System Operator and NOS BiH, the Transmission System Operator of Bosnia and Herzegovina, would join the CE/CORE region, while other Transmission System Operators from Energy Community countries would join the SEE European region.

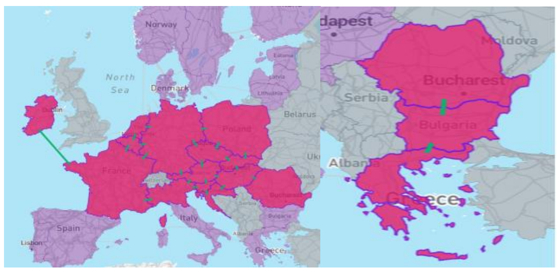

Figure 2. Overview of CCR regions in Central Europe and South-Eastern Europe

Figure 3. Definition of capacity calculation regions

This solution has already been implemented. There are several technical indicators confirming the justification of such a division, some of which are the following:

- Analysis of several major disturbances that occurred over the last twenty years, which affected the entire synchronous area, showed system separations in Croatia, Hungary, Serbia and Romania. This revealed weak points that must be analysed in a coordinated manner.

- It is important to establish coordinated transmission capacity calculations based on power flows or through the use of coordinated NTC (Net Transfer Capacity) as a transitional solution. This would avoid uncontrolled power flows (loop flows), which are one of the main sources of insecurity in the transmission network.

- The effect of achieving 70% capacity allocation, since the impacts of flows that are not controlled and originate from other zones must also be taken into account. Currently, within JSC EMS a strong influence of planned commercial flows on the Hungary–Romania border can be observed, while physical flows are closed through the transmission network of Serbia. The flow pattern is shown in Figure 4 for an atypical day during which there was a significant northbound transit, due to extremely high electricity generation from solar sources in Greece.

There are also strong influences of power flows from the South-Eastern Europe region on flows within the CORE region. For example:

- the 400 kV transmission line Ugljevik – Mitrovica has a PTDF (Power Transfer Distribution Factor) influence of up to 13% on the CORE region

- the 400 kV transmission line Trebinje – Lastva also has an influence of up to 13%

This demonstrates that there is a strong interaction between different CCR regions, which must be considered in order to calculate available transmission capacities as accurately as possible.

For these reasons, the currently predefined Shadow SEE CCR region is being reconfigured. An alternative solution is being developed in which: JSC EMS, CGES and NOSBiH would join the CE / CORE region.

Under this arrangement, daily capacity calculations would be performed using the flow-based method, where each individual network element is analysed under the most critical contingency scenarios.

From both technical and regulatory perspectives, the most optimal solution would be to define the entire continental Europe as a single flow-based capacity calculation region (flow-based CCR).

Figure 4. Scheduled exchanges and physical flows at regional borders on 9 February 2025 at 11:30

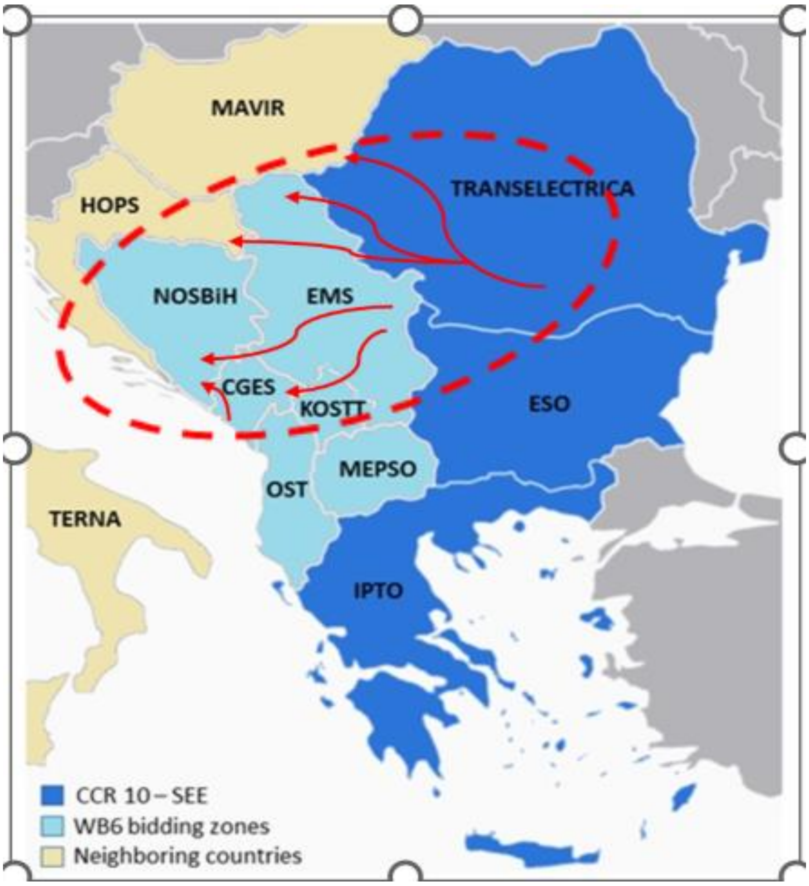

Figure 5. Impact of cross-border exchanges between the CORE region and Balkan countries

4. METHODOLOGY FOR APPLYING MACZT AS AN INDICATOR OF CROSS-BORDER CAPACITY AVAILABILITY

ACER (the Agency for the Cooperation of Energy Regulators) has developed a Recommendation for determining the minimum available capacity between bidding zones (Margin Available for Cross-Zonal Trade – MACZT), which provides the basis for calculating available capacities between bidding zones and ensures a harmonised and transparent approach across all countries in the region:

"Recommendation No 01/2019 of the European Union Agency for the Cooperation of Energy Regulators of 08 August 2019 on the Implementation of the Minimum Margin Available for Cross-zonal Trade Pursuant to Article 16(8) of Regulation (EU) 2019/943".

The Margin Available for Cross-Zonal Trade (MACZT) is used as a technical indicator of the availability of the transmission network for cross-border electricity exchanges. The application of MACZT enables the linkage between the physical constraints of the transmission system and cross-border power flows, with the aim of identifying structural and operational factors affecting the level of available capacities.

MACZT is determined and monitored for the Critical Network Element with Contingency (CNEC). For each analysed time horizon and critical network element, MACZT represents a measure of the physical capacity of the transmission network made available for cross-border trade.

MACZT is defined as the sum of the margin obtained through coordinated cross-border capacity calculation and the impact of flows not included in the coordinated capacity calculation:

$$\boldsymbol{MACZT_i = MCCC_i + MNCC_i}\ , \qquad (1)$$

where index *i* denotes the limiting critical network element with contingency.

The Margin from Coordinated Capacity Calculation (MCCC) represents the portion of the margin available for cross-border trade that results from coordinated cross-border capacity calculation within the defined coordination region.

MCCC reflects the impact of cross-border exchanges on critical network elements that are jointly planned and calculated by multiple Transmission System Operators in accordance with agreed methodologies within the same coordination region.

In the case of applying the coordinated NTC approach, MCCC is calculated as the sum of the products of positive PTDF values of the critical network element and the net transfer capacities of individual oriented cross-border directions:

$$\boldsymbol{MCCC_i = \sum_b pPTDF_{i,b} \cdot NTC_b}\ , \qquad (2)$$

where:

1. $pPTDF_{i,b}$ represents the positive value of the PTDF factor of critical network element i in the direction of the corresponding oriented cross-border direction *b,*
2. NTC_b represents the net transfer capacity determined in the capacity calculation process for cross-border direction b for the considered time horizon.

Equation (2) therefore includes all cross-border directions within the analysed coordination region.

In this way, MCCC represents the portion of available margin that is directly controlled by coordinated capacity planning and largely reflects the efficiency of the cross-border capacity calculation process within the coordination region (CCR).

The Margin from Non-Coordinated Capacity Calculation (MNCC) represents the portion of the margin that reflects the impact of flows not included in the coordinated capacity calculation, i.e. flows originating from exchanges outside the coordination region (CCR).

This component includes the impact of:

1. flows that are not subject to regional coordinated calculation,
2. net positions of bidding zones not included in the coordinated capacity calculation.

MNCC is determined based on relevant PTDF values and corresponding net exchanges/positions that cause physical power flows in the network, which Transmission System Operators cannot directly optimise within the coordinated capacity calculation framework.

MNCC is often a negative component, as non-coordinated flows may additionally load critical network elements and reduce the margin available for cross-border trade.

The application of the MACZT methodology enables quantification of the total margin available for cross-border trade and separation of its components into coordinated (MCCC) and non-coordinated (MNCC) parts.

The analysis of these components shows that limitations in cross-border capacity availability do not arise solely from the capacity calculation process, but are largely conditioned by physical constraints of the transmission network.

The part related to physical network congestion will be described in detail in Chapter 6 of this paper, which refers to the obligation of the TSO to develop an Action Plan.

5. PRELIMINARY ASSESSMENT OF COMPLIANCE WITH THE MACZT CRITERION (70% ALLOCATED CAPACITY)

JSC EMS has been implementing elements of coordinated calculations of available transmission capacities for more than a decade at the level of South-Eastern Europe, in cooperation with Transmission System Operators from the region. The main joint activities include the harmonisation of totals, exchange of monthly individual models, and the creation of a unified common grid model on which calculations are performed according to the Net Transfer Capacity (NTC) methodology. Coordination is carried out on the basis of agreements between TSOs in accordance with an annual calendar.

With the introduction of Regional Coordination Centres (RCCs), capacity calculation processes have been elevated to a significantly higher level, particularly in terms of time horizons and methodological accuracy. Our regional RCC – SCC – performs weekly calculations of NTC values for all bidding zones of operators using its services.

With the introduction of the network code “Guideline on Capacity Allocation and Congestion Management (CACM)”, which has been transposed into national legislation through the “Regulation establishing guidelines for capacity allocation and congestion management”, day-ahead and intraday calculations must be performed within RCCs using a flow-based methodology. In certain cases, the temporary application of the NTC methodology is allowed, provided that operators demonstrate that the flow-based approach would not be more efficient, assuming an identical level of system security.

In both methodological approaches to transmission capacity calculation, it is necessary to fulfil the rule of “70% allocated capacity”, also referred to as the MACZT rule.

The new Energy Law precisely defines the obligation to fulfil this criterion for both methodological approaches.

For borders between bidding zones where the harmonised Net Transfer Capacity (NTC) methodology is applied, Transmission System Operators are required to ensure that at least 70% of the capacity of the identified critical element is made available for cross-border trade, provided that security criteria for the defined contingency list are satisfied.

For borders between bidding zones where flow-based capacity calculation is applied, the minimum capacity corresponds to the margin available for flows resulting from exchanges between bidding zones for each critical network element. This margin must amount to 70% of the capacity, while the remaining 30% may be used for reliability margins, loop flows and internal flows.

JSC EMS analysed the obligation to fulfil the 70% capacity allocation criterion even before the new Energy Law entered into force and timely procured a TNA tool with the required performance characteristics. Preliminary analyses conducted by JSC EMS for 2024 and partially for 2025 indicate that the level of compliance with the MACZT criterion (70% allocated capacity for cross-border trade) ranges from 30% to 70% of MACZT, relative to the capacity calculated by JSC EMS.

However, the harmonised (final) NTC value also depends on calculations performed by neighbouring Transmission System Operators, since the lower of the two proposed values is adopted at each border. Furthermore, JSC EMS has been transparently monitoring KPI (Key Performance Indicators) for several years. It is often observed that, during bilateral harmonisation of transmission capacities, the neighbouring TSO was the cause of the lower final harmonised value that was subsequently allocated.

Nevertheless, all countries – both EU Member States and non-EU countries – are required to comply with the prescribed rule, and therefore all TSOs will strive to achieve the required 70% allocated capacity.

Table I presents an estimate of compliance with the MACZT criterion based on average allocated capacities over the last three years for selected borders. The principle applied was to adopt either the higher value of the average directional capacity or the value from 2024. The percentage of compliance, relative to winter limits, ranges from 28% to 49%.

Table I – Percentage of compliance with the MACZT criterion based on average allocated NTC values

	Agreed NTC	Maximum capacity	% of current value	MACZT 70%
RS-HU	644	1329	49	70
RS-RO	543	1770	31	70
RS-BG	392	1511	26	70
RS-MK	583	1329	44	70
RS-ME	306	868	35	70
RS-BA	539	1931	28	70
RS-HR	500	1502	33	70

The paper also presents results obtained if MACZT calculations are performed according to the defined ENTSO-E methodology, rather than based on average allocated transmission capacities. First, the principle of assessing the MACZT criterion is presented, followed by aggregated results of compliance for several months in 2025 and 2024.

In Table II, April 2025 is analysed, providing an example where the MACZT criterion is fulfilled, reaching 75% on the critical element – the 400 kV transmission line Porţile de Fier– Đerdap – under contingency scenarios involving outages of several critical 400 kV lines: Bor 2 – Đerdap, Bor 2 – Niš 2, Pančevo 2 – PRP Čibuk and Drmno – PRP Čibuk.

Table II – MACZT values for NTC calculation from Bulgaria and Romania towards Serbia

Critical outage	Critical branch	MACZT [%]
OHL 400 kV Bor 2 - Djerdap	OHL 400 kV Portile de Fier - Djerdap	74
OHL 400 kV Bor 2 - Nis 2		83
OHL 400 kV Pancevo 2 - SS Cibuk		75
OHL 400 kV SS Drmno - SS Cibuk		74

The EMS proposal for the composite NTC at the border RS → BG + RO was 1900 MW, while the NTC target required to achieve 70% capacity ranged from 1596 MW to 1801 MW.

In the opposite direction, BG + RO → RS, a MACZT value of 69% was achieved when JSC EMS proposed a composite NTC of 1900 MW. In order to reach the 70% MACZT criterion, the offered NTC would need to be 1928 MW. The results are shown in Table III.

Table III – MACZT values for NTC calculation from Bulgaria and Romania towards Serbia

Critical outage	Critical branch	MACZT [%]
TR 1 400/110 Bor 2	TR 2 400/110 Bor 2	69
TR 2 400/110 Bor 2	TR 1 400/110 Bor 2	69

An example from June 2024 was analysed for the border RS → HR, BA, where compliance with the criterion was 57%, while EMS proposed a composite NTC of 1200 MW. Already at an NTC value of 843 MW, overloading occurs on the critical branch – the 220 kV line Obrenovac – Valjevo 3 – in the contingency scenario involving outage of the 400 kV line RP Mladost – Sremska Mitrovica. To achieve the 70% MACZT criterion, an allocation of as much as 1524 MW would be required, which would result in significant loading of the critical element. The results are presented in Table IV.

Table IV – MACZT values for NTC calculation from Serbia towards Croatia and Bosnia and Herzegovina

Critical outage	Critical branch	MACZT [%]
OHL 400 kV SS Mladost - S. Mitrovica	OHL 220 kV Obrenovac - Valjevo 3	57

In the opposite direction, HR, BA → RS, the outage of the Trebinje – Lastva transmission line leads to overloading of the 220 kV line Višegrad – Požega, while the proposed NTC is 900 MW, resulting in a compliance level of 61%. The results are shown in Table V.

Table V – MACZT values for NTC calculation from Croatia and Bosnia and Herzegovina towards Serbia

Critical outage	Critical branch	MACZT [%]
OHL 400 kV Trebinje - Lastva	OHL 220 kV Višegrad - Požega	61

It can be observed that, in order to achieve the required 70% condition, the transmission network is often heavily loaded. In such cases, the issue would need to be resolved in real time through redispatching, which has financial implications.

The paper also presents MACZT calculations that consider critical network elements for several representative months in 2024 and 2025. It should be noted that the estimates were based on EMS proposals obtained from calculations in accordance with ENTSO-E methodology. The values that were actually allocated were generally reduced due to neighbouring TSOs during the harmonisation process, where the principle is to adopt the minimum of the two proposed values.

The aggregated results are presented in Tables VI–IX.

Table VI – MACZT compliance analysis for July 2024

July-24	At a critical step		NTC target [MW]	EMS's suggestion	
	NTC calculated [MW]	MACZT[%]		NTC [MW]	MACZT [%]
RS -> HU	1137	68	1278	800	55
HU -> RS	762	52	1115.2	800	54
RS -> BG + RO	2282	114	1104	1100	70
BG + RO -> RS	1245	45	1832	1400	56
RS -> BA + HR	1345	74	1256	900	49
BA + HR -> RS	454	53	610	900	73
RS -> ME + MK	1808	61	1984	1300	51
ME + MK -> RS	624	35	1358	1300	68

Table VII – MACZT compliance analysis for April 2025

April-24	At a critical step		NTC target [MW]	EMS's suggestion	
	NTC calculated [MW]	MACZT[%]		NTC [MW]	MACZT [%]
RS -> HU	682	14.7	2642	1000	24
HU -> RS	/	/	/	/	/
RS -> BG + RO	1723	64.6	1596	1900	83
BG + RO -> RS	1432	52	1928	1900	69
RS -> BA + HR	945	21	2600	1200	36
BA + HR -> RS	1044	50	1250	1200	67
RS -> ME + MK	1723	57.7	1794	1300	52
ME + MK -> RS	1263	63.7	1390	900	65

Table VIII – MACZT compliance analysis for June 2024

June-24	At a critical step		NTC target [MW]	EMS's suggestion	
	NTC calculated [MW]	MACZT[%]		NTC [MW]	MACZT [%]
RS -> HU	997	58	1156	900	55
HU -> RS	1742	81	1563	1000	53
RS -> BG + RO	1469	53	2145	800	29
BG + RO -> RS	1456	55	1930	800	42
RS -> BA + HR	843	33	1524	1200	57
BA + HR -> RS	1056	65	1634	900	61
RS -> ME + MK	1374	57	1473	1300	55
ME + MK -> RS	1526	76	1377	1400	68

Table IX – MACZT compliance analysis for August 2024

August-24	At a critical step		NTC target [MW]	EMS's suggestion	
	NTC calculated [MW]	MACZT[%]		NTC [MW]	MACZT [%]
RS -> HU	1262	54	1420	700	31
HU -> RS	1024	47	1626	700	35
RS -> BG + RO	/	/	/	/	/
BG + RO -> RS	1013	39	1865	700	22
RS -> BA + HR	1413	51.75	1945	1000	34
BA + HR -> RS	886	57	1126	1000	63
RS -> ME + MK	973	44.4	1594	1300	55
ME + MK -> RS	676	35	1389	1300	67

Several assumptions were adopted in EMS calculations:

- the results are presented using values calculated by JSC EMS with the intention of allocating all available capacity to the electricity market; however, the final allocated values are harmonised with neighbouring TSOs and adopted according to the "lower value acceptance" criterion
- the values presented in the paper refer to monthly calculations, but are higher at the daily level, since daily NTC calculations and harmonisation are performed for several borders, resulting in higher network utilisation
- the calculation must include coordination between capacity calculation regions and must be carried out on the European common grid model in order to minimise non-coordinated power flows from other zones.

6. ACTION PLAN AND STRUCTURAL CONGESTION IN THE TRANSMISSION NETWORK

Regulation (EU) 2019/943 on the internal electricity market requires Transmission System Operators to make at least 70% of available transmission capacity on interconnections relevant for cross-border trade available to market participants.

This Regulation was incorporated into the Energy Community by a Decision of the Ministerial Council on 15 December 2022. Article 15 of the Regulation stipulates that contracting parties must gradually increase available capacities along a linear trajectory so that a minimum of 70% is reached by 31 December 2027.

Until that date, if structural congestion exists, countries must adopt Action Plans for its elimination, while also increasing cross-border capacity each year. Therefore, the 70% rule becomes binding from the end of 2027, and until then, contracting parties of the Energy Community must progressively align their capacities through action plans and reporting.

The new Energy Law provides the national legal and institutional framework enabling the implementation and gradual alignment with the requirements of Regulation (EU) 2019/943 and other regulations arising from the "Clean Energy for All Europeans" package.

Amendments to the Energy Law ("Službeni glasnik RS", No. 145/2014, 95/2018 – other law, 40/2021 and 94/2024), adopted on 21 November 2024 and entering into force on 29 November 2024, introduced for the first time provisions into the national legal framework that transpose the key principles of Regulation (EU) 2019/943 on the internal electricity market.

According to paragraph 9 of Article 164 of the Energy Law, the Transmission System Operator is required to ensure an annual increase of available transmission capacities along a linear trajectory between bidding zones, until the minimum values defined in accordance with Article 165a of the Energy Law are reached. Minimum transmission capacity levels must be achieved no later than 31 December 2027.

Low or variable MACZT values indicate the existence of constraints in the transmission network that are not solely a consequence of the cross-border capacity calculation process, but are also conditioned by the physical configuration of the network, the capacities of individual network elements, and the distribution of flows within the system. For this reason, MACZT analysis represents the starting point for identifying structural congestion in the transmission network.

Therefore, in order to define effective and sustainable measures within the Action Plan, it is necessary to identify and analyse structural congestion in the transmission network, i.e. permanent or recurring network constraints that lead to a reduction of MACZT and limit the availability of cross-border capacities.

Based on technical analyses and reports prepared by Elektromreža Srbije, structural congestion has been identified in the transmission system of the Republic of Serbia, representing constraints in providing available transmission capacity for cross-border electricity trade. These constraints are not limited only to the Serbian transmission system but also include elements of neighbouring systems, given the high level of interconnection and their combined impact on power flows in the South-Eastern Europe region:

1. interconnection with Bosnia and Herzegovina (Bajina Bašta – Požega – Višegrad): limitations due to thermal capacity and insufficient automation of flow control
2. interconnection with Montenegro (Pljevlja – Bistrica)
3. 400 kV transmission line Đerdap – Portile de Fier
4. 400/110 kV transformer in substation Smederevo 3
5. 400 kV transmission line Đerdap – Drmno
6. 400/110 kV transformer in substation Bor 2
7. 220 kV transmission line Obrenovac – Belgrade 3
8. 400 kV transmission line Pančevo 2 – Belgrade 20
9. 220/110 kV transformer in substation Sremska Mitrovica 2

The Action Plan defines the planned measures for reducing identified structural congestion in the transmission system. The planned measures include:

- network development and optimization
- network expansion
- coordinated transmission capacity calculation
- reserves in the network for redispatching
- coordination of corrective measures

These measures are grouped into two main areas of action:

1. network development and optimisation – covering the first two measures
2. enhancement of congestion management – covering the remaining three measures

The development and optimisation of the transmission network, as well as the schedule for implementing these measures, are defined in the JSC EMS Development Plan. The improvement of congestion management will be carried out at the regional level in cooperation with RCCs, which, together with TSOs, will implement coordinated activities.

7. DEVELOPMENT AND OPTIMISATION OF THE TRANSMISSION NETWORK

In order to adequately address future challenges, including new requirements defined in Article 16(8) of the Regulation on the electricity market, sustainable expansion of network infrastructure represents one of the key prerequisites for reliable and efficient system operation.

The transmission network is continuously developing, and within the cyclical planning process future needs are regularly identified and appropriate measures are defined to meet them. JSC EMS has legally prescribed obligations aimed at ensuring the sustainable development of the transmission system of the Republic of Serbia.

Through its medium-term and long-term development strategy, JSC EMS plans significant investments in the refurbishment of existing infrastructure and the construction of new transmission capacities over the next ten- and twenty-year periods.

These infrastructure projects will improve the reliability of supply to transmission system users and increase cross-border capacities for electricity exchange, which is of major international (regional) importance.

Planned international projects in which JSC EMS participates, considered within the pan-European Ten-Year Network Development Plan (TYNDP package), as shown in the following figure, will contribute to increasing transmission capacities at as many as six borders of the Republic of Serbia.

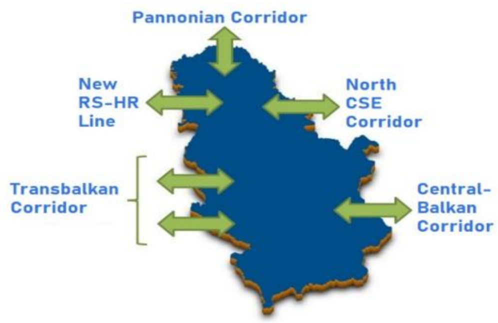

Figure 7. Overview of main transmission corridors and dominant power flow directions in the Serbian power system and the region

In accordance with the Energy Development Strategy of the Republic of Serbia, development plans of the generation and distribution systems, and the business strategy of JSC EMS, investments in electricity transmission infrastructure are directed towards the following objectives:

- increasing the operational security of the transmission system and the reliability of supply to transmission system users, which is also a legal obligation of JSC EMS
- increasing cross-border transmission capacities of the Republic of Serbia that have regional and pan-European significance
- balanced, sustainable and timely development of the transmission system with the aim of integrating new conventional and renewable energy sources, as well as customer facilities
- development of the electricity market at both national and regional levels

In accordance with the provisions of the Energy Law of the Republic of Serbia, JSC EMS adopts a development plan for the next ten-year period at least once every two years.

According to Article 111 of the Serbian Energy Law of 2024, the necessary network development projects are summarised in Network Development Plans, which are prepared every two years by the Transmission System Operator JSC EMS and must be approved by the regulatory authority.

A strong and reliable network is a key factor in achieving the minimum capacity required to be made available for cross-border trade, in accordance with Article 16(8) of the Regulation.

The Ten-Year Network Development Plan is updated annually and aims to increase transmission capacity, reduce network congestion and facilitate the achievement of objectives. Measures to achieve these goals include reinforcement and optimisation of the existing network, as well as the development of new infrastructure.

A strong and reliable network is a key factor in achieving the 70% criterion defined by the Regulation. In the coming years, reinforcement or optimisation of several existing transmission lines and substations is planned.

In accordance with Article 15(1) of the Regulation on the electricity market, the Action Plan must include provisions related to monitoring its implementation. Monitoring is essential to ensure that the planned measures for increasing cross-border capacity and reducing structural congestion are actually implemented in line with the defined linear trajectory, without compromising the operational security of the power system.

8. CONCLUSION

After defining and establishing the operational framework of regions for coordinated transmission capacity calculation, calculations will be performed at the regional level within RCCs in a coordinated manner, initially for the day-ahead and intraday time horizons. By applying a flow-based methodological approach, the loading of each network element is analysed individually.

Through coordinated flow-based calculations within RCCs, transmission capacity domains will be defined in a more transparent manner, and only after market transactions will it become clear whether critical network elements exist and which ones they are. During the calculations, compliance with the 70% requirement is considered for each critical element from the predefined contingency list.

This will represent a challenge both for planning and for real-time operation, where critical congestion situations in the network must be resolved through redispatching or counter-trading, both of which entail financial implications.

Experience from European countries that have already implemented the 70% rule shows that TSOs, in order to allocate 70% of capacity, may operate in regimes where network overloads occur. This raises the question of whether this rule leads to “insecurity of the 70% rule”. Additionally, questions remain as to whether sufficient potential for counter-trading exists.

In the calculation and validation of transmission capacities, potential corrective measures (“remedial actions”) are also taken into account, which must be implemented in real time when their feasibility is in question.

Within JSC EMS, structural congestion has been identified, and in accordance with this, an Action Plan has been developed to eliminate the identified network constraints. JSC EMS is required to ensure an annual increase of transmission capacities along a linear trajectory between bidding zones until the minimum value is reached, no later than the end of 2027.

By defining the Action Plan, JSC EMS is provided with additional time to fully comply with the MACZT criterion and to further strengthen transmission infrastructure.

REFERENCES

[1] ENERGY COMMUNITY, CLEAN ENERGY PACKAGE, https://www.energy-community.org/implementation/package/EL.html
[2] Uredba o uspostavljanju smernica za rad međusobno povezanih sistema za prenos električne energije
[3] Commission Regulation (EU) 2015/1222 of 24 July 2015 establishing a Guideline on Capacity Allocation and Congestion Management (CACM), https://eur-lex.europa.eu/legal-content/EN/TXT/?uri=CELEX%3A32015R1222
[4] ACER, Day-ahead Capacity Calculation Methodology of the CORE Capacity Calculation Region, Annex Ia, 21 February 2019, https://documents.acer.europa.eu/Official_documents/Acts_of_the_Agency/ANNEXESTODECISIONOFTHEAGENCYNo022019/Annex%20I%20-%20ACER%20Decision%20on%20Core%20CCM.pdf
[5] Zakon o energetici („Službeni glasnik RS“, br. 145/2014, 95/2018 – dr. zakon, 40/2021 и 94/2024)
[6] Uredba o raspodeli prenosnog kapaciteta I upravljanje zagušenjima („Sl. Glasnik RS”, br. 102/2024)

BIOGRAPHIES

Marija Đorđević was born in 1972 in Serbia. She graduated from the Faculty of Electrical Engineering, University of Belgrade, in 1997. She obtained her MSc degree in 2003 at the same faculty and her PhD in the field of energy in 2013 at the University of Belgrade. She is currently the Head of the Centre for Operational Planning and Analysis of Transmission System Operation. Her areas of interest include short-term planning and operation analysis, market aspects, and the implementation of European regulations in the Serbian power system.

Srđan Mladenović was born in 1982 in Kruševac, where he completed his primary and secondary education. He graduated from the Faculty of Electrical Engineering, University of Belgrade, in 2010. He has been employed at Elektromreža Srbije for over 15 years, where he has progressed through various professional roles. He currently works as Head of the Department for Planning and Analysis of Transmission System Operation.

Ivana Stamenić was born in 1993 in Užice. She completed her primary and secondary education in Bajina Bašta. She graduated in 2016 from the Faculty of Electrical Engineering, University of Belgrade, Department of Power Engineering. She completed her Master's academic studies in 2017 at the same faculty. Since 2018, she has been employed at Elektromreža Srbije, currently holding the position of Head of the Unit for Transmission System Operation Planning.

Branko Šumonja was born in 1969. He graduated from the Faculty of Electrical Engineering, University of Belgrade, majoring in Power Engineering. Since 1998, he has been working in the Serbian energy sector, initially in Electric Power Industry of Serbia and later in Elektromreža Srbije since its establishment in 2005. He has gained extensive experience in transmission system management, from NDC dispatcher to various managerial positions in operation and planning of the transmission system. He currently holds the position of Director of the Transmission System Operation Directorate.

UDK: 621.311.1(497.11)
621.311:351.824.11(497.11:4-6EU)

Marija Đorđević[1], Srđan Mladenović[1], Ivana Stamenić[1], Branko Šumonja[1]

Implementacija evropskih procesa u operativni rad EMS AD

[1] Akcionarsko društvo Elektromreža Srbije, Beograd, Srbija*

Stručni rad

Ključne poruke

- Ovaj rad razmatra koordinisane procese koji se odvijaju na nivou evropskih operatora prenosnih sistema i glavne promene koje se sprovode u operativnom radu EMS AD
- Opisana su dva najbitnija procesa i to koordinisana sigurnost i koordinsani proračuni prenosnih kapaciteta
- Date su tehničke osnove za definisanje regionâ za koordinisani proračun kapaciteta u regionu Jugoistočne Evrope
- Sagledane su mogućnosti srpskog operatora prenosnog sistema da ispuni regulatornu obavezu dodele prenosnog kapaciteta prema MACZT metodologiji

Kratak sadržaj

Na nivou ENTSO-E i Evrope odvijaju se procesi koji direktno utiču na elektroenergetski sektor Srbije i svakodnevni rad Operatora prenosnog sistema. Dva ključna procesa u okviru ENTSO-E – koordinisana analiza sigurnosti i koordinisani proračuni prenosnih kapaciteta – sprovode se na usklađen način. U okviru proračuna prenosnih kapaciteta primenjuju se dva metodološka pristupa: NTC i flow-based metod. Ovaj rad prikazuje regulatorni proces priključenja EMS AD evropskim regionima za proračun kapaciteta – CORE i SEE regionu – uz poseban osvrt na izazove sa kojima se EMS AD suočava u ovom kontekstu. Takođe, predstavljeni su osnovni koncepti koordinisanih procesa, koji će se delom realizovati unutar Operatora prenosnog sistema, a delom kroz regionalne koordinacione centre. Bez obzira na primenjenu metodologiju proračuna prenosnih kapaciteta u različitim fazama, neophodno je ispuniti pravilo dodele 70% kapaciteta kritičnog elementa. U radu su prikazani preliminarni rezultati ispunjenja ovog pravila, uzimajući u obzir da je njegova primena obavezna u skladu sa Zakonom o energetici.

Ključne reči

ENTSO-E, MACZT (*Margin Available for Cross-Zonal Trade*), RCC (*Regional Coordination Centre*), TSO (OPS)

Primljeno: 19. novembra 2025. Recenzirano: 11. marta 2026.
Izmenjeno: - / bez primedbi / Odobreno: 12. marta 2026.

* Korespondirajući autor: Marija Đorđević, +381 64/840-86-69
Imejl: marija.djordjevic@ems.rs

Napomena:
Ovaj članak predstavlja proširenu, unapređenu i dodatno recenziranu verziju rada „*Koordinisani procesi u EMS AD u skladu sa najnovijom evropskom regulativom*” (https://doi.ub.kg.ac.rs/doi/cigre37-c5-08/), nagrađenog u Studijskom komitetu STK-C5 *Tržište električne energije i regulacija,* na 37. Savetovanju CIGRE Srbija, 26-30. maja 2025.

EDITORIAL POLICY AND TOPICS OF THE JOURNAL

When the Journal *Elektroprivreda* was relaunched, it was decided that it would take on a scientific and professional focus and be redesigned with a broader concept. It is now published in both Serbian and English.

English-language publication is reserved for manuscripts authored by individuals from Serbia and the surrounding region who wish to publish in English, provided the Editorial Board and peer reviewers determine the work offers significant contributions and may be of interest to readers beyond the Serbian-speaking community. The Journal also welcomes submissions from international authors whose original manuscripts are in English. With their consent, accepted papers will be translated and published in Serbian as well. Serbian-language articles are available in both Cyrillic and Latin scripts.

The Journal is published twice a year exclusively in digital format, following an Open Access model. There are no publication fees for accepted manuscripts—authors are not charged, nor are they compensated by the Publisher for submitted or published work.

Submissions must be original and must not have been published or publicly presented anywhere in the world prior to their debut in *Elektroprivreda*. Exceptions apply only to special issues of the Journal featuring selected papers from partner conferences. In these cases, the manuscript must be expanded by at least 30% compared to the original conference presentation, undergo improvements, and pass the same peer review process as regular submissions.

Only manuscripts that receive at least two positive reviews from qualified experts in the relevant field – or a majority of favorable evaluations if more reviewers are involved – can be published.

The Journal accepts and publishes original scientific and research-oriented papers, particularly those that align with its thematic scope:

- new technologies for providing, processing and exploitation of primary energy resources,
- generation, transmission and distribution of electricity,
- storage and conversion of electricity and heating energy,
- rational consumption of electricity and heating energy,
- development of renewable energy sources,
- information and telecommunication systems,
- organization of power system operations,
- environmental protection,
- rehabilitation of power facilities,
- inventions and innovations,
- restructuring and privatization process in an energy sector,
- electricity markets,
- application of EU legal regulations within the scope of energy; and
- other related disciplines.

The Journal is envisioned as a platform for sharing expertise, fostering constructive dialogue, and encouraging the exchange of professional viewpoints among practitioners, researchers, and innovators from academic and industrial settings. Its aim is to promote open discourse on strategic development and the adoption of emerging technologies. Such collaboration may help identify effective technical, technological, legal, economic, and organizational responses to the pressing challenges posed by decarbonization, digitalization, and the transition of the power sector toward sustainable development.

On behalf of the Editorial Board,

Mr. Vladimir Šiljkut, Ph.D.E.E.
Editor-in-Chief

CLASSIFICATION (RANKING) OF MANUSCRIPTS

When reviewing manuscripts and completing a Reviwer's Report, reviewers propose and Editorial Board - in case manuscripts are accepted for publication - determine their category (rank). Classification (ranking) of manuscripts will be done as per the *Rulebook for classification and ranking of scientific journals* (Official Gazette of Republic of Serbia, No. 80/2024 as of 4 October 2024) and the table provided herein:

Scientific articles:	
Original scientific and research paper	Paper presenting previously unpublished results of own research done by a scientific method
Review paper	Paper including original, detailed and critical view of a research problem or discipline where the author(s) made some contribution
Short or pre-communication	An original scientific paper in full form, but less extensive or preliminary in nature
Scientific critique, i.e., discussions and reviews	Discussion of some scientific topic based only on scientific arguments and by applying scientific methods
Professional articles:	
Professional paper	Article offering experience useful in promoting professional practice, but which are not necessarily based on a scientific method
Information article	Editorials, comments, and similar
Report	A book report, computer program report, case report, scientific event report, and similar
Expert critique, i.e., discussions and reviews	Discussion of a certain professional topic

UDC: (Editor's input)

First A. Author[1], Second B. Author[2], Third C. Author[3], ...

Instructions for the Preparation of Article - the Title of the Article

(NOT MORE THAN FOUR LINES)

[1] Affiliation of the first author - institution, city, country[*]
[2] Affiliation of the second author - institution, city, country (if differs from 1)
[3] Affiliation of the third author - institution, city, country (if differs from 1, 2)
…

DOI: (Editor's input)
Category of article: (Editor's input)

Highlights

- Key aspects and messages of the work should be presented in a maximum of four short items/bullets
- The sentences of these items must be short, concise, auxiliary verbs can be omitted
- E.g.: The structure and design of work for publication are considered by the instruction

Abstract

The Abstract of the article should contain a concise description of the problem, applied methods and conclusions. It is an essential part of the article and should be clear and concise. The Abstract should be informative, giving an overview of the issues, the procedure and the main conclusions, results, and their significance. Do not write in the first person, do not list references and equations, and avoid abbreviations. It should not contain more than 300 words (in Serbian) to 350 (in English, including definite and indefinite articles before nouns).

Keywords

Specify up to six keywords, separated by commas

Received: (Editor's input) Reviewed: (Editor's input)
Modified: (Editor's input) Accepted: (Editor's input)
[*]Corresponding author: (phone)
E - mail:

1. INTRODUCTION

The *Elektroprivreda* journal publishes categorized articles: original scientific papers, previous announcements, reviews and technical papers in the field of electrical engineering and energy.

All papers are subject to review. The authors are solely responsible for the originality of the paper, the quality and reliability of the results. By submitting the paper, the authors accept all the rules specified in these Instructions.

This document contains paper preparation instructions. Authors are requested to fully comply with these Instructions when preparing their paper to avoid any problems when printing the paper.

The document is a sample for *Microsoft Word* (version 7 and higher) and is also an example of the desired paper formatting. It contains all the necessary information about the paper format, font type and size, as well as the rules explaining the procedures related to equations, units of measurement, figures, tables and other parts of the paper.

The complete paper containing the manuscript, tables, diagrams, drawings, photographs and full names and surnames of authors with affiliations should be submitted by uploading it to the Manuscript Handling Application, available on the Journal's website, https://epijournal.eps.rs/prijava or, alternatively, by sending it to the following e-mail: epijournal.editor@eps.rs.
The paper should not be more than ten pages long (without the list of references and the title, key messages, short content and keywords in English), except in the case of review papers and special editions of the Journal with extended award-winning papers from conferences, in which case the number of pages is not limited, nonetheless it is recommended that it should not be more than 16 pages long.

The original paper should be presented in A4 format (210x297) mm. The text of the paper should be justified. All margins should be set to 2 cm. The text of the paper should be single-spaced. The paper can be written in Serbian or English. (The editorial board decides which paper will be translated into another language, in order to make them available to as many readers as possible.) The font size for individual parts of the text is as in these Instructions. Complete mathematical derivations should be avoided in the paper. The necessary derivation may be given, if necessary, as a whole, in the form of one or more attachments.

This document can be downloaded directly from the following web address https://epijournal.eps.rs and used as the basis to prepare the manuscript, simply by entering parts of the paper text in certain places in this document.

It is recommended that the paper text begins with an introduction where the problem and task of the paper are formulated. An overview and commentary of the used literature from the specified area should be given and the position and contribution of the paper in relation to the specified literature should be indicated.

2. CHAPTER TITLE (for example: TEXT PREPARATION)

For greater clarity, the text of the paper should be divided into chapters and subchapters. Chapters and subchapters should be numbered with Arabic numerals, subchapters with numbers separated by a period. Please separate the titles of chapters and subchapters from the text before and after the title with one blank line. Line breaks in the text title or subtitle should be avoided.

2.1 Subchapter levels

With subchapters, it is not desirable to go lower than the second level, for example 2.1, 3.3, etc.

2.1.1 Third subchapter level. It is allowed only exceptionally, if this contributes to the methodological and general clarity of the paper text and if written, similar to the subchapter titles, in bold lowercase letters, but ending with a period, after which, in continuation of such line and written in normal font, the first sentence of this subchapter begins.

2.2 Positioning of tables and diagrams

Tables, figures and diagrams may, if necessary, be in one or both columns. All figures and tables should be placed in the text close to, but not in front of, the place in the text where they are first mentioned. Figures and tables in the appendices should be marked in the same way as in the text of the paper.

2.3 First page

In the middle of the first page, the paper title is indicated in bold letters, size 16, *Times New Roman* type. Below the title, the full names and surnames of the authors are listed in size 11 letters. The author's affiliations are listed below the names and surnames, in size 10 letters. After specifying the authors' data, the first page lists the key messages of the paper, a summary of the paper and keywords, in size 11 letters.

If the paper is written and approved for publication only in the Serbian language, after the content described in the previous paragraph, the title of the paper, key messages, summary of the paper and key words in English are listed in the final version of the paper for publication.

If the work was written in English and approved for publication, it will be fully translated and published in Serbian, with identical formatting.

If the paper was written in Serbian and approved for publication in both languages, it will be fully translated and published in English, with identical formatting.

In the lower left corner of the first page, the full information needed to contact the first author of the paper should be specified.

All this is easily realized by using the provided first page template by simply entering the anticipated text in places provided under the Instructions.

2.4 Subtitle (for example: Text of the paper)

The text of the paper should simply be entered instead of the text of the Instructions in this format by entering or copying parts of the text that have been done in accordance with these instructions in places provided for this in the Instructions.

2.5 Equations

Equations should be placed in the middle of the text and numbered with Arabic numerals in small (round) brackets along the right margin of the text. Mathematical software (*Microsoft Equation Editor for MS Word* or *MathType*) should be used for equations. E.g:

$$I_F = I_B = -I_C = \frac{-J\sqrt{3}E_A}{Z_1 + Z_2} \quad (1)$$

Equations should be separated from the text before and after the text with a 6pt space. Symbols used in an equation must be defined before they appear in the equation or immediately after the equation. Reference to an equation in the text is made by specifying the equation number in round brackets (1). If the sentence begins with a reference to an equation, then please use "Equation (1) is ...".

2.6 Tables

Tables should be inserted in the text where they are first mentioned or immediately after. They should be marked with Roman numerals, and the number and name of the table should be placed above the table. E.g:

Table I Duration of simulations and memory usage

ISCAS circuit	CPU time [s]	Memory usage [MB]
c17	2	3.9
c432	62	68.7
c880	160	152.6
c1355	283	178.8

2.7 Figures

Figures should be carefully prepared and inserted into the text in the designated place. The figure number and name must be below the image. Figure number should be marked with Arabic numerals. For the sake of better understanding, please avoid excessive information in the figures. All comments related to figures should be in the header. Typescripts should be chosen carefully to ensure clarity. Please attempt to describe the figure axes with words, not just symbols. For example, it is better to specify the ***time t***, rather than just ***t***. Symbols for units of measurement should be placed in parentheses.

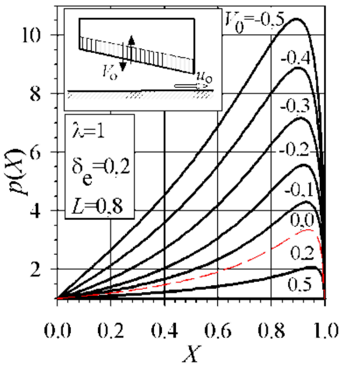

Figure 1. Figure description

3. CONCLUSION

Although the conclusion should contain an overview of the key results of the paper, it should not repeat the part stated in the Summary. The conclusion may explain the importance of the paper or suggest possible applications of the achieved results and provide guidelines for further research on the issues covered by the paper.

ACKNOWLEDGMENTS

Acknowledgments for sponsorship, funding or assistance, if any, should be given as a separate, unnumbered section before the list of references. Please use the singular in the title even when there are several acknowledgements.

REFERENCES

The list of references should be provided at the end of the paper in a separate, unnumbered section. References should be numbered with Arabic numerals in square brackets, according to the order of citation in the text of the paper. When citing, please make sure that the references are accurate and complete, ie. they should fully describe the data sources.

All mentioned references must be directly cited in the text of the paper by stating the reference number in square bracket. Please do not limit yourself to listing your references, but also list relevant references from the field under consideration.

Below are examples of how to cite references: a paper published in a journal [1], a book [2], a chapter in a multi-authored book [3], a paper published in a conference proceedings [4] and an article taken from a website [5].

[1] Šiljak D. D, Stipanović D. M, "Robust Stabilization of Nonlinear Systems - the LMI Approach", *Mathematical Problems in Engineering*, Vol. 6, No. 5, pp. 461-493, 2000.
[2] Marković Z., "Granična stanja čeličnih konstrukcija prema evrokodu", Akademska misao, Beograd, 2014.
[3] Deavours D., "UHF RFID Antennas", in: Bolić M. (Ed.), *RFID Systems - Research Trends and Challenges,* Ch. 3, Wiley, New York, 2010.
[4] Ocokoljić G., Živković S., Subotić S., "Aerodynamic Coefficients Determinations for the ATM Model with

Lateral Jets Simulation – Experimental and Numerical Methods", Proc. 4th *International scientific conference on defensive technologies OTEH 2011*, Belgrade, Serbia, pp. 17-22, 6-7 October 2011.
[5] Vukić B., „Društvene igre za visokopozicionirane poslovne ljude" [Internet]. Beograd; Novi Sad: Adizes Southeast Europe; 2010 [citirano 19.03.2012]. Dostupno na: http://www.asee.rs/?page=142&oi=69

APPENDIX (ATTACHMENT) 1

Appendices, if necessary, should be listed after the References. If there are more, they should be numbered with Arabic numerals. In case the attachments contain tables or figures, they should be numbered with the letter "A" followed by a period and a serial number (namely: for tables in Roman, from "I" onwards, in a uniform order for all attachments; and for figures in Arabic, from "1" onwards, uniform for all attachments).

APPENDIX (ATTACHMENT) 2

Depending on their content, attachments can be formatted as double-column or single-column. In the case when this allows better visibility for the reader, figures and tables in attachments can be rotated to the left by 90°.

Table A.I Name of the first table of the appendix

Heading	Column 1	Column 2	Column 3	Column 4	Column 5	Column 6	Column 7
Row 1							
Row 2							
Row 3							
Row 4							
Row 5							
Row 6							

BIOGRAFIJE

A short biography should be provided for each author. Please start with the author's first and last name and give his/her short, mostly professional biography. A photo of the author should also be included. A sample biography is provided below.

Nikola Tesla was born in Smiljan in the Austrian Empire on 9 July 1856. He graduated from the Austrian Polytechnic School in Graz and studied at the University of Prague. His work experience included American Telephone Company, Budapest, Edison Machine Works, Westinghouse Electric Company and Nikola Tesla Laboratories. His particular fields of interest were high frequency fields. Tesla received honorary degrees from institutions of higher learning including Columbia University, Yale University, University of Belgrade and University of Zagreb. He received the Elliott Cresson Medal from the Franklin Institute and the Edison Medal from the IEEE. In 1956, the term "tesla" (T) was adopted as the unit of magnetic flux density in the MKS system of units. In 1975, the Power Engineering Society established the Nikola Tesla Award in his honor. Tesla died on 7 January 1943.
ORCID: xxxx-yyyy-zzzz-wwww.
/ Each author should provide their ORCID (*Open Researcher and Contributor ID*), if available /

Authors shall submit a signed Declaration of Authorship, Originality of the Manuscript and Transfer of Copyright to the Journal's Editorial Board following acceptance of the paper; The form may be downloaded from the Journal's website, https://epijournal.eps.rs.

/ Please delete this text box once the paper has been finalised /

UDK: (*unosi Redakcija*)

Prvi A. Autor[1], Drugi B. Autor[2], Treći C. Autor[3], ...

Uputstvo za pripremu radova - naslov rada

(*NE VIŠE OD ČETIRI REDA*)

[1] Afilijacija prvog autora - institucija, grad, zemlja[*1]
[2] Afilijacija drugog autora - institucija, grad, zemlja (ako se razlikuje od 1)
[3] Afilijacija trećeg autora - institucija, grad, zemlja (ako se razlikuje od 1,2)
…

Kategorija rada: (*unosi Redakcija*)

Ključne poruke

- U najviše četiri kratke stavke/*bullets* treba izložiti ključne aspekte i poruke rada
- Rečenice ovih stavki moraju biti kratke, jezgrovite, pomoćni glagoli mogu biti izostavljeni
- Npr: Uputstvom sagledani struktura i oblikovanje rada za publikovanje

Kratak sadržaj

Kratak sadržaj rada treba da sadrži sažet opis problema, primenjene metode i zaključke. On je esencijalni deo rada i treba da bude jasan i koncizan. Kratak sadržaj treba da bude informativan, dajući pregled problematike, postupka i glavnih zaključaka, rezultata i njihovog značaja. Ne treba pisati u prvom licu, ne navoditi reference i jednačine i izbegavati skraćenice. Ne treba da sadrži više od 300 reči (na srpskom) do 350 (na engleskom, uključujući i određene i neodređene članove ispred imenica).

Ključne reči

Navesti do maksimalno šest ključnih reči, odvojenih međusobno zapetama

Primljeno: (unosi Redakcija) Recenzirano: (unosi Redakcija)
Izmenjeno: (unosi Redakcija) Odobreno: (unosi Redakcija)
[*]Korespondirajući autor: (ime i prezime, telefon)
E - mail:

In memoriam

UDC: 621.3:929 Katić V.

Professor Vladimir Katić, PhD

(1954–2026)

It is with deep sadness that we inform the readership, authors and contributors of our journal that, following a brief but severe illness, Professor Vladimir Katić, PhD, Chairman of our Editorial Board, passed away in early April 2026.

Professor Katić graduated in 1978 from the Faculty of Technical Sciences (FTN) in Novi Sad, obtained his MSc in 1981, and his PhD in 1991 from the Faculty of Electrical Engineering in Belgrade. He was an outstanding scientist and educator, a highly respected professor at FTN in Novi Sad, and served several terms as Vice-Dean.

Over the course of his remarkable career, he published more than 600 scientific papers and authored 22 monographs and textbooks. With close to 2,100 citations and an *h*-index of 20 (according to Google Scholar), Professor Katić was one of the most influential researchers in the fields of power electronics and power quality, renewable energy sources, and electric vehicles. As a reviewer with more than 500 recognised reviews, he was highly esteemed within the editorial boards of the world's most prestigious scientific journals.

Professor Katić left an indelible mark on both the academic and professional communities. Through his dedicated work, exceptional knowledge and vision, he made a significant contribution to the development of electrical engineering, as well as to the international standing of our scientific community. He initiated and for many years organised numerous scientific conferences, most notably the "Power Electronics" conference, which helped place our universities and experts firmly on the global scientific map.

As an IEEE Life Member, Professor Katić embodied lifelong dedication to the engineering profession. Until his final days, he remained active as Chair of the IEEE Life Member Affinity Group. For many years, he also chaired the IEEE Joint Chapter for Industry Applications, Industrial Electronics and Power Electronics (IE-13/IA-34/PEL-35), where, through his expertise, authority and organisational skills, he successfully bridged academia and industry. From 2006 to 2010, he served as Chairman of the IEEE Serbia and Montenegro Section.

He was a member of the executive boards of international associations such as EPE (Brussels) and PEMC (Budapest). He chaired numerous conferences, among which EPE-PEMC 2012 ECCE Europe stands out, placing Novi Sad and Serbia at the centre of the global power electronics community. The last major event in this field that Professor Katić organised and led was the XXIII International Symposium on Power Electronics (Ee 2025), held from 8 to 10 October 2025 in Belgrade and Novi Sad.

As one of the most distinguished experts in the field, he was the founder and president of the Power Electronics Society of Serbia, and also served as president of the ETRAN Society, where he devoted his knowledge, energy and organisational skills to maintaining continuity and advancing one of the most significant scientific conferences in the region.

He also served for many years as Chairman of Expert Commission 2 – *Power Quality in Electricity Distribution Systems* – of the Serbian National Committee of CIRED, of which he was a founder and a member of its Executive Board. He made an outstanding contribution to this area of power engineering, to the work and development of this association, and to the advancement of the conferences it has organised over the past three decades.

Since the relaunch of the journal *Elektroprivreda* in 2023, Professor Katić had headed its Editorial Board, making a major contribution to the effort to revive, establish and continuously develop the publication. Until his final days, he remained actively involved in preparing this very issue, never revealing that he was battling a serious illness. His passing therefore came as a shock to all his colleagues and collaborators, making the loss all the more profound and irreplaceable. To all who had the honour and privilege of working with him, however, even such dedication comes as no surprise, as Professor Katić was distinguished by immense energy, selflessness, commitment to the advancement of science and the profession, as well as by kindness, composure, dignity and quiet strength. In the very same way he lived and worked, he departed this worldly life, leaving behind an enduring legacy and, to all who knew him, a sense of loss and many cherished memories.

With deep respect and gratitude,
the Editorial Board

Attached to this memorial and brief overview of the career and works of Professor Vladimir Katic, we provide an extract from his extensive bibliography

Excerpt from the Bibliography of Professor Vladimir Katić

Books, textbooks and monographs (in Serbian):

1. **Vladimir Katić**, Energetska elektronika 1: Komponente i AC/x pretvarači, univerzitetski udžbenik, Fakultet tehničkih nauka, Novi Sad, 2020, ISBN: 978-86-6022-243-7
2. **Vladimir Katić**, Energetska elektronika 2: DC/x pretvarači i napajači, univerzitetski udžbenik, Fakultet tehničkih nauka, Novi Sad, 2020, ISBN: 978-86-6022-266-6
3. **Vladimir Katić**, Rešeni zadaci iz Energetske elektronike 1, udžbenik, Fakultet tehničkih nauka, Novi Sad, 2020, ISBN: 978-86-6022-264-2
4. **Vladimir Katić**, Stevan Grabić, Ivan Todorović, Zoltan Čorba, Praktikum iz energetske elektronike, univerzitetski praktikum/udžbenik, Fakultet tehničkih nauka, Novi Sad, 2016, ISBN: 978-86-7892-835-2
5. **Vladimir Katić**, Amir Tokić, Tatjana Konjić, Kvalitet električne energije, knjiga, Fakultet tehničkih nauka, Novi Sad, 2007, ISBN: 978-86-7892-064-6
6. **Vladimir Katić**, Izudin Kapetanović, Vangel Fuštić, Obnovljivi izvori električne energije, knjiga, Fakultet tehničkih nauka, Novi Sad, 2007, ISBN: 978-86-7892-066-0
7. **Vladimir Katić**, Vlado Porobić, Darko Marčetić, Primena mikroprocesora u energetici: praktikum laboratorijskih vežbi, udžbenik, Fakultet tehničkih nauka, Novi Sad, 2006, ISBN: 86-7892-013-0; 978-86-78920-13-4
8. **Vladimir Katić**, Kvalitet električne energije – viši harmonici: monografija, Fakultet tehničkih nauka, Novi Sad, 2002, ISBN: 86-80249-57-2
9. **Vladimir Katić**, Darko Marčetić, Dušan Graovac, Energetska elektronika: praktikum laboratorijskih vežbi, udžbenik, Fakultet tehničkih nauka, Novi Sad, 2000, ISBN: 86-499-0081-X
10. **Vladimir Katić**, Energetska elektronika: zbirka rešenih zadataka, udžbenik, Fakultet tehničkih nauka, Novi Sad, 1987, COBISS-ID: 195530249
11. **Vladimir Katić**, Borislav Pantić, Zbirka rešenih zadataka iz industrijske elektronike, udžbenik, Naučno-obrazovni institut za energetiku i elektroniku, Fakultet tehničkih nauka, Novi Sad, 1980, COBISS-ID: 39513095

Selected articles from international journals (since 2000):

1. Joeri Van Mierlo, Michael Fowler, **Vladimir Katic**, Aymeric Rousseau and Peter Van den Bossche, “Establishment of Ten New Sections in WEVJ2”, Editorial, *World Electric Vechicle Journal*, Vol.16, No.521, 16.09.2025, pp. 1-3, https://doi.org/10.3390/wevj16090521
2. Nebojša Horvat, Dušan B. Gajić, Petar Trifunović, Veljko B. Petrović, Dinu Dragan, **Vladimir A. Katić**, “Performance Evaluation of a Distributed Ledger-Based Platform for Renewable Energy Trading”, *IEEE Access*, Vol. 14, 19.06.2024, pp. 86013-86033, DOI: 10.1109/ACCESS.2024.3416612
3. **Vladimir Katić**, “PV Solar Energy Supply in Smart Cities”, *IPSI Transactions on Internet Research*, Vol.18, No.1, April 2022, pp. 28-33, DOI: 10.58245/ipsi.tir.22jr.06
4. Radovan Turović, Dinu Dragan, Gorana Gojić, Veljko B. Petrović, Dušan B. Gajić, Aleksandar M. Stanisavljević and **Vladimir A. Katić**, “An End-to-End Deep Learning Method for Voltage Sag Classification”, *Energies*, Vol.15, No 8, 2898, 15.04.2022, https://doi.org/10.3390/en15082898
5. Dušan B. Gajić, Veljko B. Petrović, Nebojša Horvat, Dinu Dragan, Aleksandar Stanisavljević, **Vladimir Katić** and Jelena Popović, “A Distributed Ledger-Based Automated Marketplace for the Decentralized Trading of Renewable Energy in Smart Grids”, *Energies*, Vol.15, No 6, 2121, 14.03.2022, https://doi.org/10.3390/en15062121
6. Aleksandar Stanisavljević, **Vladimir A. Katic**, Srdan Lj. Milicevic, “A Method for Real-Time Prediction of the Probability of Voltage Sag Duration Based on Harmonic Footprint”, *IEEE Access*, Vol. 10, 24.02.2022, pp. 23757-23773, DOI: 10.1109/ACCESS.2022.3154058
7. Zoltan Čorba, Bane Popadić, Dragan Milićević, Boris Dumnić and **Vladimir Katić**, “A Long-Term Condition Monitoring and Performance Assessment of Grid Connected PV Power Plant with High Power Sizing Factor under Partial Shading Conditions”, *Energies*, MDPI, Switzerland, Vol.13, No.4810, pp.1-20, 14.09.2020., Open Access, [Online]. Available: DOI: 10.3390/en13184810
8. Aleksandar Stanisavljevic, **Vladimir A. Katic**, Boris Dumnić and Bane Popadić, “A comprehensive overview of digital signal processing methods for voltage disturbance detection and analysis in modern distribution grids with distributed generation”, *Acta Polytechnica Hungarica*, ISSN: 0278-0046, Vol. 16, No.5, June 2019, pp.125-149, DOI: https://doi.org/10.12700/APH.16.5.2019.5.8.

9. Aleksandar Stanisavljevic and **Vladimir A. Katic**, “Magnitude of voltage sags prediction based on harmonic footprint for application in DG control system”, *IEEE Transactions on Industrial Electronics*, USA, ISSN: 0278-0046, Vol. 66, No.11, Nov.2018, pp. 8902-8912, [Online]. Available: DOI: 10.1109/TIE.2018.2881934

10. **Vladimir A. Katic,** Aleksandar M. Stanisavljevic, “Smart Detection of Voltage Dips Using Voltage Harmonics Footprint”, *IEEE Transaction on Industry Application*, Vol.54, No.5, Sep./Oct. 2018, pp.5331-5342, ISSN 0093-9994, [Online]. Available: DOI: 10.1109/TIA.2018.2819621

11. Bane P. Popadic, Boris P. Dumnic, Dragan M. Milicevic, **Vladimir A. Katic** and Damir Šljivac, “Grid connected converter control during unbalanced grid conditions based on delay signal cancellation”, *International Transactions on Electrical Energy Systems*, ISSN 2050-7038, Vol.28, No.12, e2636, June 2018, [Online] Available: DOI: https://doi.org/10.1002/etep.2636

12. Saša Mujović, Slobodan Djukanović, **Vladimir A. Katić**. "Simultaneous Operation of Personal Computers and Mathematical Assessment of Their Harmonic Impact on the Grid", *Advanced Technologies, Systems, and Applications*; Editors: Mirsad Hadžikadić and Samir Avdaković, Lecture Notes in Networks and Systems 3, Springer International Publishing AG, 2017. pp.57-79., [Online] Available: DOI: 10.1007/978-3-319-47295-9_2

13. Zoltan Corba, **Vladimir A. Katic**, Bane Popadic, Dragan Milicevic, “New string reconfiguration technique for residential PV system generation enhancement”, *Advances in Electrical and Computer Engineering*, ISSN: 1582-7445, Vol. 16, No.1, Feb. 2016, pp.19-26, [Online]. Available: http://dx.doi.org/10.4316/AECE.2016.01003

14. Saša Mujović, Slobodan Djukanović, Vladan Radulović, **Vladimir A. Katić**, “Multi-parameter mathematical model for determination of PC cluster total harmonic distortion of input current”, *COMPEL: The International Journal for Computation and Mathematics in Electrical and Electronic Engineering*, ISSN 0332-1649, Vol. 35, No.1, Jan. 2016, pp.305-325, [Online]. Available: DOI: http://dx.doi.org/10.1108/COMPEL-03-2015-0149,

15. Ivan Subotic, Nandor Bodo, Emil Levi, Boris Dumnic, Dragan Milicevic, **Vladimir A. Katic**, “Overview of Fast On-Board Integrated Battery Chargers for Electric Vehicles Based on Multiphase Machines and Power Electronics”, *IET Electric Power Applications*, ISSN 1751-8660, Vol.10, Issue.3, March 2016, pp.217-229, [Online]. Available: DOI: 10.1049/iet-epa.2015.0292

16. Boris P. Dumnic, Dragan M. Milicevic, Bane P. Popadic, **Vladimir A. Katic**, Zoltan J. Corba, “Speed-Sensorless Control Strategy for Multi-Phase Induction Generator in Wind Energy Conversion Systems”, *Thermal Science*, ISSN 0354-9836, Vol. 20, Suppl. 2, 2016, pp. S481-S493, [Online]. Available: DOI: 10.2298/TSCI151019032D

17. Boris Dumnic, Bane Popadic, Dragan Milicevic, **Vladimir Katic**, Djura Oros, “Artificial intelligence based vector control of induction generator without speed sensor for use in wind energy conversion system”, *International Journal of Renewable Energy Research*, ISSN 1309-0127, Vol.5, No.1, 2015, pp.299-307. [Online]. Available: https://ijrer.org/ijrer/index.php/ijrer/article/view/2030/pdf_41

18. Evgenije M. Adžić, Vlado B. Porobić, Marko S. Vekić, Zoran R. Ivanović, **Vladimir A. Katić**, “Vector-Controlled Induction Motor Drive with Minimal Number of Sensors”, *Electronics,* ISSN 1450-5843, Vol.19, No.1, June 2015, pp.21-31. DOI: 10.7251/ELS1519021A

19. **Vladimir A. Katić**, Boris Dumnić, Zoltan Čorba, Dragan Milićević, „Electrification of The Vehicle Propulsion System – An Overview”, *Facta Universitatis, Series: Electronics and Energetics*, ISSN 0353-3670, Vol.27, No.2, 2014, pp.299-316, [Online]. Available: DOI: 10.2298/FUEE1402299K.

20. Saša Mujović, Slobodan Djukanović, Vladan Radulović, **Vladimir Katić**, Mladen Rašović, “Least Squares Modeling of Voltage Harmonic Distortion Due to PC Cluster Operation”, *Advances in Electrical and Computer Engineering*, ISSN: 1582-7445, Vol. 13, No.4, 2013, pp.133-138, [Online]. Available: http://dx.doi.org/10.4316/AECE.2013.04022

21. Evgenije M. Adzic, Milan S. Adzic, **Vladimir A. Katic**, Darko P. Marcetic, Nikola L. Celanovic, “Development of High-Reliability EV and HEV AC Propulsion Drive with Ultra-Low Latency HIL Environment”, *IEEE Transactions on Industrial Informatics*, ISSN 1551-3203, Vol. 9, No.2, May 2013, pp.630-639, [Online]. Available: 10.1109/TII.2012.2222649

22. Dragan Milićević, **Vladimir A. Katić**, Zoltan Čorba, Marian Greconici, „New Space Vector Scheme for VSI Supplied Dual Three-Phase Induction Machine“, *Advances in Electrical and Computer Engineering*, ISSN: 1582-7445, Vol. 13, No.1, Feb.2013, pp.59-64, [Online]. Available: http://dx.doi.org/10.4316/AECE.2013.01010

23. Velimir Lj. Strugar, **Vladimir A. Katic**, Jovica V. Milanovic, “Generic Model of Coastal Distribution Network for Power System Harmonics Studies”, *Przeglad Elektrotechniczny (Electrical Review)*, ISSN 0033-2097, Vol. 89, No.1a, Jan. 2013, pp.149-155. Online]. Available: http://pe.org.pl/articles/2013/1a/40.pdf

24. Marko Vekić, Stevan Grabić, Dušan Majstorović, Ivan Čelanović, Nikola Čelanović, **Vladimir A. Katić**, “Ultralow Latency HIL Platform for Rapid Development of Complex Power Electronics Systems”, *IEEE Transaction on Power Electronics*, ISSN 0885-8993, Vol. 27, No.11, Nov.2012, pp.4436-4444, [Online]. Available: 10.1109/TPEL.2012.2190097

25. Zoran R. Ivanovic, Evgenije M. Adzic, Marko S. Vekic, Stevan U. Grabic, Nikola L. Celanovic, **Vladimir A. Katic**, "HIL Evaluation of Power Flow Control Strategies for Energy Storage Connected to Smart Grid Under Unbalanced Conditions", *IEEE Transaction on Power Electronics*, ISSN 0885-8993, Vol. 27, No.11, Nov.2012, pp.4699-4710, [Online]. Available: 10.1109/TPEL.2012.2184772

26. Boris Dumnic, **Vladimir A. Katic**, Veran Vasic, Dragan Milicevic, Marko Delimar, "An Improved MRAS Based Sensorless Vector Control Method for Wind Power Generator", *Journal of Applied Research and Technology – JART*, ISSN: 1665-6423, Vol. 10, No. 5, October 2012, pp. 687-697, [Online]. Available: http://www.jart.ccadet.unam.mx/volumen10_5.htm

27. Zoltan J. Čorba, **Vladimir A. Katić**, Boris P. Dumnić, Dragan M. Milićević, "In-Grid Solar-to-Electrical Energy Conversion System Modeling and Testing", *Thermal Science*, ISSN 0354-9836, Vol. 16, Suppl.1, 2012, pp. S159-S171, [Online]. Available: DOI: 10.2298/TSCI120224069C.

28. **Vladimir A. Katić**, Boris P. Dumnić, Nenad A. Katić, Dragan M. Milićević, Stevan U. Grabić, „Potentials and Market Prospects of Wind Energy In the Province of Vojvodina", *Thermal Science*, ISSN 0354-9836, Vol. 16, Suppl.1, 2012, pp. S141-S157, [Online]. Available: DOI: 10.2298/TSCI120229068K

29. Duško Majstorović, Ivan Čelanović, Nikola Teslić, Nikola Čelanović, **Vladimir A. Katić**, „Ultralow-Latency Hardware-in-the-Loop Platform for Rapid Validation of Power Electronics Designs", *IEEE Transactions on Industrial Electronics*, ISSN: 0278-0046, Vol. 58, No.10, Oct.2011, pp.4708-4716, [Online]. Available: http://dx.doi.org/10.1109/TIE.2011.2112318

30. Jovan Knežević, **Vladimir Katić**, "Hybrid Method for On-line Harmonic Analysis", *Advances in Electrical and Computer Engineering*, ISSN: 1582-7445, Vol. 11, No.3, 2011, pp.29-34, [Online]. Available: http://dx.doi.org/10.4316/AECE.2011.03005.

31. **Vladimir A. Katić**, Saša V. Mujović, Vladan M. Radulović, Jadranka S. Radović: „The Impact of the Load Side Parameters on PC Cluster's Harmonics Emission", *Advances in Electronics and Computer Engineering,* ISSN: 1582-7445, Vol. 11, No.1, 2011, pp.103-110. [Online]. Available: http://dx.doi.org/10.4316/AECE.2011.01017

32. Saša Mujović, **Vladimir Katić** and Jadranka Radović, "Improved Analytical Expression for Calculating Total Harmonic Distortion of PC Clusters", *Electric Power Systems Research*, ISSN: 0378-7796, 2011, [Online]. Available: http://dx.doi.org/10.1016/j.epsr.2011.01.023

33. Saša Mujović, **Vladimir Katić** and Jadranka Radović, "Power quality based classification and modelling of small loads and generators", *International Journal on Electrical Engineering Education*, ISSN: 0020-7209, Vol.47, No.3, July 2010, pp.229-247, [Online]. Available: https://doi.org/10.7227/IJEEE.47.3.1

34. Ivan Čelanović, Peter Haessig, Eric Carol, **Vladimir Katić**, Nikola Čelanović, "Real-Time Digital Simulator: Enabling Rapid Development of Power Electronics", *Electronics*, ISSN 1450-5843, Vol.14, No.1, June 2010, pp.15-19, [Online]. Available: http://electronics.etfbl.net/journal/Vol14No1/xPaper_03.pdf

35. Velimir Strugar, **Vladimir Katić, "**Power Quality Measurement in a Modern Hotel Complex", *Electronics*, ISSN 1450-5843, Vol.14, No.1, June 2010, pp.98-102, [Online]. Available: http://electronics.etfbl.net/journal/Vol14No1/xPaper_19.pdf.

36. Evgenije Adžić, Zoran Ivanović, Milan Adžić, **Vladimir Katić**: "Maximum Power Search in Wind Turbine Based on Fuzzy Logic Control", *Acta Polytechnica Hungarica, Journal of Applied Sciences*, ISSN 1785-8860, Vol.6, No.1, 2009, pp.131-149, [Online]. Available: https://uni-obuda.hu/journal/Adzic_Ivanovic_Adzic_Katic_17.pdf

37. Stevan Grabić, Nikola Čelanović, **Vladimir Katić**: "Permanent Magnet Synchronous Generator Cascade for Wind Turbine Application", *IEEE Transaction on Power Electronics*, ISSN 0885-8993, Vol.23, No.3, May 2008, pp.1136-1142, [Online]. Available: DOI: 10.1109/TPEL.2008.921181.

38. Dušan Graovac, **Vladimir Katić**, Alfred Rufer: "Power Quality Problems Compensation with Universal Power Quality Conditioning System", *IEEE Transaction on Power Delivery*, ISSN 0885-8977, Vol.22, No.2, April 2007, pp.968-976, [Online]. Available: DOI: 10.1109/TPWRD.2006.883027

39. **Vladimir Katić**, Jovan Knežević, Dusan Graovac: "Application-Oriented Comparison of the Methods for AC/DC Converter Harmonics Analysis", *IEEE Transaction on Industrial Electronics*, ISSN 0278-0046, Vol. 50, No. 6, 2003, pp.1100-1108, [Online]. Available: DOI: 10.1109/TIE.2003.819580

40. **Vladimir Katić**, Dusan Graovac: "A Method for PWM Rectifier Line Side Filter Optimization in Transient and Steady States", *IEEE Transaction on Power Electronics*, ISSN 0885-8993, Vol. 17, No. 3, 2002, pp.342-352, [Online]. Available: DOI: 10.1109/TPEL.2002.1004242.

41. Dušan Graovac, **Vladimir Katić**: "On-Line Control Of Current Source Type Active Rectifier Using Transfer Function Approach", *IEEE Transaction on Industrial Electronics*, ISSN 0278-0046, Vol. 48, No. 3, 2001, pp. 526-553, [Online]. Available: DOI: 10.1109/41.925579.

42. Dušan Graovac, **Vladimir Katić**, Alfred Rufer: "Power Quality Compensation Using Universal Power Quality Conditioning System", *IEEE Power Engineering Review*, ISSN 0272-1724, Vol. 20, No. 12, 2000, pp. 58-60, [Online]. Available: DOI: 10.1109/39.890381

Selected articles in English in national and regional journals (since 2000):

1. Aleksandar M. Stanisavljević, **Vladimir A. Katić**, Boris P. Dumnić, Bane P. Popadić, "A Brief Overview of the Distribution Test Grids with a Distributed Generation Inclusion Case Study", *Serbian Journal of Electrical Engineering*, Vol. 15, No. 1, February 2018, pp. 115-129, DOI: https://doi.org/10.2298/SJEE1801115S
2. Bane Popadić, **Vladimir Katić**, Boris Dumnić, Dragan Milićević, Zoltan Čorba, "Synchronization Method for Grid Integrated Battery Storage Systems During Asymmetrical Grid Faults", *Serbian Journal of Electrical Engineering*, Vol. 14, No. 1, February 2017, pp. 113-131, DOI: 10.2298/SJEE1701113P
3. **Vladimir A. Katić**, Boris Dumnić, Zoltan Čorba, Dragan Milićević, "Electrification of the Vehicle Propulsion System – An Overview", *Facta universitatis* – series: *Electronics and Energetics*, Vol. 27, No 2, June 2014, pp. 299-316, DOI: 10.2298/FUEE1402299K
4. Nikola Čelanović, Ivan Čelanović, Stevan Grabić, **Vladimir Katić**, Zoran Ivanović, and Marko Vekić, "Cyber Physical Systems Approach to Power Electronics Education", *Electronics ETF*, Vol. 16, No. 2, December 2012, pp. 125-129, DOI: 10.7251/ELS1216125C
5. Jovan M. Knežević and **Vladimir A. Katić**, "Comparison of Methods for On-Line Harmonic Estimation", *Electronics ETF*, Vol. 16, No. 1, June 2012, pp. 16-21, DOI: 10.7251/ELS1216016K
6. Jordan Shikoski, **Vladimir Katic**, Risto Rechkoski, "New Infratechnologies in the Deregulated Power Sector", *Turkish Journal of Electrical Engineering and Computer Sciences*, Vol. 11, No. 2, 1-1-2003, pp. 130-141, available at: https://journals.tubitak.gov.tr/cgi/viewcontent.cgi?article=3669&context=elektrik [accessed on 3. 8. 2026]

Sources of data for the Excerpt from the Bibliography:

ORCID: https://orcid.org/0000-0002-0138-8807

COBBIS PLUS, https://plus.cobiss.net/cobiss/sr/sr/search/cobib?q=Vladimir+Katić

Research Gate, https://www.researchgate.net/profile/Vladimir-Katic-3/research

Publication (in Serbian) „Srpski naučnici u energetskoj elektronici", Chapter: „Kvalitet električne energije – Međunarodni simpozijum Energetska elektronika – Doprinos profesora Vladimira Katića", Catalogue No. 43 of the Gallery of Science and Technology of Serbian Academy of Science and Art, SANU, 2020, pp. 40-41, Biography and References, link: http://esp.etf.rs/cvkatic.pdf

Prepared by:

Vladimir Šiljkut, PhD, Dipl. El. Ing.

I_P
$N_P : N_S$
I_S
V_P
E_P
E_S
V_S
$\frac{V_P}{V_S} = \frac{I_S}{I_P} = \frac{N_P}{N_S}$
D
G
S
C_{gd}
R_g
I_{ch}
C_{ds}
C_{gs}
$CH_4 + H_2O \rightarrow CO + 3H_2$
3.33 ms
3.33 ms
V [p.u.]
A
B
C
t (ms)